2007

Death by Frustration: How Defects in Cell Differentiation Trigger Apoptosis

Ann H. Tang

DEATH BY FRUSTRATION: HOW DEFECTS IN CELL DIFFERENTIATION TRIGGER APOPTOSIS

A Thesis Presented to the Faculty of

The Rockefeller University

In Partial Fulfillment of the Requirements for

The degree of Doctor of Philosophy

by

Ann H. Tang

June 2007

DEATH BY FRUSTRATION: HOW DEFECTS IN CELL DIFFERENTIATION TRIGGER APOPTOSIS

Ann H. Tang, Ph.D.

The Rockefeller University 2007

Apoptosis plays a crucial role in the growth, development, and homeostasis of multicellular organisms by removing excess cells and sculpting tissues. The implications of its misregulation in diseases such as cancer, neurodegeneration, and autoimmunity bespeak of its importance. A family of proteases called caspases brings about the orderly deconstruction of a cell through an evolutionarily-conserved process. A bewildering number of molecules have been implicated to either directly or indirectly regulate these enzymes. Since the net outcome between inhibitory and activational mechanisms ultimately determines a cell's fate, caspases and their regulation still continue to be subjects of intense study.

Studies with *dcp-1* described here have clarified its role as a *Drosophila* effector caspase. From the original descriptions of its somatic phenotypes, a possible role for *dcp-1* in cell proliferation was initially explored, but these phenotypes were eventually found to be associated with a disruption in another gene encoded in the same locus. RNAi studies with *dcp-1* and *drice*, another effector caspase, have provided *in vivo* confirmation of their epistatic relationship to *rpr*, *hid*, and *grim* and have revealed that they may work synergistically.

rpr indirectly activates caspases by derepressing their inhibitors, and many proapoptotic signals trigger its transcriptional upregulation. An analysis of its promoter described here has furthered the understanding of how developmental mutations cue *rpr* transcription. As a consequence of signaling resulting from developmentally aberrant cells, *rpr* is transcriptionally activated via different elements in its promoter region, rather than through a single one, suggesting the role of different pathways and hence different transcription factors. A yeast 1-hybrid assay performed with a narrow region that can mediate upregulation in *crb* and *srp3* backgrounds has led to the identification of a transcriptional modulator of *rpr*, *p8*. Its mammalian homolog has been implicated in stress response and apoptosis. The induced RNA and protein levels of *p8*, the RNA *in situ* pattern, and a reduction of reporter signal in *p8* mutants in *crb* and *srp3* backgrounds support a role for *p8* in transducing a pro-apoptotic response resulting from developmental mutants to the activation of *rpr* transcription.

Dedicated to my loving parents.

Acknowledgments

First and foremost, I thank Hermann Steller for the privilege of working with him and for his support, mentorship, enthusiasm, and patience. I am grateful to him for allowing me the time, space, and freedom to learn to independently solve problems I encountered along the way. I especially appreciate that he assembles a lab with talented and dedicated people, encourages good rapport amongst ourselves, and sets a tone of high integrity for research. I thank the members of my committee, Shai Shaham and Michael Young, for their encouragement, comments, and interest. In addition, I thank Michael Young for having welcomed me into his lab for my first rotation at the beginning of my graduate career. And I thank my outside committee member, Kristin White, for her time and insight.

I thank the current and former members of the Steller Lab for their help, friendship, and invaluable discussions. I especially want to thank Eli Arama and Joe Rodriguez for their generosity, moral support, and entertaining discussions in all matters scientific and otherwise. I am grateful to them and Gabrielle Rieckhof for helping me through the final stretch.

I thank Steve Anderson for always believing in me, encouraging me, and thinking of me.

Finally, I thank my family and friends for their unwavering love and support.

Table of Contents

List of Figures

List of Tables

Abbreviations

AED: after egg deposition
Apaf-1: apoptotic protease activating factor-1
Ark: Apaf-1-related killer
ARTS: apoptosis-related protein in TGFβ signaling pathway
bcd: bicoid
bcl-2: B-cell lymphoma leukemia-2
BIR: Baculovirus IAP repeats
CAD: caspase-activated DNAse
CARD: caspase activation and recruitment domain
ced: cell-death abnormal
crb: crumbs
dark: *Drosophila* Apaf-1-related killer
dcp-1: death caspase-1
debcl: death executioner bcl-2 homolog
DED: death effector domain
dfd: deformed
DIABLO: direct IAP binding protein with low PI
diap-1: *Drosophila* inhibitor of apoptosis protein-1
dl: dorsal
dpp: decapentaplegic
egl: egg-laying defective
en: engrailed
ER: endoplasmic reticulum
esg: escargot
GFP: green fluorescent protein
GH3: grim homology 3
GMR: glass multiple repeats
hac-1: homolog of Apaf-1 and ced-4
hh: hedgehog
hid: head involution defective

hs: heat shock

HtrA2: high temperature requirement A 2

IAP: inhibitor of apoptosis protein

IBM: IAP-binding motif

ICAD: inhibitor of CAD

ICE: interleukin-1 β-converting enzyme

JNK: c-Jun N-terminal kinase

PCD: programmed cell death

ph: polyhomeotic

RHG: reaper hid grim

RING: really interesting new gene

RNAi: RNA interference

rpr: reaper

sens: senseless

Smac: second mitochondria-derived activator of caspase

srp: serpent

Tunel: Terminal deoxynucleotidyl transferase-mediated dUTP nick end labeling

XIAP: X-linked IAP

X-gal: 5-bromo-4-chloro-3-indolyl-β-D-galactopyranoside

yw: yellow white

1 Introduction to Programmed Cell Death

1.1 The Prologue

While the observation that cell death occurs during normal development was documented by Carl Vogt in 1842 (Jacobson et al., 1997), many years passed before cell death research evolved into a hotly pursued field. In the interim, additional observations of this phenomenon trickling into the literature had led to a more generalized view of developmental cell death. In 1965, Richard Lokshin coined “programmed cell death” (PCD) originally to describe the predictable, and hence “programmed”, nature of this developmental cell death that he and his colleagues had observed in insect metamorphosis (Lockshin and Williams, 1965). After documenting the nature of dying cells in various contexts and noting their general structural similarities, Kerr and colleagues applied the term “apoptosis” to describe this death process as one with morphological features distinct from necrosis in displaying a reduction in cell volume, membrane blebbing, DNA fragmentation, chromatin condensation, and phagocytosis (Kerr *et al.*, 1972). Their hypothesis that an underlying genetic program controls this process would only be born out more than a decade later.

Interest in cell death increased as initial studies from mammalian and *Caenorhabditis elegans* models began to stream in. Mammalian data provided the first link between apoptosis and cancer when *bcl-2*, a proto-oncogene translocated in follicular lymphoma, was found to unexpectedly block apoptosis rather than stimulate proliferation under various conditions (Vaux *et al.*, 1988;McDonnell *et al.*, 1989). *C. elegans*, with a precisely defined lineage for

each of the 1090 cells that comprise a hermaphrodite, including 131 that are destined to die with all the morphological manifestations of programmed death (Sulston and Horvitz, 1977), proved to be the ideal model organism to substantiate the idea that a genetic program controls this stereotypical cell death. A genetic screen that yielded mutations in two genes abrogating these deaths provided a foundation for studying PCD at a genetic and molecular level (Ellis and Horvitz, 1986). The subsequent revelation that one of those genes, *ced-3*, encodes a unique protease connected the genetics data to a molecular mechanism for the first time and galvanized the field (Yuan *et al.*, 1993). Insects made reappearance in the cell death field in the form of *Drosophila melanogaster*. Cell death in this organism had already been previously observed (Fristrom, 1968;Fristrom, 1969), but an assiduous documentation of embryonic apoptosis (Abrams *et al.*, 1993) and a landmark discovery of a novel locus that regulates it (White *et al.*, 1994) officially heralded the fly into this field. The flow of findings has since swollen into an inundation, and as with all fields of lasting importance, new discoveries have left ever more questions that continue to intrigue and tantalize.

1.2 Relevance

The direct relevance of apoptosis to our health and well-being fuels the motivation to gain further understanding of this process. When appropriately deployed, PCD serves as a vital counterweight to cell growth and proliferation in assuring the proper development and homeostasis of all multicellular organisms

and as a stringent quality control mechanism to remove defective and potentially dangerous cells (Jacobson *et al.*, 1997;Tittel and Steller, 2000). A developing organism generates many more cells than it needs, and its ultimate well-being requires their precise elimination. Furthermore, an adult organism requires apoptosis to balance cell divisions that continue to occur as well as to limit neoplastic growth. Finally, apoptosis serves to remove damaged or malfunctional cells, such as virally-infected cells or self-reactive lymphocytes. For these reasons, body parts are sculpted, unnecessary structures are destroyed, cell numbers are maintained, and abnormal or harmful cells are eliminated. Examples include the removal of interdigital webbing to create individual digits, the elimination of a tadpole's tale when it is no longer needed, and the culling of excess neuronal and immune cells. Lesions in cell death pathways may lead to pathogenesis of disease, such as AIDS, cancer, autoimmune, and neurodegenerative diseases (Thompson, 1995;Hanahan and Weinberg, 2000;Yuan and Yankner, 2000). For example, abnormal activation of cell death pathway may lead to Parkinson's disease and ischemia in the brain on the one hand, but failure to trigger cell death may lead to cancer on the other (Degterev *et al.*, 2003c). Moreover, the use of apoptotic components for non-apoptotic outcomes plays an important role in proper differentiation, such as in the terminal differentiation of spermatids (Arama *et al.*, 2003;Huh *et al.*, 2004;Arama *et al.*, 2006), muscle development (Fernando *et al.*, 2002), and dendritic pruning (Kuo *et al.*, 2006;Williams *et al.*, 2006). Apoptosis, therefore, plays a crucial role in development and homeostasis, and insight gained from

studying its regulation can be harnessed for developing therapies for treating diseases caused by its mis-regulation.

1.3 The Core Apoptotic Pathway

C. elegans first paved the way to identifying and genetically and molecularly dissecting the components of the core apoptotic pathway. During its normal development, the precise elimination of 131 cells through PCD from a total of 1090 leaves a properly-differentiated hermaphrodite consisting of 959 cells (Sulston *et al.*, 1977;Kimble and Hirsh, 1979;Sulston *et al.*, 1983). Any aberration from this invariant developmental pattern would therefore signify a lesion in a developmental pathway. Genetic screens seeking perturbations in the cell death pattern of this organism yielded four genes that comprise the core cell death pathway: *cell death abnormal* genes *ced-3*, *ced-4*, and *ced-9*, and *egg-laying defective egl-1* (Trent *et al.*, 1983;Ellis *et al.*, 1986;Hengartner *et al.*, 1992). The survival of almost all of the 131 cells normally programmed to die in *ced-3*, *ced-4*, and *egl-1* loss-of-function mutants revealed the pro-apoptotic nature of these genes (Ellis *et al.*, 1986;Desai and Horvitz, 1989;Conradt and Horvitz, 1998), while *ced-9* was found to be anti-apoptotic (Hengartner *et al.*, 1992). The later realization of the evolutionary conservation of these genes elevated interest even further, and the model that arose from genetic epistasis experiments in *C. elegans* still serves as the centerpiece in many subsequent models for apoptotic pathways (Hengartner *et al.*, 1992;Shaham and Horvitz, 1996;Conradt *et al.*, 1998;Danial and Korsmeyer, 2004;Hay and Guo, 2006).

Revolutionary insight into the mechanism by which cells die came from discovery that *ced-3*, the gene occupying the most downstream position in the pathway responsible for killing 131 cells in *C. elegans*. It encodes a protein that bears similarity to the human and murine Interleukin-1 beta-Converting Enzyme-1 (ICE) and whose protease activity is required for cell death (Thornberry *et al.*, 1992;Yuan *et al.*, 1993;Xue *et al.*, 1996). ICE became the founding member of a family of proteases later to be named as caspases, short for cysteine aspartic proteases that cleave specifically after Aspartate residues (Alnemri *et al.*, 1996). At least ten mammalian caspases have heretofore been identified, and many of them have been implicated in apoptosis (Degterev *et al.*, 2003b); the *Drosophila* genome contains a total of seven caspase family members (Boyce *et al.*, 2004). Whatever their function may be, they all have a highly conserved active site containing a Cysteine residue for proteolyzing after an Aspartic acid residue (Thornberry and Lazebnik, 1998). Most caspase molecules comprise an inhibitory or pro- amino-terminal domain and a large and small subunit; cleavage between these domains results in the formation of an active heterodimer from the large and small subunit, and two heterodimers form a heterotetramer. The apoptotic caspases are usually classified into two groups: those with long prodomains are usually considered to be the initiator or upstream caspases, and those with short prodomains are the effector or downstream caspases. The long prodomain of the initiator caspases contain motifs for homotypic protein-protein interactions, such as death effector domain (DED) and the caspase activation and recruitment domain (CARD) that are also found on proteins with which they

interact. These procaspases can auto-catalyze, and their resulting mature forms, in turn, activate the effector caspases. Rather than randomly cleave at every consensus site, these effector caspases target specific substrates, such as components directly involved in cellular integrity, positive regulators of cytoskeletal strurcture, or negative regulators of apoptosis (Fischer *et al.*, 2003). Cleavage of nuclear lamin, for example, results in shrinkage of the nucleus and condensation of chromatin (Takahashi *et al.*, 1996;Orth *et al.*, 1996). And cleavage of the inhibitor of caspase-activated DNAse ICAD allows CAD to fragment DNA (Liu *et al.*, 1997;Enari *et al.*, 1998). The central role of caspases in executing the cell death program therefore requires stringent mechanisms to tightly regulate their activation, and many genes identified thus far that participate in the apoptotic process, by and large, do influence caspase activity either directly or indirectly.

ced-4, the other gene isolated in the same screen as *ced-3*, was eventually proven to be a caspase activator. While *ced-4* was also shown to be pro-apoptotic like *ced-3* and to act upstream of *ced-3* (Ellis *et al.*, 1986;Yuan and Horvitz, 1990;Shaham *et al.*, 1996), further elucidation of its mode of action came from *in vitro* studies which led to the identification of its mammalian homolog, Apoptotic Protease Activating Factor-1 (APAF-1). It, in a complex that includes Caspase-9 and Cyctochrome c was found to be necessary and sufficient in reconstituting dATP-dependent Caspase-3 activation (Zou *et al.*, 1997;Li *et al.*, 1997;Zou *et al.*, 1999). Soon thereafter, the physical interaction of CED-4 and CED-3 was demonstrated to be necessary for CED-3 activation and apoptosis

(Seshagiri and Miller, 1997;Yang *et al.*, 1998), and the mammalian holoenzyme with APAF-1 and Caspase-9 was shown to have orders of magnitude greater enzymatic activity than Caspase-9 alone (Rodriguez and Lazebnik, 1999). The *Drosophila* homolog Ark, also known as Dark/Hac-1/Dapaf-1, functions similarly in its requirement, along with Cytochrome c in certain cell types, in its activation of Dronc, the initiator caspase in flies (Zhou *et al.*, 1999;Kanuka *et al.*, 1999;Rodriguez *et al.*, 1999;Arama *et al.*, 2003;Mendes *et al.*, 2006;Arama *et al.*, 2006). CED-4 and its homologs, therefore, serve as adaptor proteins that, when oligomerized together with caspases, form active apoptosomes (Zou *et al.*, 1999). Differences among the homologs appear to stem in part from the protein structure of CED-4. All homologs contain an N-terminal CARD domain for interacting with CARD-carrying caspases, but CED-4 lacks a WD40 domain present in homologs of other species. In *C. elegans*, unless CED-4 is otherwise held in check, it will bind to and activate CED-3. In contrast, WD40 repeats inhibit APAF-1 function until a proapoptotic signal causes the translocation of Cytochrome c into the cytoplasm where it releases the inhibition on APAF-1 by binding to the WD40 repeats and causing a conformational change that allows the CARD domain to interact with that of Caspase-9 (Hu *et al.*, 1998;Benedict *et al.*, 2000).

Upstream regulation of *ced-3* and *ced-4* occurs via the function of anti-apoptotic *ced-9* and pro-apoptotic *egl-1*, both of which turned out to be members of the *bcl-2* superfamily (Hengartner *et al.*, 1992;Hengartner and Horvitz, 1994a;Hengartner and Horvitz, 1994b;Conradt *et al.*, 1998). Previous studies

had already established a relationship between the founding member *bcl-2* with apoptosis (Vaux *et al.*, 1988), and further experiments showing the ability of *bcl-2* to block cell death in *C. elegans* as well as to function anti-apoptotically in *ced9-/-* animals provided additional evidence for the evolutionary conservation of the PCD pathway (Hengartner *et al.*, 1992;Vaux *et al.*, 1992). Both pro- and anti-apoptotic genes comprise this superfamily, and their antagonistic function upstream of apoptosome formation constitutes an important control point in the decision to proceed with PCD. In *C. elegans*, until a pro-apoptotic signal triggers the activation of the cell death pathway, CED-4 is sequestered in its dimeric form by its interaction with CED-9 bound at the outer mitochondrial membrane (James *et al.*, 1997;Spector *et al.*, 1997;Wu *et al.*, 1997a;Wu *et al.*, 1997b). In an apoptotic situation, EGL-1 binds to CED-9 and causes the release of CED-4 from the mitochondrial membrane, thus allowing it to complex with and to activate CED-3 (Seshagiri *et al.*, 1997;Conradt *et al.*, 1998;Yang *et al.*, 1998;Del *et al.*, 1998;Chen *et al.*, 2000;Del *et al.*, 2000). Mammalian Bcl-2 proteins, on the other hand, do not physically interact with APAF-1, but rather regulate its activation indirectly (Kluck *et al.*, 1997;Yang *et al.*, 1997). The ratio of anti- to pro-apoptotic members in mammalian cells serves as a rheostat that sets the threshold of susceptibility to apoptosis; if the death program is turned on, pro-apoptotic Bcl-2 proteins alter the architecture of the outer mitochondrial membrane and cause the release of pro-apoptotic proteins that aid in apoptosome formation and inhibit Inhibitor of Apoptosis (IAP) function, respectively (Danial *et al.*, 2004). Two *bcl-2* members have thus far been described in *Drosophila*: the pro-apoptotic *death*

executioner bcl-2 homolog (*debcl*)/ *Drosophila ortholog of bcl-2 family-1*(*drob-1*)/ *Drosophila bcl-2 ortholog* (*dborg-1*)/ *Drosophila bok* (*dbok*) and the anti-apoptotic *buffy/dborg-2* (Brachmann *et al.*, 2000;Igaki *et al.*, 2000;Colussi *et al.*, 2000;Zhang *et al.*, 2000;Quinn *et al.*, 2003). However, their mode of action remains unclear. Studies at this point disagree on the requirement of *ark* and caspases in the cell death resulting from *debcl* overexpression.

In addition to regulating the activation of caspases via apoptosome formation, their activity is also subject to control by Inhibitor of Apoptosis proteins (IAPs) and their antagonists, the RHG (*rpr hid grim*) family members. The very first screen done in *Drosophila* seeking cell death genes led to the identification of a small deficiency *Df(3L)H99* that abrogated embryonic cell death (White et al, 1994). Rather than harboring homologs of known genes, this small deletion was found to contain three novel genes: *reaper* (*rpr*) (White *et al.*, 1994;White *et al.*, 1996), *head involution defective* (*hid*) (Grether *et al.*, 1995), and *grim* (Chen *et al.*, 1996), which became the founding members of the RHG family. Studies in later years led to the identification of two other *Drosophila* proteins that share conserved sequence motifs with the RHG family (Tenev *et al.*, 2002;Christich *et al.*, 2002;Srinivasula *et al.*, 2002;Wing *et al.*, 2002). In particular, these five proteins all share a small motif called the IBM (IAP-binding motif). In its minimal form, this motif can be reduced to a conserved tetrapeptide that is necessary and sufficient to binding IAPs (Wing *et al.*, 2001;Shi, 2002a;Shi, 2002b). The novelty of the original members, *rpr*, *hid*, and *grim*, provided the basis upon which the discovery of their apparent mammalian homologs was made: Smac/Diablo (Du

et al., 2000;Verhagen *et al.*, 2000) and Htr2A/Omi (Suzuki *et al.*, 2001;Martins, 2002;Hegde *et al.*, 2002;van *et al.*, 2002;Verhagen *et al.*, 2002). ARTS, a functional ortholog lacking any recognizable IBM, was also found to activate apoptosis similarly in antagonizing IAPs (Larisch-Bloch *et al.*, 2000;Gottfried *et al.*, 2004;Lotan *et al.*, 2005).

A modifier screen seeking mutations enhancing or suppressing the eye-ablation phenotypes in the adult *Drosophila* eye caused by *GMR-rpr* and *GMR-hid*, transgenic flies overexpressing *rpr* and *hid* under the *glass multiple repeats* promoter, provided insight into the mechanism of the pro-apoptotic activity of RHG proteins (Agapite, 2002). Among the mutants obtained in this screen were alleles of *Drosophila* homologs of Inhibitor of Apoptosis proteins, *diap-1* (Hay *et al.*, 1995;Wang *et al.*, 1999b;Goyal *et al.*, 2000;Agapite, 2002) and *dbruce* (J. Agapite Ph.D. thesis, MIT, 2002;(Vernooy *et al.*, 2002;Arama *et al.*, 2003). This evolutionarily conserved family, founded by *Op-iap* in baculovirus (Crook *et al.*, 1993), contains genes with at least one baculovirus IAP repeat (BIR) motif (Miller, 1999), and those members functioning in apoptosis usually contain RING (really interesting new gene) domains that function as ubiquitin E3 ligases (Vaux and Silke, 2005). *C. elegans*, however, does not have IAPs that function in apoptosis (Fraser *et al.*, 1999). Structural studies reveal similar modes of binding for the mammalian IAPs and fly Diap-1 with caspases downstream and RHG proteins upstream. Mammalian XIAP, cIAP-1, and cIAP-2 had previously been shown to directly inhibit effector caspase-3 and -7 and initiator caspase-9 (Deveraux *et al.*, 1997;Roy *et al.*, 1997), and later structural analysis elucidated the precise

binding mechanism with which the BIR domain and its neighboring residues hinder substrate access to the active site of caspases (Chai *et al.*, 2001;Huang *et al.*, 2001;Riedl *et al.*, 2001;Shiozaki *et al.*, 2003). Likewise, Diap-1 also uses its BIR2 domain to interact with and inhibit the caspases Dronc in its unprocessed form and Drice and Dcp-1 in their activated forms (Kaiser *et al.*, 1998;Hawkins *et al.*, 1999;Wang *et al.*, 1999b;Meier *et al.*, 2000;Zachariou *et al.*, 2003;Chai *et al.*, 2003;Yan *et al.*, 2004;Tenev *et al.*, 2005). Releasing caspases from Diap-1 or XIAP requires the binding of the IBM of their respective IAP antagonist to displace caspases from the BIR domain (Wu *et al.*, 2000;Liu *et al.*, 2000;Wu *et al.*, 2001). These protein interactions, therefore, exhibit an impressive level of conservation at the structural level.

The similarities revealed by X-ray crystallography, however, belie the actual differences and importance in mechanism between the mammalian and fly RHG and IAP members. While mammalian tissue culture and biochemical studies with XIAP have revealed an anti-apoptotic role (Duckett *et al.*, 1996;Uren *et al.*, 1996;Deveraux *et al.*, 1997), the inhibition of caspase-9 appears to be its main mode of action. Even though XIAP does have a ubiquitin E3 ligase encoding RING domain that can ubiquitinate caspases *in vitro*, its physiological relevance has yet to be demonstrated (Vaux *et al.*, 2005). Unfortunately, the apparent redundancy of IAP family member function has confounded an *in vivo* analysis XIAP (Harlin *et al.*, 2001). Furthermore, the inhibition of IAPs by the mammalian RHG proteins identified thus far probably does not play a major role in caspase activation. Since the release of these proteins from their normal

place of residence in the mitochondria occurs only after a pro-apoptotic stimulus disrupts the mitochondrial membrane, their function would enhance, rather than initiate, the apoptotic process already in progress (Du *et al.*, 2000;Verhagen *et al.*, 2000;Suzuki *et al.*, 2001;Hegde *et al.*, 2002). Based on our current state of knowledge, it appears that mammals rely more heavily on the activation of caspases to trigger apoptosis. However, few decisive studies have been done so far, particularly under *in vivo* conditions, and it is possible that genuine mammalian homologs of RHG-family proteins will be discovered in the future. Studies demonstrating the ability of *Drosophila* RHG proteins to potently kill mammalian cells support this possibility (Claveria *et al.*, 1998;Haining *et al.*, 1999;Varghese *et al.*, 2002;Claveria *et al.*, 2004b).

Extensive studies with *diap-1*, on the other hand, have led to the model that the initiation of caspases in *Drosophila* requires the release of Diap-1 inhibition. Homozygous strong mutant *diap-1* alleles display an immense elevation of cell death in embryos and never hatch, revealing a vital role (Wang *et al.*, 1999b;Goyal *et al.*, 2000;Lisi *et al.*, 2000). *In vitro* binding experiments demonstrate a physical interaction between DIAP-1 and RPR and HID, and genetic epistasis experiments with *Df(3L)H99*, the deficiency deleting *rpr*, *hid*, and *grim*, place *diap-1* downstream of *Df(3L)H99* (Wang *et al.*, 1999b;Goyal *et al.*, 2000). Structural studies discussed above corroborate these observations. RHG proteins, therefore, activate the cell death program by unleashing activated effector caspases and allowing pro-Dronc to oligomerize with Dapaf-1 by

competing for the binding of Diap-1 at its BIR domain. Furthermore, DIAP-1 does not alter the catalytic activity of Dronc the way XIAP-1 does for Caspase-9 (Yan *et al.*, 2004). The RING domain of Diap-1 plays an important role in tagging pro-Dronc for degradation, but self-ubiquinates when bound to an RHG protein (Holley *et al.*, 2002;Ryoo *et al.*, 2002;Yoo *et al.*, 2002;Wilson *et al.*, 2002). The mechanisms governing the interplay between caspase activation and inhibition have been conceptualized in the "Gas and Brake" model of apoptosis: the apoptosome-mediated activation of caspases provides the gas driving cell death, and the IAPs are the brakes that keep the caspases in check (Song and Steller, 1999;Salvesen and Abrams, 2004). In mammals, stepping on the gas via caspase activation is thought to play the more prominent role in causing cell death, whereas in *Drosophila*, the releasing of the brakes via the derepression of Diap-1 inhibition on activated effector caspases is the more important mechanism.

Intense study in the field of PCD over the last two decades in worms, flies, and mammals has yielded vast insight into a process that was documented 165 years ago. Illustrations of models integrating current knowledge depict a vast array of molecules in intersecting pathways. Described in this section is the current view on the core intrinsic pathway (Figure 1.1). Close scrutiny has revealed some differences in regulation, but more notable is the high degree of evolutionary conservation. The picture is far from complete, and current studies in the nematode, fly, and mammalian models will continue to synergistically further our understanding.

Figure 1.1: Core Apoptotic Machinery. In the "Gas and Brake" Model of apoptosis, activation of caspases constitutes stepping on the gas and their inhibition constitutes stepping on the brake. Caspases are the most downstream components of the core apoptotic machinery, and their proteolytic activity ultimately dismantles a cell. Worms have only one apoptotic caspase, ced-3; flies and mammals have multiple ones. Caspases are synthesized as zymogens that contain an N-terminal domain, a large subunit, and a small subunit, and cleavage between these domains is required for their activation. In flies and mammals, caspases are categorized into "initiator" and "effector" classes with Dronc and Caspase-9 as examples of the former and Drice/Dcp-1 and Caspase-3 as examples of the latter. The initiator class differs from the effector class in that members of the former contain longer prodomains with motifs for homotypic protein-protein interactions for the recruitment of adaptor proteins, such as CED-4 in worms and its homologs Ark and Apaf-1 in flies and mammals, respectively. Constitutively active in worms, CED-4 binds to and activates CED-3 in the absence of inhibition. In a non-apoptotic situation in worms, anti-apoptotic Bcl-2 family member CED-9, residing on the outer mitochondrial membrane, binds directly to CED-4 and sequesters it. In an apoptotic situation, the inhibition that CED-9 has on CED-4 is relieved by the direct binding of pro-apoptotic Bcl-2 family member EGL-1 to CED-9. Apoptosis proceeds because CED-4 is then free to complex with CED-3. The mechanism by which CED-4 homologs Ark and Apaf-1 activate caspases differs because they contain additional inhibitory WD-40 repeats that prevent their constitutive activation of caspases in the absence of an apoptotic signal. In mammals, this signal is governed upstream by pro- and anti-apoptotic Bcl-2 members that, rather than interact directly with Apaf-1, alter the architecture of the mitochondrial membrane such that its contents would be released in a pro-apoptotic situation. The released Cytochrome C then binds to the WD-40 repeats, thereby relieving its inhibition of Apaf-1 and allowing it to activate caspases. A similar requirement for Cytochrome C has been demonstrated in certain tissues in flies to activate Ark, but fly Bcl- 2 homologs, Debcl and Buffy, need to be studied further to confirm their roles in the apoptotic process. Unlike worms, flies and mammals have an additional mechanism regulating caspases: IAP family members that usually contain at least one BIR domain and a RING domain. DIAP-1 in flies inhibits active effector caspases using a BIR domain and neighboring residues and tags pro-DRONC for degradation with its RING domain. An in vivo function for degradation of mammalian caspases by XIAP-1 has not been demonstrated, and while it is capable of inhibiting effector and initiator caspases, inhibiting the catalytic activity of the latter seems to be the most important function. When DIAP-1, in turn, is negatively regulated by Rpr, Hid, and Grim via their IBM motifs binding to DIAP-1, the inhibition on caspases is released and apoptosis is allowed to proceed. Mammalian counterparts are mitochondrial proteins Smac/Diablo and HtrA2/Omi, which contain the IBM motif, and ARTS, which has no IBM motif. They are IAP-binding molecules, but their weaker in vivo significance in inhibiting XIAP-1 suggests that true homologs of Rpr, Hid, and Grim may not have been found.

"Gas and Brake" Model of Apoptosis

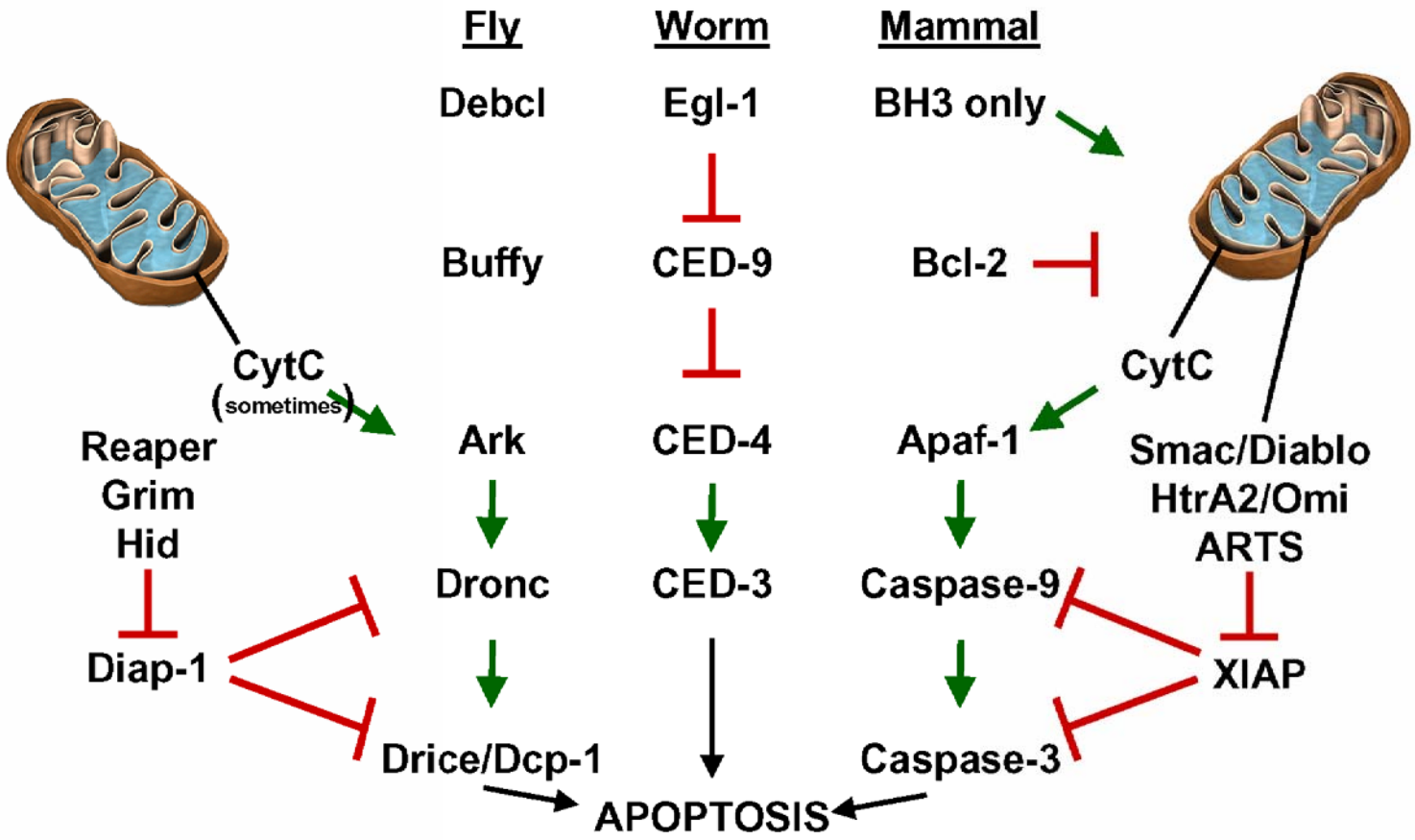

1.4 Studying Apoptosis with *D. melanogaster*

While the utilization of *D. melanogaster* in studying PCD may have begun later than the other model organisms, it has proven itself to be an equal partner, and crucial insights gained from its use has fueled further studies in the field. The advantages the fly has over other systems stem from its position as the nonpareil compromise between the worm and the mouse in terms of the ease of genetic manipulation and organismal complexity. Its genetic tractability and rich history as a research organism has conferred it an unrivaled breadth of tools to test hypotheses in an *in vivo* setting. Its relative simplicity compared to the mouse reduces the level of genetic redundancy that often confounds the results of murine studies, while its relative complexity compared to the worm allows for experiments in which plasticity in development may be the desired setting.

Initial groundwork demonstrated the suitability of *Drosophila* as a model organism to study apoptosis and described the nature and pattern of cell death, as visualized by electron microscopy and staining with vital dyes (Abrams *et al.*, 1993). Embryonic cell death in the fly begins at stage 11 and possesses all the morphological hallmarks of apoptosis. Inhibition of protein synthesis right before the onset of apoptosis does not affect normal embryonic cell deaths but does suppress those resulting from X-irradiation. The variability observed at the onset of CNS apoptosis suggested a plasticity that may be exploited in future studies on how the cellular environment may influence the cell death decision. That *Drosophila* would use genes homologous to the ones found in nematodes and mammals to drive this apparently apoptotic cell death was predictable, and those

discoveries did occur in swift succession. Such was the case with the seven caspases, *ark*, *bcl-2* family members, *diap-1* and *-2*. Both *in vivo* and *in vitro* studies with this repertoire have greatly furthered our understanding of the apoptotic process. But in addition to that, the fly has also been instrumental in identifying novel cell death genes. Indeed, the major discovery of a small chromosomal region that controls almost all PCD in the embryo immediately proved *Drosophila* to be an important player. Continuing studies with this organism therefore promises to lead to further substantial and relevant findings.

1.5 *Drosophila* Caspases

Because their activation ultimately leads to the stereotypical morphological changes associated with an apoptotic cell, caspases play a central role as executioners of apoptosis. Studying their function and regulation is, therefore, fundamental to understanding the cell death process. The lower degree of genetic redundancy in simpler model organisms generally facilitates the evaluation of genetic function. With *ced-3* as the only apoptotic caspase in the *C. elegans* genome, for example, loss-of-function alleles exhibiting an unambiguous phenotype of the survival of almost all 131 cells normally eliminated in development and epistasis experiments placing it in the final position in the core pathway reveal a crucial role for this gene (Ellis *et al.*, 1986;Yuan *et al.*, 1993;Shaham *et al.*, 1996). More than ten caspases, on the other hand, have been identified in humans and mice, and targeted gene knock-outs in mice have yielded a spectrum of phenotypes ranging from embryonic lethality for *caspases* -

7 and *-8* and perinatal lethality with neuronal hyperplasia for *caspases-3* and *-9* to apparently normal development for *caspases-1*, *-6*, *-11*, and *-12*, signifying a dedication of each caspase to different functions with possible redundancy (Degterev *et al.*, 2003a). Studying how caspases are differentially regulated is of great interest, and *Drosophila* offers a good compromise between the organism that has only one caspase and the one that has more than ten.

Seven caspases have been identified in *Drosophila*: *dcp-1*, *dronc*, *drice*, *dredd*, *decay*, *damm*, and *strica* (Boyce *et al.*, 2004). As with many caspases, the length of their prodomains usually determines their classification into either initiator or effector caspases. By this measure, three should fall into the initiator class, but *strica* remains an enigma because of the absence of known domains for homotypic protein-protein interactions in its prodomain (Doumanis *et al.*, 2001) and because of its phylogenetic similarity to effector caspases (Lamkanfi *et al.*, 2002). The remaining two caspases with long prodomains, *dredd* and *dronc*, are bona fide initiator caspases. Evidence supporting a role of *dredd* in apoptosis includes an accumulation of mRNA in cell destined to die, the suppression of its mRNA in a *Df(3L)H99* background, and resistence of *dredd-/-* flies to UV irradiation (Chen *et al.*, 1998;Georgel *et al.*, 2001). Much stronger evidence, however, points more solidly to a role in the regulation of relish, a NFkB homolog, in the *Drosophila* innate immune response (Leulier *et al.*, 2000;Elrod-Erickson *et al.*, 2000;Stoven *et al.*, 2000;Georgel *et al.*, 2001). The function of a pro-apoptotic initiator caspase, then, falls on *dronc*. Indeed, *in vitro* experiments have shown the ability of Dronc to cleave Drice (Hawkins *et al.*, 2000;Meier *et al.*,

2000). That *dronc* mutants display defects in developmental apoptosis in some tissues and a decrease in stress-induced apoptosis demonstrates a major role *in vivo*, supporting previous observations made with dominant-negative mutations or RNAi loss-of-function studies (Meier *et al.*, 2000;Quinn *et al.*, 2000;Muro *et al.*, 2002;Daish *et al.*, 2004;Chew *et al.*, 2004;Xu *et al.*, 2005). Furthermore, ecdysone pulses governing metamorphosis transcriptionally regulate *dronc*, leading to the histolysis of tissues no longer needed (Dorstyn *et al.*, 1999a;Cakouros *et al.*, 2004).

Four caspases with short prodomains that fall into the effector class are *dcp-1*, *drice*, *damm*, and *decay*. Not much is known about the latter two. Decay was found to have a similar substrate specificity as mammalian Caspase-3, and it is expressed in a subset of tissues known to undergo apoptosis (Dorstyn *et al.*, 1999b). The expression pattern of *damm* also coincides with tissues known to undergo apoptosis, its overexpression causes cell death, and overexpression of its catalytically inactive form suppresses the *GMR-hid* eye-ablated phenotype (Harvey *et al.*, 2001). *dcp-1* and *drice* are the better characterized of these effector caspases, and they do not have completely redundant functions. They are broadly expressed in embryos but may be found in different temporal and spatial patterns in other tissues (Song *et al.*, 1997;Fraser and Evan, 1997a;Peterson *et al.*, 2003). Initial biochemical experiments revealed that these two caspases may have similar, overlapping substrate specificities, but they are not identical (Fraser *et al.*, 1997a;Fraser *et al.*, 1997b;Song *et al.*, 2000). Loss-of-function RNAi experiments showed that *drice-RNAi*, but not *dcp-1-RNAi*,

suppresses *GMR-diap1-RNAi* and *GMR-hid* phenotypes, but *dcp-1-RNAi* enhances the suppression seen with *drice-RNAi* alone (Leulier *et al.*, 2006). The isolation of *drice* and *dcp-1* mutants has substantiated some of these findings. *dcp-1* null flies are viable but suffer a block in starvation-induced germline cell death at mid-oogenesis and an alteration in the localization of Drice (Laundrie *et al.*, 2003). *drice* null alleles obtained by different groups have reduced viability (Muro *et al.*, 2006;Xu *et al.*, 2006). Loss of *dcp-1*, as in the RNAi studies (Leulier *et al.*, 2006), was found to enhance *drice* null phenotypes: no *dcp-1-/-; drice-/-* animals eclose, and *dcp-1-/-; drice-/-* embryos show a greater suppression of normal developmental apoptosis than do *drice -/-* embryos. Furthermore, a *drice -/-* background suppresses *GMR-rpr*, *-hid*, and *-grim* eye ablation phenotypes and *diap-1-/-* -induced embryonic apoptosis, but does not suppress *GMR-dronc* or *GMR-dcp-1*. And additional midline glial cells as well as interommatidial cells survive normal developmental elimination in *drice -/-* animals (Muro *et al.*, 2006;Xu *et al.*, 2006). But because the numbers of these extra cells are lower than those found in *Df(3L)H99* and *dronc* mutants, another caspase in addition to *drice* likely plays a role in apoptosis in those contexts (Xu *et al.*, 2006).

1.6 *Drosophila* RHG Genes

In a deficiency screen covering ~50% of the *Drosophila* genome, *Df(3R)H99* was found to dramatically abrogate acridine orange staining that marks normal developmental cell death in embryos (Abrams *et al.*, 1993;White *et al.*, 1994). From a series of overlapping cosmid clones tested for their ability to

rescue this lack of death, only one, from which *rpr* was cloned, has the ability to significantly, but not completely, restore embryonic cell death (White *et al.*, 1994). Further analysis led to the identification of two other genes in the region, *hid* and *grim* (Grether *et al.*, 1995;Chen *et al.*, 1996). Single mutants in the *Df(3L)H99* region have been isolated as well (Grether *et al.*, 1995;Peterson *et al.*, 2002). Loss-of-function alleles for *hid* showed reduced apoptosis for embryogenesis and contain extra cells, but this phenotype is much less severe than the global cell death defect seen in *Df(3L)H99* homozygotes (Grether *et al.*, 1995). This suggested a redundancy in the function of these three genes. Indeed, overexpression studies demonstrated that each of the three is sufficient in inducing caspase-dependent cell death (Grether *et al.*, 1995;Hay *et al.*, 1995;Chen *et al.*, 1996;White *et al.*, 1996;Pronk *et al.*, 1996;Evans *et al.*, 1997;Claveria *et al.*, 1998;McCarthy and Dixit, 1998;Haining *et al.*, 1999). Furthermore, a 14-amino acid stretch of homology at the amino-terminus of these otherwise dissimilar proteins indicates a similarity in protein function (Grether *et al.*, 1995;Chen *et al.*, 1996). This trio would become the founding members of the RHG protein family (Wing *et al.*, 2001). Subsequent studies ushered in two other *Drosophila* RHG-bearing genes into the family: *skl* and *jafrac2* (Tenev *et al.*, 2002;Christich *et al.*, 2002;Srinivasula *et al.*, 2002;Wing *et al.*, 2002). As discussed above, genetic, biochemical, and structural experiments have provided corroborating data in support for a model of a mechanism by which the IBM tetrapeptide relieves the inhibition that DIAP-1 has on caspases by competing for

binding to Diap-1 at its BIR domain. Therefore, these RHG members do, by virtue of a short stretch of homology, share similar function.

The mRNA distribution of these genes, however, is not the same and suggests a difference in upstream regulation. *rpr* mRNA is broadly expressed in the embryo in a pattern similar to normal developmental death and foretells the death of a cell (White *et al.*, 1994). On the other hand, although *hid* is detected broadly except in the ventral nerve cord, it is also expressed in cells that are not necessarily destined to die (Grether *et al.*, 1995). Additionally, type II neurons that die after the completion of metamorphosis express *rpr* and *grim* but not *hid* (Robinow *et al.*, 1997). Likewise, vCrz neurons that apoptose after the onset of metamorphosis require *rpr* but not *hid* or *grim* for this task (Choi *et al.*, 2006). *skl*, shown to be coexpressed with *rpr*, *hid*, or *grim* in some cells, has a much more limited distribution as compared to the pattern of embryonic PCD, but can act synergistically with *grim* in inducing apoptosis (Christich *et al.*, 2002;Srinivasula *et al.*, 2002;Wing *et al.*, 2002). Furthermore, that a synergism between *rpr* and *hid* is needed for the death of midline glial cells shows that *rpr*, *hid*, and *grim* alone are not necessarily sufficient in killing in all contexts (Zhou *et al.*, 1997a). And overexpression of *grim* can induce apoptosis at an earlier stage than *rpr* can (Chen *et al.*, 1996). Finally, flies transgenic for chimeric genes in which the IBM domain of *grim* replaces that of *rpr* and vice versa do not possess identical killing abilities (Wing *et al.*, 2001). These observations show, therefore, that these genes are differentially regulated and not completely redundant.

Furthermore, the functions of these genes may not be exclusively dictated by the IBM. Overexpression of *rpr* or *grim* without this domain, for example, may induce apoptosis in a caspase-dependent and independent manner (Chen *et al.*, 1996;Wing *et al.*, 1998;Kaiser *et al.*, 1998;Wing *et al.*, 2001;Tait *et al.*, 2004). More specifically, a Trp block or GH3 domain predicted to conform to an α helix, identified in *grim*, was found to be sufficient in killing in a manner independent of IAP binding. Homologous regions exist in *rpr* and *skl* and are proposed to function similarly (Claveria *et al.*, 1998;Wing *et al.*, 2001;Claveria *et al.*, 2002;Claveria *et al.*, 2004a). *In vitro* analyses with truncated regions of Rpr confirm that the stretch encompassing the Trp block/GH3 region does induce death independent of Ark or Diap-1 binding (Chen *et al.*, 2004). In addition, translational inhibition has also been demonstrated to be another function of *rpr* and *grim* that is independent of its RHG domain (Holley *et al.*, 2002;Yoo *et al.*, 2002). These studies thus indicate that domains outside of the RHG motif may confer to these proteins additional, unique functions that extend beyond DIAP-1 binding.

RHG proteins, therefore, have a well-characterized role in derepressing the inhibition that Diap-1 has on caspases by competitive binding of the RHG domain with the BIR domain. Other domains on these proteins may confer different properties, that, when combined with differential upstream signals, likely results in the diverse functions of the various RHG proteins.

1.7 *reaper* and its transcriptional regulation

rpr was the first gene to be cloned within the *H99* region (White *et al.*, 1994). It encodes a small protein of only 65 amino acids in length, and yet its promoter region regulating its transcription spans over 11 kb, since transgenic animals made with a 11kb promoter region driving a LacZ reporter mostly, but not completely, recapitulate the mRNA *in situ* pattern of endogenous *rpr* (White *et al.*, 1994;Nordstrom *et al.*, 1996)Lamblin and Steller, unpublished). Expression of *rpr* precedes cell death by 1-2 hours, and the broad distribution of its transcript in the embryo reflects a similar pattern of PCD (White *et al.*, 1994). *rpr* is sufficient, but not necessary, in inducing apoptosis in a caspase-dependent manner (Nordstrom *et al.*, 1996;White *et al.*, 1996;Peterson *et al.*, 2002). Indeed, transheterozygotes for deletions at the *rpr* locus are homozygous viable, despite the abundance of its transcript during embryogenesis in *wt* animals (White *et al.*, 1994;Peterson *et al.*, 2002). The sterility of males for this deletion is attributed to an inability to bend its genitalia rather than to a spermatogenesis or behavioral defect (Peterson *et al.*, 2002). The only cell death defect detected in *rpr* null animals is the persistence of neuronal cells that normally die post eclosion and a reduction of apoptotic cells in response to X-irradiation (Peterson *et al.*, 2002). But apparently, p53-induced cell death as well as the histolysis of larval tissues that normally occur with an increase in *rpr* transcript can also occur in a *rpr*-independent manner (Jiang *et al.*, 1997;Brodsky *et al.*, 2000;Ollmann *et al.*, 2000;Jin *et al.*, 2000;Peterson *et al.*, 2002). A

functional redundancy most likely from the other RHG genes accounts for this mild phenotype.

Despite of a lack of a dramatic phenotype in *rpr* null animals, studying its regulation is nonetheless worthwhile. As discussed above, other RHG genes possess functions that can compensate for *rpr* as well as possibly unique functions, but each may be differentially regulated at the transcriptional level since different transcripts are detected in different cells. Studying how upstream signals lead to the transcriptional activation of RHG genes will provide insight on events causing a release of the brakes on caspase activity. The vast stretch of promoter sequences of *rpr* is a prime candidate for the integration of those signals. Accumulating evidence shows support for the importance of the transcriptional regulation of *rpr* in response to various signals. Indirect data usually show a correlating change in *rpr* transcript. For example, n4 neurons that normally die after eclosion of the fly require a factor from the head to upregulate transcription of *rpr* (Robinow *et al.*, 1997). And cells protected from death show a corresponding downregulation of *rpr*. For instance, *senseless* (*sens*) represses transcription of *rpr* as well as *hid* in embryonic salivary glands, presumably to protect them from apoptosis (Chandrasekaran and Beckendorf, 2003). And posterior dMP2 and MP1 pioneer neurons are spared the death meted out to the anterior neurons by the repressive action of Hox gene *abdominal B* (*abd-B*) on *rpr* and *grim* transcription in those posterior cells (Miguel-Aliaga and Thor, 2004). In some cases, direct binding of a protein onto the *rpr* promoter has been demonstrated. Ecdysone pulses during metamorphosis, for example, induce *rpr*

expression by engaging the EcR/USP response elements in the *rpr* promoter (Jiang *et al.*, 2000). X-irradiation-triggered apoptosis occurs via the direct transcriptional activation *rpr* by the binding of Dmp53 onto its promoter (Brodsky *et al.*, 2000). Localized apoptosis can create physiological boundaries defined by the spatial upregulation of *rpr*. The mandibular-maxillary boundary in embryos is created by the binding of Hox protein Deformed (Dfd) onto the *rpr* promoter (Lohmann *et al.*, 2002). And the morphogenesis of the joint in the *Drosophila* leg depends on *rpr* activation triggered by a Jun kinase cascade in response to a sharp interruption of Dpp signaling that occurs during normal segmentation (Manjon *et al.*, 2007). Many diverse signals, hence, impinge upon the *rpr* promoter, and since the presence of its mRNA spells inexorable death to a cell, investigating how the signals are integrated would be a fascinating endeavor.

1.8 Transcriptional Regulation of Apoptotic Genes

Regulation of the core apoptotic machinery can occur through a number of mechanisms, such as the activation, upregulation, or downregulation of pro- and anti-apoptotic components. While all these components are generally constitutively expressed in cells, the activation of the apoptotic program still requires new RNA and protein synthesis (Jacobson *et al.*, 1994;Weil *et al.*, 1996). The first compelling piece of evidence for this requirement came from the identification of *rpr*, *hid*, and *grim* locus in *Drosophila* and the observation that *rpr* is usually transcriptionally activated one to two hours prior to a cell's demise and suggested a wider significance of transcriptional control in the cell death process

(Abrams *et al.*, 1993;White *et al.*, 1994;Jacobson *et al.*, 1997). The prevalence of this strategy described in subsequent publications has indeed demonstrated the importance of transcriptional regulation as a mechanism in controlling the core apoptotic machinery in all three model organisms in which apoptosis is studied.

In addition to the regulation of *rpr* described above, other *Drosophila* apoptotic genes are also under transcriptional control. *hid* and *ark*, like *rpr*, are upregulated by ionizing radiation (Zhou *et al.*, 1999;Sogame *et al.*, 2003;Luo *et al.*, 2007). *hid* has additionally been shown to be transcriptionally activated in mis-specified cells (Werz *et al.*, 2005). Furthermore, ecdysone pulses that signal metamorphosis induce histolysis of unnecessary tissues by upregulating the pro-apoptotic *rpr*, *hid*, *dark*, *dronc*, and *drice* genes and downregulating the anti-apoptotic genes *diap-1* and *-2* (Dorstyn *et al.*, 1999a;Jiang *et al.*, 2000;Lee *et al.*, 2000;Lee and Baehrecke, 2000;Cakouros *et al.*, 2002;Lee *et al.*, 2002;Daish *et al.*, 2004;Kilpatrick *et al.*, 2005).

In *C. elegans*, the pro-apoptotic *bcl-2* family member *egl-1* plays a crucial role in initiating the cell death pathway and hence requires stringent control (Huang and Strasser, 2000). Studies from the past several years indicate that transcriptional regulation constitutes an important mechanism in that control. For example, TRA-1A, a transcription factor that specifies sex of the organism, was found to transcriptionally repress *egl-1* in cells of the HSN (hermaphrodite-specific) lineage to allow for their survival in hermaphrodites (Conradt and Horvitz, 1999). Furthermore, a specific *cis*-regulatory region in the *egl-1* promoter has

been found to play a role in the fate of NSM (neuron-secretory motor) sister cells: *egl-1* is transcriptionally activated when a heterodimer of HLH-2/HLH-3 (helix-loop-helix) binds to Snail-binding sites/E-boxes in the region, but is transcriptionally repressed when those same sites are occupied by CES-1 (cell-death specification), a Snail-like DNA-binding protein (Thellmann *et al.*, 2003). Finally, a complex comprising of Hox protein MAB-5 (Male Abnormal-5) and CEH-20 (C. Elegans Homeobox-20) binds to a consensus sequence in the *egl-1* promoter to direct apoptosis of a P11 cell lineage (Liu *et al.*, 2006). However, *egl-1* does not play a major role in inducing apoptosis in all cell types. The temporal control of tail-spike cell death was recently shown to be controlled by the transcriptional activation of *ced-3* by the binding of a homeodomain transcription factor PAL-1 (Maurer *et al.*, 2007).

Studies in mammalian models thus far have shown that from their repertoire of apoptotic molecules, *bcl-2* family members, *apaf-1*, *smac*/*diablo*, and caspases are transcriptionally regulated. Pro- and anti-apoptotic members of the *bcl-2* family are subject to transcriptional regulation. *hrk* (*harakiri*)/*dp5* transcript, for instance, is upregulated in neuronal tissues with a significant apoptotic population (Imaizumi *et al.*, 1997). Transcript levels of two other family members, *noxa* and *puma*, are induced by DNA damage in a p53-dependent manner (Oda *et al.*, 2000;Nakano and Vousden, 2001;Han *et al.*, 2001;Yu *et al.*, 2001;Villunger *et al.*, 2003;Jeffers *et al.*, 2003;Shibue *et al.*, 2003). In addition, *puma* was found to be upregulated by E2F-1 to cause apoptosis of melanoma cells (Hao *et al.*, 2007). *bim* was found to be induced in response to growth

factor deprivation in neuronal and hematopoietic cells (Dijkers *et al.*, 2000;Putcha *et al.*, 2001;Shinjyo *et al.*, 2001;Whitfield *et al.*, 2001). Glutocorticoid induces apoptosis by indirectly activating *bim* probably through the binding of a *forkhead* transcription factor (Wang *et al.*, 2003) that are known to transcriptionally regulate *bim* in other contexts (Dijkers *et al.*, 2000;Stahl *et al.*, 2002;Linseman *et al.*, 2002;Gilley *et al.*, 2003). Finally, Gfi-1 has the ability to directly repress *bax* expression in immortalized T cell lines and primary thymocytes by binding to Gfi-1consensus sites in the promoter (Grimes *et al.*, 1996). Among the anti-apoptotic *bcl-2* members regulated transcriptionally, *bcl-2* is transcriptionally repressed by AP-2α (activator protein 2α) (Wajapeyee *et al.*, 2006). Furthermore, mcl-1 transcript is induced in myeloid leukemia cell lines and is regulated by CREB transcription factor in IL-3-stimulated cells (Zhou *et al.*, 1997b;Wang *et al.*, 1999a).

The other apoptotic genes regulated transcriptionally have been less extensively studied, but the reports nonetheless highlight the importance of this mechanism. Transcriptional regulation of *apaf-1* has been demonstrated to occur via P53 (Kannan *et al.*, 2001;Rozenfeld-Granot *et al.*, 2002) and E2F-1 (Moroni *et al.*, 2001;Furukawa *et al.*, 2002). And cAMP transcriptionally upregulates *smac*/*diablo* by binding to CRE consensus site at the promoter (Martinez-Velazquez *et al.*, 2007). Various mammalian caspases are also transcriptionally regulated. P53, for example, has been demonstrated to upregulate *caspase-1*, *-8*, and *-10* (Gupta *et al.*, 2001;Liedtke *et al.*, 2003;Rikhof *et al.*, 2003). *caspase-1* has been shown to additionally be induced by the ETS

transcription factor. Finally, INF-γ treatment of human breast tumor cells results in an elevation of *caspase-8* transcript levels via the binding of IRF-1 (Interferon Regulatory Factor-1) onto the ISRE (Interferon-stimulated response element) in the promoter (Ruiz-Ruiz *et al.*, 2004).

Transcriptional regulation, therefore, is a common strategy for cells to alter the quantity of apoptotic molecules in the cell. The body of data accumulated so far shows molecules from different pathways playing roles in the transcriptional control and reveals a complex intersection of upstream pathways involved in initiating the core apoptotic machinery.

2 Characterization of *dcp-1*

2.1 Introduction

The identification of *dcp-1* and P-element insertions disrupting its locus provided tools for the *in vivo* analysis of its function. In particular, the intriguing phenotypes associated with these mutations afforded the opportunity of linking caspase function to a non-apoptotic role. Initial studies using two loss-of function P-element alleles, *l(2)2132* and *l(2)1862*, described the somatic phenotypes of 3rd instar larval lethality with melanotic tumors and no imaginal discs and a germline phenotype of aberrant nurse cell death (Song *et al.*, 1997;McCall and Steller, 1998). X-gal staining of the *l(2)2132* line recombined with *esg-LacZ* for the visualization of imaginal discs has revealed the presence of very small discs in the homozygotes (Figure 2.1D and E) and posed a puzzling phenotype to study. A phenotype of an excess number of cells, rather than one of fewer cells, would be an intuitive prediction from a loss or reduction of caspase function. A loss of *dcp-1* function resulting in smaller imaginal discs, rather than larger ones, may point to an unexpected role for a caspase.

At the inception of my undertaking this project, a growing body of evidence implicating additional functions for caspases outside the context of conventional PCD was beginning to challenge the notion that their activation represents unequivocal demise for a cell. For example, activation of *caspase-3* and caspase-3-like proteases that is not followed by apoptosis had been observed in proliferating T lymphocytes (Miossec *et al.*, 1997;Wilhelm *et al.*, 1998;Posmantur *et al.*, 1998). Furthermore, *in vivo* studies from knockout mice had provided

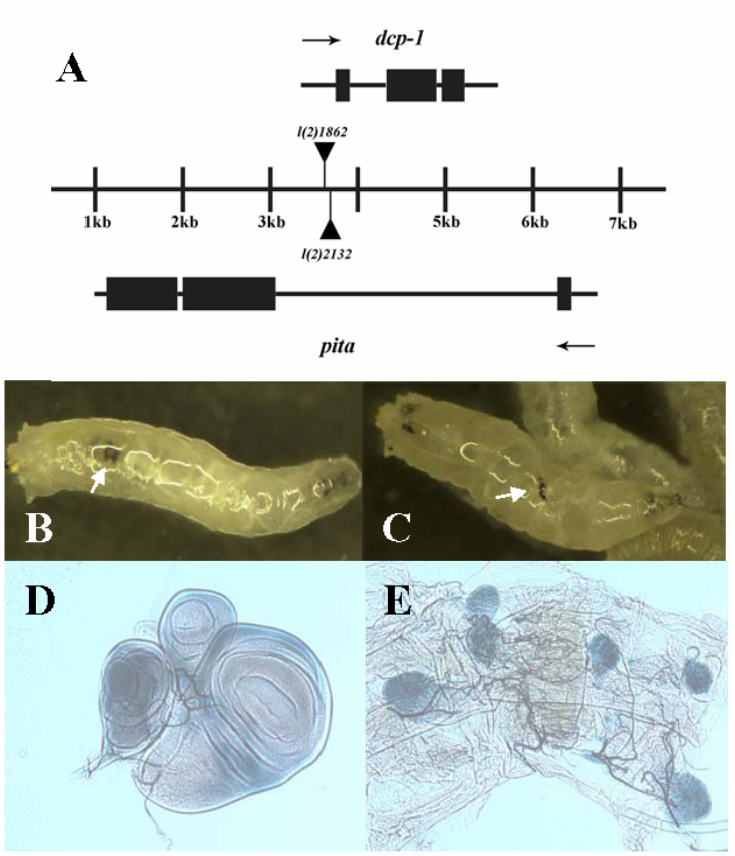

Figure 2.1: Mutant phenotypes associated with *l(2)1862* and *l(2)2132*

(A) Genomic locus depicting the relative locations of *dcp-1*, *pita*, and two P-element alleles, *l(2)1862* and *l(2)2132*. The arrows indicate the relative directions in which each gene is transcribed. Melanotic tumors (white arrows) are prevalent in *l(2)2132* homozygous **(B)** and *l(2)1862/ l(2)2132* transheterozygous **(C)** wandering 3rd instar larvae. Imaginal discs are dissected from wandering 3rd instar larvae of *l(2)2132, esg-LacZ/CyO-GFP* **(D)** and *l(2)2132, esg-LacZ/l(2)2132* **(E)** genotypes and stained with X-gal. **(D)** and **(E)** were taken at the same magnification.

circumstantial, yet tantalizing, data suggesting a possible role of caspases in cell proliferation. In particular, *caspase-8-/-* mice produce hematopoietic precursors with decreased ability for colony formation and insufficient number of T-cell progenitors (Varfolomeev *et al.*, 1998). And *fadd-/-* mice exhibit a similar phenotype as well as the production of T cells deficient in activation-induced proliferation (Newton *et al.*, 1998;Walsh *et al.*, 1998). That caspases may activate a positive regulator or inactivate a negative regulator of cell cycle was already a topic of conjecture (Los *et al.*, 2001). But establishing a link between caspases and proliferation required more concrete evidence. *dcp-1* mutants with small imaginal discs that may have defects in either differentiation or proliferation seemed to be useful as tools to reveal the mechanisms by which caspases may function in processes that are intuitively contrary to apoptosis.

However, the phenotypes of *dcp-1* first had to be confirmed. Indeed, subsequent sequencing and annotation of the *Drosophila* genome showed that a second gene *CG3491*, now named *pita* (Peterson *et al.*, 2003), is transcribed at the same locus (Figure 2.1A). *dcp-1* and the two P-alleles are located entirely within the first intron of *pita*. Northern analysis revealed the loss of both transcripts in *l(2)2132* homozygotes (Figure 2.2). This necessitated the determination of which phenotypes were actually caused by the loss of which gene in addition to further characterization of the phenotypes before studies with the P-alleles could proceed.

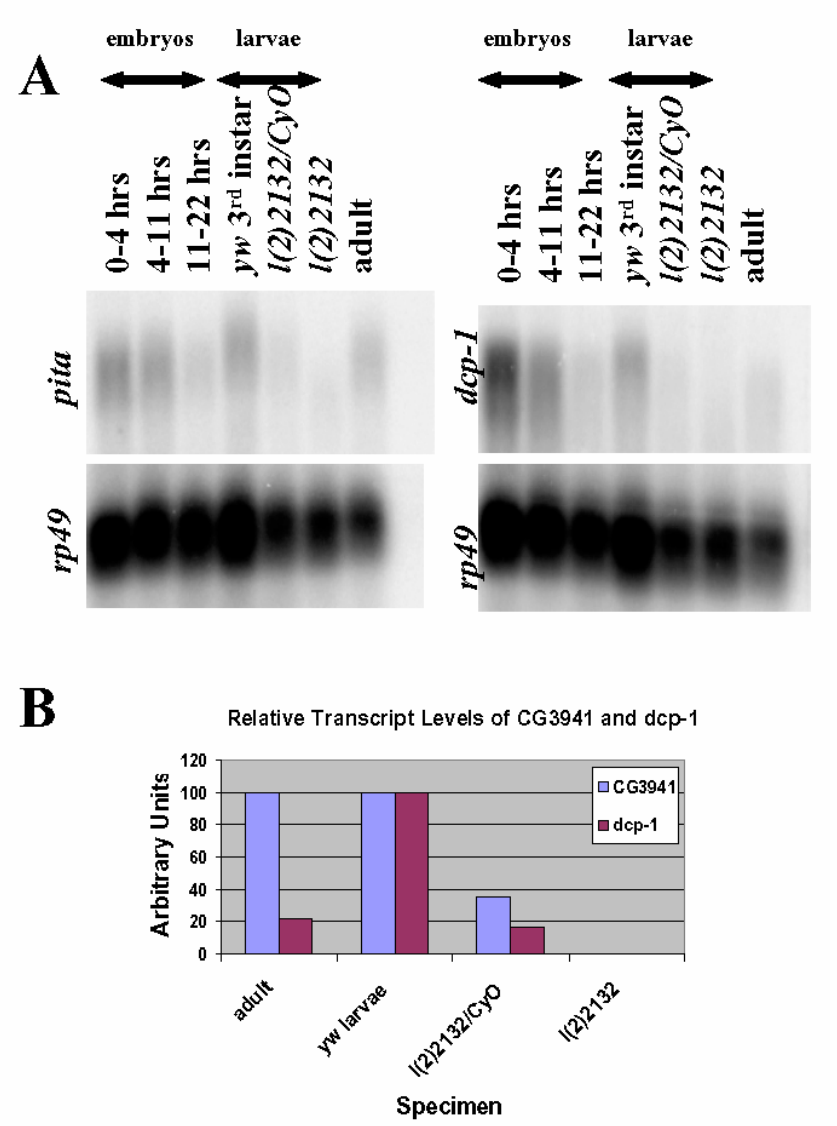

Figure 2.2: Northern analysis for *dcp-1* and *pita* (*CG3941*) transcripts

(A) 30 µg total RNA was loaded in each lane. The blots were hybridized with *dcp-1*, *pita* (*CG3941*), and *rp49* radio-labeled probes, and the signal was detected with a phosporimager.
(B) The signal was quantitated in arbitrary units, normalized against *rp49*, and plotted on a bar graph.

2.2 Materials and methods

2.2.1 *Drosophila* stocks

Fly stocks were maintained on conventional cornmeal-agar-molasses medium at 25°C. The following fly lines were used in these studies:

l(2)1862	*l(2)2132*
esg-LacZ	*flp122; tub>y+ GFP>Gal4*
dpp-LacZ	*hh-LacZ*
FRT G13^{w+} ubi-nls-GFP	*FRT G13^{w+}*
UAS-GFP	*UAS-LacZ*
UAS-p35; UAS-dn-prodronc	*en-Gal4*
ey-Gal4	*69B*
GMR-dn-dcp-1	*GMR-dcp-1-RNAi*
UAS-dn-dcp-1	*UAS-dcp-1-RNAi*
UAS-drice-RNAi	*GMR-ΔN-dcp-1*
GMR-Gal4	*UAS-pita*
yw	*Sco/CyO-GFP*
hs-Gal4	

2.2.2 Generation of transgenic flies

GMR-dn-dcp-1 and *UAS-dn-dcp-1* constructs were made by inserting the cDNA of the dominant-negative form of dcp-1 with a C285A point mutation in its conserved catalytic site into the *pGMR* and *pUAST* vectors, respectively. To make *GMR-dcp-1-RNAi* and *UAS-dcp-1-RNAi* constructs, 2 copies *dcp-1* cDNA was first cloned into Bluescript in opposite orientation with a GFP linker in the

middle and then finally cloned into either *pGMR* or *pUAST*. *UAS-pita* constructs were made by cloning the cDNA of *pita* into *pUAST*. All constructs were injected into *yw* embryos using standard protocols.

2.2.3 Generation of αDCP-1 antibody

The coding sequence of *dcp-1* with a C285A mutation was excised out of pBluescript by an EcoRI and NcoI digest and cloned into pGEX4T3 at those sites. The construct was expressed in Bl21 and GST-tagged DCP-1 was purified from the bacterial lysate with Glutathione Sepharose 4B beads (Amersham) using a recommended standard protocol from the manufacturer. Purified protein was electrophoresed through a 10% Tris-HCl gel, and the relevant band was excised and sent for antibody production in guinea pigs (Cocalico).

2.2.4 X-gal staining of imaginal discs

Imaginal discs were dissected from larvae in PBS and fixed in 1% glutaraldehyde in PBS for 15 minutes with shaking at room temperature. They were then washed for 3 X 10 minutes in PBS. X-gal is added at a final concentration of 2mg/mL in X-gal staining solution preheated to 65°C containing 10mM phosphate buffer, pH7.4, 150 mM NaCl, 1mM $MgCl_2$, 3mM $K_4FeII(CN)_6 \bullet 3H_2O$, 3mM $K_3FeIII(CN)_6$, and 0.3% Triton X-100. The discs were rocked at room temperature until a desired level of staining is achieved, rinsed once in PBS, and allowed to equilibrate in 80% glycerol in PBS at 4°C. The imaginal discs were then dissected away from all unwanted tissues and mounted.

2.2.5 Antibody staining of imaginal discs

Imaginal discs were dissected from larvae in PBS and fixed in 4% paraformaldehyde with shaking for 20 minutes at room temperature and were washed for 3 X 10 minutes in $PBT_{0.1\%}$ (PBS + 0.1% Triton X-100). A one-hour blocking step in 5% normal goat serum and 1% BSA in $PBT_{0.1\%}$ took place at room temperature. Primary antibody was incubated overnight at 4°C with rocking, followed by 3 X 10 minutes washes in $PBT_{0.1\%}$. The discs were then rocked at room temperature for 2 hours in secondary antibody, followed by at least 3 X 10 minutes washes in $PBT_{0.1\%}$. If a HRP-conjugated secondary was used, then the development of the signal was obtained with the Vectastain ABC Elite Kit according to recommended protocol. The imaginal discs were finally dissected away from unwanted tissue and mounted in 80% glycerol in PBS. The following antibodies and dilutions were used in these studies:

GFP (Molecular Probes)	1:500
Engrailed (DHSB)	1:10
ß-gal (Promega)	1:500
ß-gal (Cappel)	1:2500
Cyclin B (DSHB)	1:5
Phospho H3 (Upstate)	1:500
BrdU (BD)	1:20
CM1 (Idun)	1:2000
Elav (DSHB)	1:50
Dcp-1	1:1000

HRP-conjugated anti mouse (Jackson Laboratories) 1:500

All fluorescent 2° antibodies (Jackson Laboratories) 1:250

2.2.6 BrdU incorporation

Imaginal discs were dissected from larvae in Schneider's medium and were allowed to incubate in 10 μM BrdU in Schneider's medium for 30 minutes at room temperature. They were then washed 1 X 5 minutes in Schneider's medium and 2 X 5 minutes in PBS. The fixation step required an overnight incubation at 4°C with rocking in 1% paraformaldehyde in PBS. The discs were then washed 2 X 10 minutes in PBS, hydrolyzed in 2N HCl for 15 minutes, and neutralized in 0.1M sodium borate. A 1 X 10 minute wash in PBS and 2 X 10 minute washes in $PBT_{0.1\%}$ followed. The discs were rocked first in αBrdU antibody in 5% normal goat serum in $PBT_{0.1\%}$ for 2 hours at room temperature, washed for 3 X 10 minute in $PBT_{0.1\%}$, and then rocked in secondary antibody in 5% normal goat serum in $PBT_{0.1\%}$ for 2 hours at room temperature. After 3 X 10 minute washes in $PBT_{0.1\%}$, the discs were dissected away from unwanted tissues and mounted in 80% glycerol in PBS.

2.3 Results

2.3.1 Analysis of small imaginal disc phenotype

Small imaginal discs may be a result of a defect in proliferation or one in patterning. *decapentaplegic* (*dpp*) and *hedgehog* (*hh*) expression patterns were initially used to assess whether the latter was disrupted. Imaginal discs were dissected from *l(2)2132/CyO-GFP; dpp-LacZ* of the wandering 3rd instar stage (Figure 2.3A) and of the newly molted 3rd instar stage (Figure 2.3B) and their

Figure 2.3: Evaluation of patterning in imaginal discs of *l(2)2132* 3rd instar larvae

Imaginal discs in all panels were dissected from wandering 3rd instar, except for those in (B), which came from newly-molted 3rd instar larvae. Discs in panels A-G were stained with X-gal, and those in panels H-I were stained with an Elav antibody. Genotypes: (A, B) *l(2)2132/CyO-GFP; dpp-LacZ.* (C, D) *l(2)2132; dpp-LacZ.* (E) *l(2)2132/CyO-GFP; hh-LacZ.* (F, G) *l(2)2132; hh-LacZ.* (H) *l(2)2132/CyO-GFP.* (I, J) *l(2)2132.* Abbreviations: ed = eye disc, hd = haltere disc, ld = leg disc, wd = wing disc.

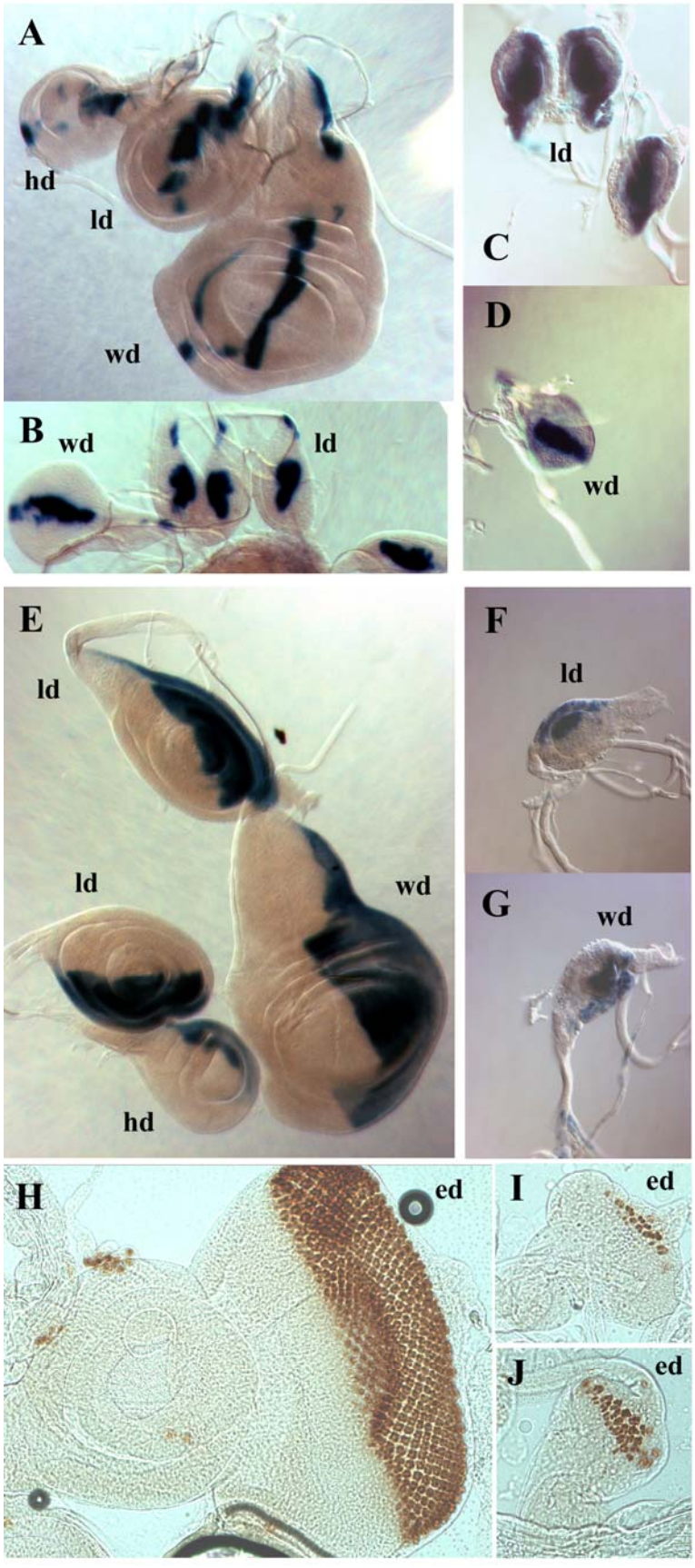
A
hd
ld
wd
B
wd
ld
C
ld
D
wd
E
ld
ld
wd
hd
F
ld
G
wd
H
ed
I
ed
J
ed

l(2)2132; dpp-LacZ wandering 3rd instar siblings (Figure 2.3C and D) and stained with X-gal. Normal wing and leg discs from the *l(2)2132/CyO-GFP* heterozygotes express *dpp* in a stripe along the anterior-posterior (AP) boundary (Figure 2.3A), and that stripe is wider at an earlier age (Figure 2.3B). A similar pattern of staining is seen in *l(2)2132* discs from older wandering 3rd instar larvae (Figure 2.3C, D), indicating that *dpp* is expressed properly in the homozygotes but that the growth of the discs have halted. Likewise, small discs from *l(2)2132; hh-LacZ* (Figure 2.3F and G) stain for X-gal in the posterior compartment as do the larger discs from their *l(2)2132/CyO-GFP; hh-LacZ* (Figure 2.3E) siblings of the same age. Eye discs were also stained for Elav to detect neuronal cells, and although the morphogenetic furrow for those from *l(2)2132* (Figure 2.3I and J) had not moved as anteriorly as for *l(2)2132/CyO-GFP* eye discs (Figure 2.3H), positive staining for Elav is evident. The imaginal discs from *l(2)2132*, therefore, appear to be able to differentiate properly.

To determine whether there is a cell-autonomous requirement for the gene disrupted by *l(2)2132*, clones were induced by a one-hour heat shock at 37ºC administered to the progeny *of hs-flp; FRT G13^{w+} ubi-nls-GFP* virgin females and *FRT G13^{w+} l(2)2132/CyO* at 24 (Figure 2.4A), 48 (Figure 2.4B), or 72 (Figure 2.4C and D) hours after egg deposition (AED). The observations that only twin spots appear when recombination is induced at the earlier time points of 24 and 48 hours AED and that mutant clones appear only when they are induced at 72 hours AED indicate that there is, indeed, a cell-autonomous requirement. Furthermore, mutant clones from animals heat shocked at 72 hours AED stained

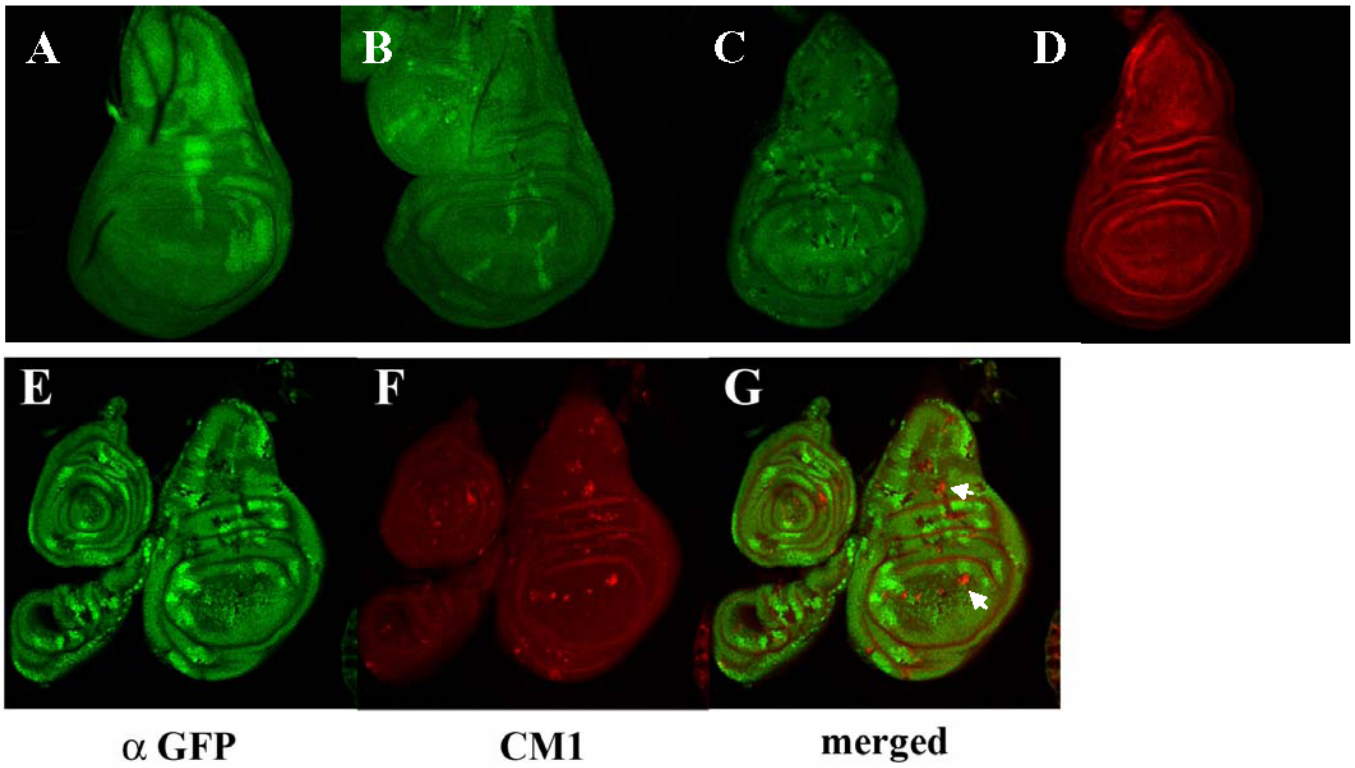

Figure 2.4: Cell autonomous requirement for gene disrupted by *l(2)2132*
Progeny from *hs-flp; FRT G13^{W+} ubi-nls-GFP* virgin females X *FRT G13^{W+} l(2)2132/CyO* were heat shocked for 1 hour at 37°C at **(A)** 24 hrs, **(B)** 48 hrs, or **(C-G)** 72 hrs. AED, dissected for wing discs at the wandering 3rd instar larval stage, and stained for GFP **(A-C, E)**, phalloidin **(D)**, and CM1 **(F)**. White arrows in the merged image in **(G)** point to examples of mutant clones immunoreactive to the CM1 antibody.

positively with the CM1 antibody that detects activated caspases, indicating that they die by apoptosis (Figure 2.4E-G).

l(2)2132 may be causing a growth or proliferation defect, since cells with such defects are out-competed by their *wt* or more highly metabolic neighboring cells (Diaz and Moreno, 2005). To test that possibility, imaginal discs from larvae heat shocked at 72 hours AED were stained with antibodies against Cyclin B, Phospho H3, and BrdU. Cyclin B, a marker for cells that have passed the G1/S checkpoint but have not divided yet, normally stains cells just posterior to the morphogenetic furrow of the eye imaginal disc (Figure 2.5B;(Baker and Yu, 2001b), and that stripe of cells remains uninterrupted by mutant clones generated along its path (Figure2.5C, white arrow). Phospho H3 is normally detected randomly throughout the imaginal discs (Figure 2.5E and H), and cells staining positive for it can be found in mutant clones (Figure 2.5F and I, white arrows). Incorporated BrdU accumulates, among other places, in a sharp band posterior to the morphogenetic furrow of the eye imaginal disc (Baker and Yu, 2001a), and, like Cyclin B, positive staining can be found inside mutant clones (Figure 2.5L, white box). Similarly, BrdU can also be found in mutant clones in the wing imaginal disc (Figure 2.5O). *l(2)2132* clones, therefore, do not appear to have a defect in proliferation.

2.3.2 Determination of the gene responsible for phenotypes

Since the cell autonomous requirement for either *dcp-1* and/or *pita* is the cause of the loss of *l(2)2132* mutant clones (Figure 2.4), then testing whether a block or decrease in *dcp-1* could phenocopy the loss of clones would determine if

Figure 2.5: Absence of cell cycle defect in *l(2)2132* clones

Progeny from *hs-flp; FRT G13^{w+} ubi-nls-GFP* virgin females X *FRT G13^{w+} l(2)2132/CyO* were heat shocked for 1 hour at 37°C at 72 hrs AED, dissected for imaginal discs at the wandering 3rd instar larval stage, and stained for GFP **(A, D, G, J, M)** and Cyclin B **(B)**, Phospho H3 **(E, H)**, or BrdU **(K, N)**. Merged images are represented in **(C, F, I, L, O)**. White arrows and white boxes indicate examples of mutant clones which stained positively with Cyclin B or Phospho H3 antibodies or for BrdU incorporation.

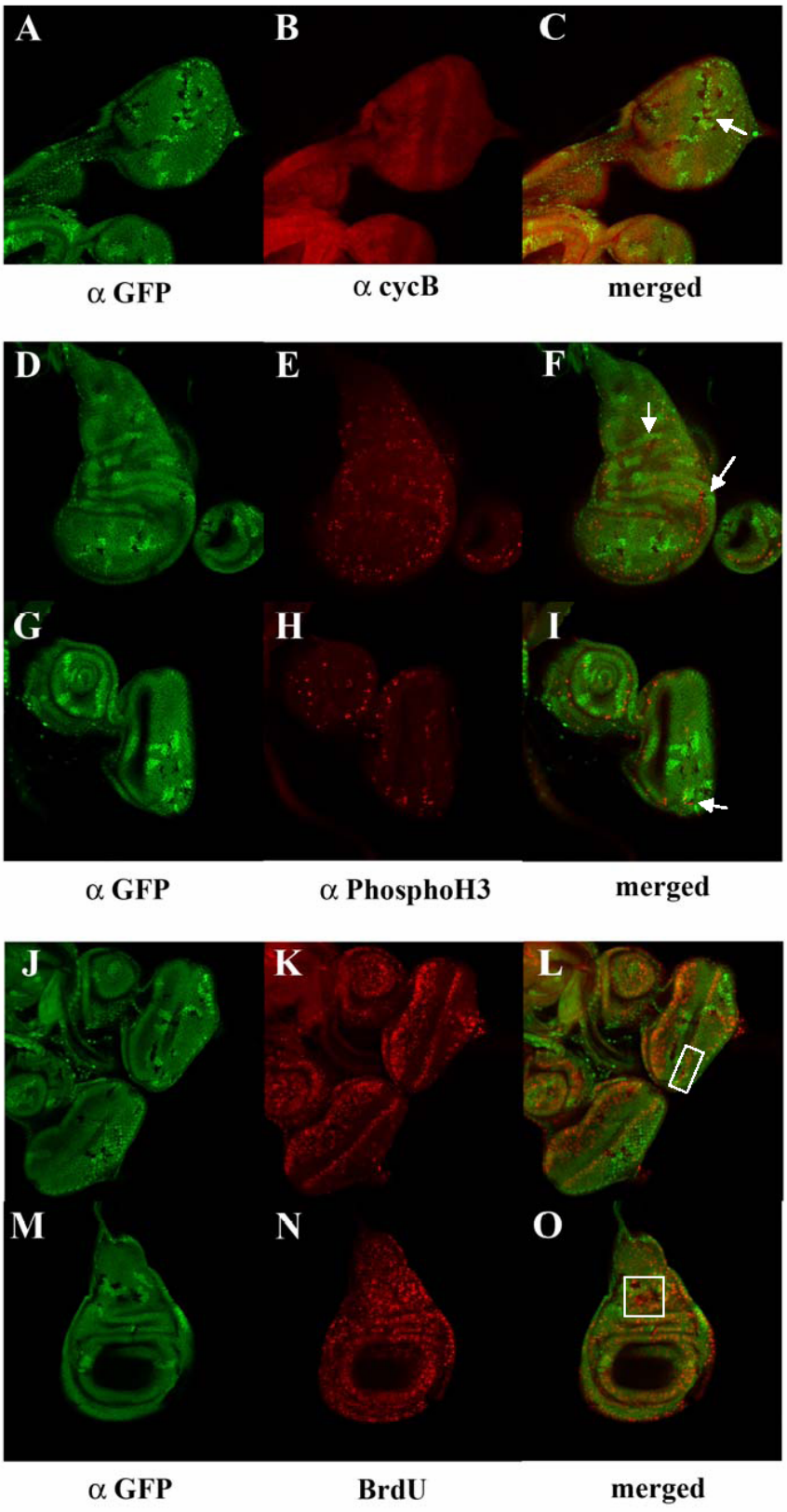
A
B
C
α GFP
α cycB
merged
D
E
F
G
H
I
α GFP
α PhosphoH3
merged
J
K
L
M
N
O
α GFP
BrdU
merged

the disruption of *dcp-1*, indeed, causes the small imaginal disc phenotype. To this end, pan-caspase inhibitor *p35* and a dominant-negative form of the initiator caspase *dronc* were first used to indirectly inhibit Dcp-1 function. Flip-out clones were, therefore, generated to overexpress *p35* and *dn-dronc* by crossing flp122*; tub> y+ GFP> Gal4* virgin females with *UAS-p35; UAS-dn-prodronc* males. Progeny were subjected to a 1 hour heat shock at 37ºC at 24, 48, and 72 hours AED (Figure 2.6). In all cases, the clones overexpressing *p35* and *dn-dronc* were qualitatively similar in size than to those not overexpressing anything.

The next option in strategy was to generate clones overexpressing a dominant-negative form of *dcp-1* to attempt a more direct interference of Dcp-1 function. Transgenic flies for *UAS-dn-dcp-1* and *GMR-dn-dcp-1* were created with a point mutation at its active site. Wing discs from *en-gal4/+; UAS-dn-dcp-1/+* larvae exhibited increased immunoreactivity to αDCP-1 antibody in the posterior compartment, showing that DN-Dcp-1 is overexpressed there (Figure 2.7). One copy of *GMR-dn-dcp-1* modestly suppresses the eye phenotype caused by one copy of *GMR-ΔN-dcp-1* (compare Figure 2.7C and D) and slightly suppresses *2XGMR-rpr CyO/ScO* (compare Figure 2.7 E and F). However, the sizes of clones overexpressing *dn-dcp-1* beginning at 24 hours (data not shown), 48 hours (data not shown), and 72 hours (Figure 2.7G and H) are again comparable to the ones overexpressing nothing.

UAS-dcp-1-RNAi and *GMR-dcp-1-RNAi* transgenic flies were also made as another attempt to create *dcp-1* loss-of-function clones. Wing discs from *en-Gal4/UAS-GFP; UAS-dcp-1-RNAi/+* flies do show a decrease in immunoreactivity

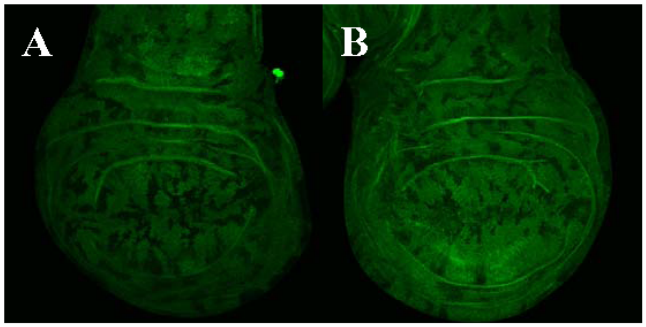

Figure 2.6: Absence of effect of inhibition of activated caspases on clonal size
Progeny of *flp122; tub>y+ GFP>Gal 4* virgin females X *yw* **(A)** or *UAS-p35; UAS-dn-prodronc* **(B)** were heat shocked for 1 hour at 37°C at 72 hrs AED, dissected for their wing discs at the wandering 3rd instar stage, and stained for GFP.

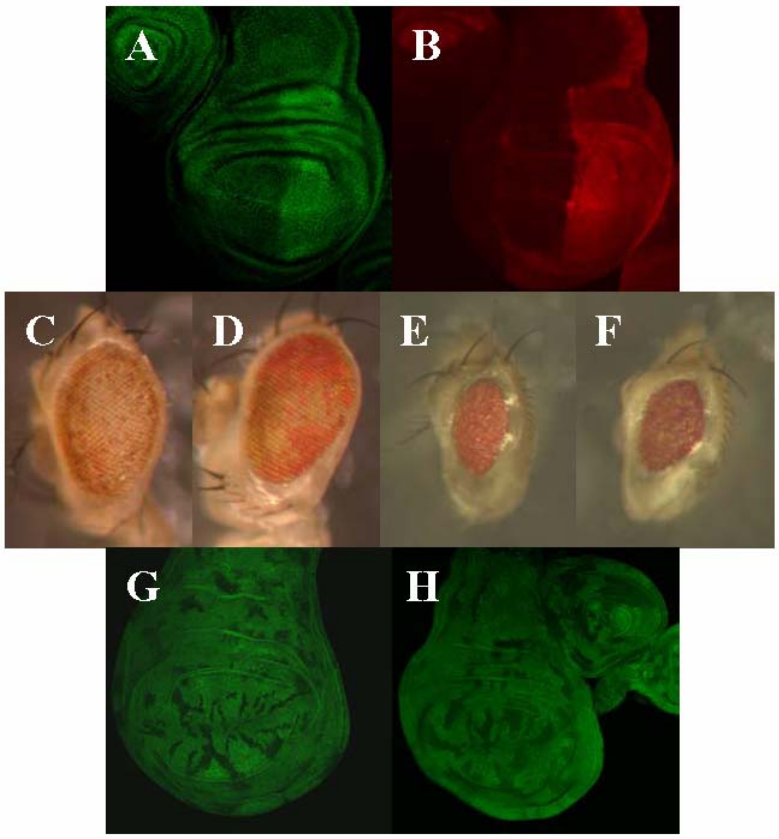

Figure 2.7: Absence of effect of reduction of DCP-1 by DN-DCP-1 on clonal size

Wandering 3rd instar larvae of the *en-Gal4/+; UAS-dn-dcp-1/+* genotype were dissected for wing discs and stained for Engrailed **(A)** and DCP-1 **(B)**. Eye phenotype of *GMR-ΔN-dcp-1/+* flies **(C)** is modestly suppressed by *GMR-dn-dcp-1/+; GMR-dn-dcp-1/GMR-ΔN-dcp-1* **(D)**. Eye ablation phenotype of *2XGMR-rpr CyO/Sco* **(E)** is very slightly suppressed by *2XGMR-rpr CyO/ScO; GMR-dn-dcp-1/+* **(F)**. Progeny of *flp122; tub>y+ GFP>Gal 4* virgin females X *yw* **(G)** or *UAS-dn-dcp-1* **(H)** were heat shocked for 1 hour at 37°C at 72 hrs AED, dissected for their wing discs at the wandering 3rd instar stage, and stained for GFP.

to the αDCP-1 antibody (Figure 2.8A-C) and one copy of *GMR-dcp-1-RNAi* dramatically rescues the eye phenotype of *GMR-ΔN-dcp-1* (compare Figure 2.8G and H), demonstrating a knockdown of *dcp-1* transcript by its RNAi construct. But again, flip-out clones overexpressing two copies of *dcp-1-RNAi* do not alter clonal size (compare Figure 2.8I-N). These experiments may indicate that there is no cell-autonomous requirement for *dcp-1* and therefore the small imaginal disc phenotype may not be attributable to the loss of *dcp-1*. However, that *dcp-1* has not been sufficiently knocked down in these experiments remains a possibility.

To determine whether *dcp-1* or *pita* is responsible for 3rd instar larval lethality, an EMS screen was undertaken to isolate point mutations allelic to *l(2)2132* (Figure 2.9). Out of approximately 7000 males screened, two candidates, C7.8 and HH10.3, could not complement each other or either of *l(2)2132* or *l(2)1862 in trans* (Table 2.1). Sequencing the genomic region encompassing *dcp-1* and *pita* revealed that the only alteration C7.8 contains is a H4167 point mutation in one of the C2H2 Zinc finger domains of Pita (Figure 2.10). Loss of *pita*, therefore, is responsible for 3rd instar larval death.

Flies transgenic for *UAS-pita* were generated for genetic rescue experiments in which transheterozygous combinations of *pita* mutants could be rescued to adulthood with either the *ey-Gal4* driver that is expressed in the eye or the *69B* driver that is expressed in imaginal discs (Table 2.2). That *l(2)2132/l(2)1862; 69B/UAS-pita* adult progeny could be recovered from a *l(2)2132/CyO; 69B* X *l(2)1862/CyO; UAS-pita/TM6B* cross in Mendelian

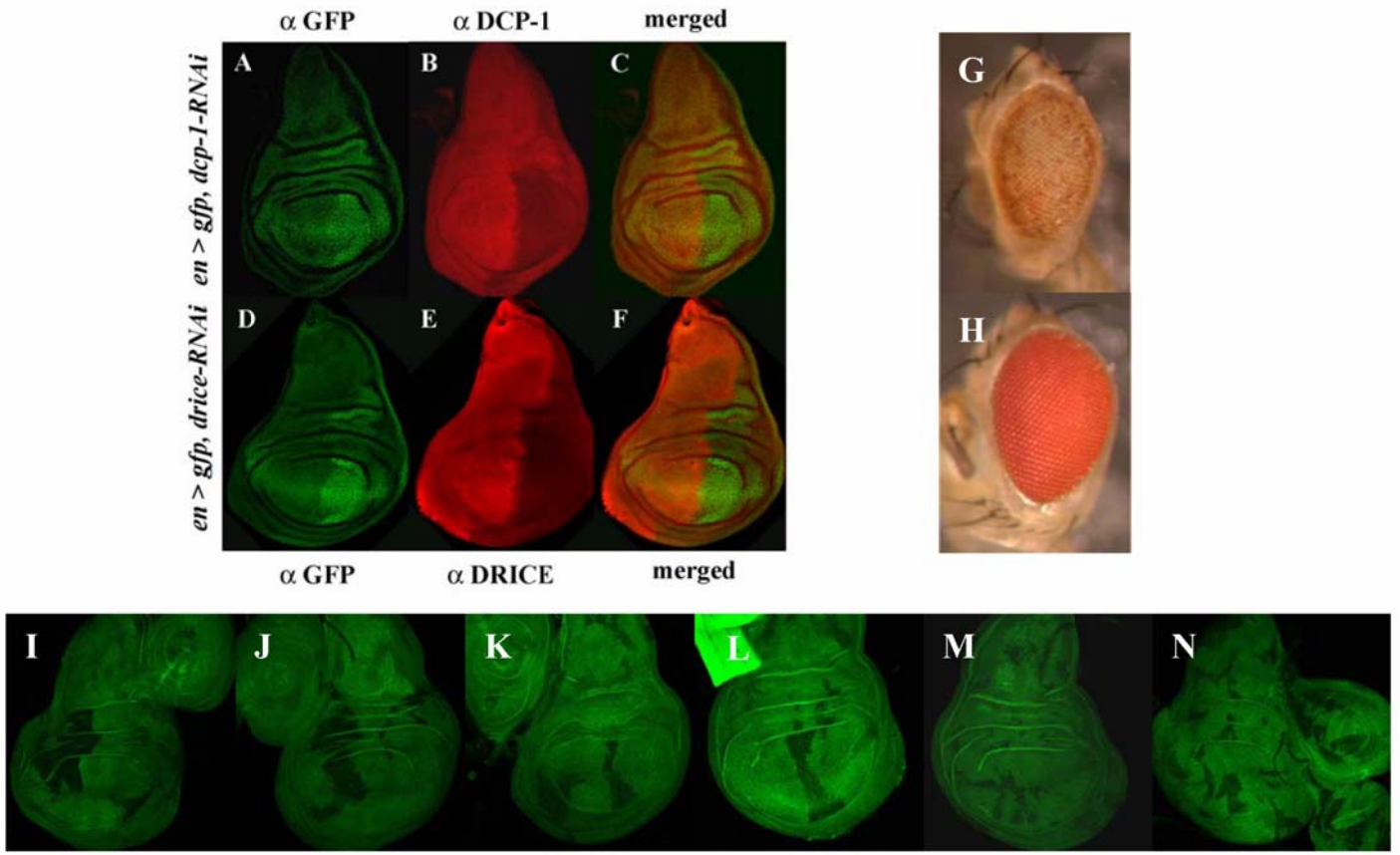

Figure 2.8: Absence of effect of reduction of DCP-1 by *dcp-1-RNAi* on clonal size
Wandering 3rd instar larvae of the *en-Gal4/+; UAS-dcp-1-RNAi/+* **(A, B, C)** or *en-Gal4/+; UAS-drice-RNAi/+* **(D, E, F)** genotypes were dissected for wing discs and stained for Engrailed **(A, D)** and DCP-1 **(B)** or DRICE **(E)**. Eye phenotype of *GMR-ΔN-dcp-1/+* flies **(G)** is completely suppressed by *GMR-ΔN-dcp-1/+; GMR-dcp-1-RNAi* **(H)**. Progeny of *flp^{122}; tub>y+ GFP>Gal 4* virgin females X *yw* **(I, K, M)** or *UAS-dcp-1-RNAi (2X)* **(J, L, N)** were heat shocked for 1 hour at 37°C at 24 hrs **(I, J)**, 48 hrs **(K, L)**, or 72 hrs **(M, N)** AED, dissected for their wing discs at the wandering 3rd instar stage, and stained for GFP.

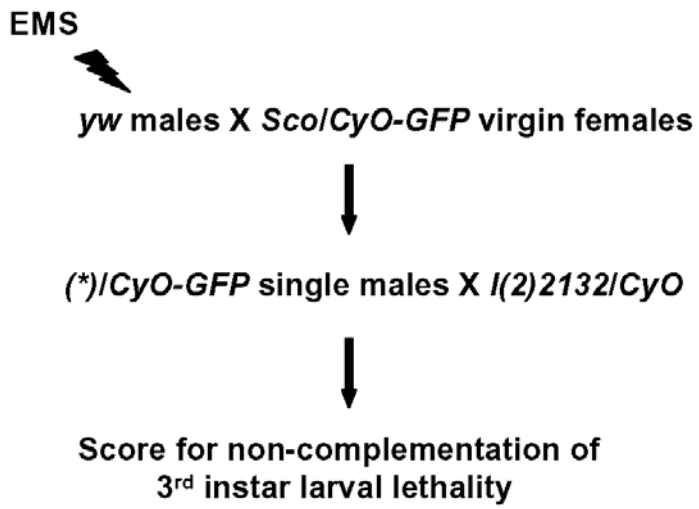

Figure 2.9: Scheme for isolation of additional *l(2)2132* alleles
EMS-mutagenized males will be crossed *en masse* to *Sco/CyO-GFP* females, and males from the progeny will be individually balanced and tested for lethality *in trans* with *l(2)2132*.

Table 2.1: Complementation of EMS mutants with P-alleles

	l(2)2132/CyO		*l(2)1862/CyO*		*HH10.3/CyO*	
	CyO	non CyO	CyO	non CyO	CyO	non CyO
C7.8/CyO	187	0	247	0	178	0
HH10.3/CyO	196	0	212	0		

EMS mutants *C7.8* and *HH10.3* were crossed to each other and to each ot the P-alleles, and progeny were scored for the presence of CyO.

N		51	61	71	81	91
1	MAAKLEVREA	MLTEKRVCRF	CLTEQKLASI	FEENPRVKTT	ANLPLQIMAI	TAIEVYAGDG
61	MPGHICLECR	LLFEHCYRFK	QMCKRAETLL	RQYPLTGNWP	SPLEKPRAPM	TMVASKKLLV
121	VPAKTAEPSE	TPKKLLNTMA	KSSSQVIIED	VQVLESAMVT	PRTVAGSSPV	PRRSHAYELK
181	VDNNQELSMD	DVQSMLEDMA	SELEKEFPDI	PQKASPVKPK	VLNKSSIRIL	NKGPAAPVEP
241	RLATPKVKRD	DSGNVAIVTE	VLDSDLPLDD	QDDPTKNAEK	VATDVFPCPD	CERSFPLQQL
301	LEIHRLNHTR	SRSFQCLLCE	KSFFSKYDLA	KHNFVHTGER	PFKCAICSKA	FTRKALLHRH
361	ERTHTDVPKF	ICVYCEKPFL	SRQEMEKHAE	RHQKKRPFQC	GVCTKSFAFK	QGLERHETVH
421	STNLPFPCQH	CERSFSTASK	LARHLVAHAG	KRAYPCKYCH	KSYMLSHHLS	RHLRTHTQTS
481	DASFVCSECK	VSYSNYNDLL	DHALIHATAS	LKCPMCRKQI	EDIDSVESHM	DQHKQSERHA
541	CEFCDHIFLT	QKCLQRHIED	DHVVEMEPYQ	NEFEDDGEGE	GGVDEKEEHL	DDFEDMDNVK
601	QEEFVTEYLE	DDALYEDHLD	DSDESFTPPP	PKQRKTNPPK	DAQQSVRQTR	SRDAQRITQK
661	TGKNEGKPHH	KLERNLKNRR	SAK			

Figure 2.10: Mutant C7.8 from genetic screen
C7.8 is a H416Y (highlighted in yellow) mutation in a C2H2 Zn finger domain of Pita. The zinc fingers are highlighted in blue.

Table 2.2: Rescue of EMS mutants with *UAS-pita*

	l(1862)/CyO; UAS-pita/TM6B		*C7.8/CyO; UAS-pita/TM6B*		*HH10.3/CyO; UAS-pita/TM6B*	
	A	B	A	B	A	B
l(2)2132/CyO; ey-G4			0.16	96	0.07	42
l(2)2132/CyO; 69B	0.18	108	0.21	126	0.19	114
l(2)1862/CyO; ey-G4			0.09	54		
l(2)1862/CyO; 69B			0.22	132	0.16	96

Column A = # non CyO and non TM6B/ total # progeny

Column B = (Column A/ theoretical fraction of progeny that can be rescued) X 100

frequency indicates that the loss of *dcp-1* does not play a role in causing larval lethality. Optimal rescue of *l(2)2132* animals could also be obtained using a *hs-Gal4* driver and subjecting the animals to a one-hour heat shock at four days AED (Table 2.3). Multiple rounds of heat shock, however, killed the animals harboring both *hs-G4* and *UAS-pita* transgenes. Rescued *l(2)2132; hs-Gal4/UAS-pita* appear grossly normal; males are fertile, but females are sterile.

The rescue of pita mutants to adulthood indicates that imaginal disc development has also proceeded normally. To test whether *pita* has a role in proliferation, flip-out clones were again used to overexpress *pita*, and no differences were observed (Figure 2.11). If the normal function of *pita* were to drive proliferation, then its overexpression is not sufficient to increase cell division.

2.3.3 Epistatic relationship of *dcp-1* and *drice* to *rpr*, *hid*, and *grim*

Evidence supporting that *rpr*, *hid*, and *grim* kill in a caspase-dependent manner came from showing that the death could be suppressed by *p35* (Grether *et al.*, 1995;Chen *et al.*, 1996;White *et al.*, 1996) and or enhanced by the loss of *diap-1* (Hay *et al.*, 1995;Wang *et al.*, 1999b;Goyal *et al.*, 2000), but direct genetic interaction linking the RHG genes and caspases was lacking. This could now be tested by using *UAS-dcp-1-RNAi* and *GMR-dcp-1-RNAi* transgenic flies as well as *UAS-drice-RNAi* flies (Arama and Steller, unpublished). Like dcp-1-RNAi, UAS-drice-RNAi flies were first confirmed for their ability to decrease Drice protein levels (Figure 2.8D-E). Progressively better rescue of the rough eye phenotype of *GMR-rpr* could be obtained by using more copies of *UAS-dcp-1-*

Table 2.3: Rescue of 3rd instar larval lethality with *UAS-pita*

Administration of HS at the following days AED						% of population that are
1	2	3	4	5	6	l(2)2132; hs-G4/UAS-CG3941
X						6
	X					0
		X				5
			X			25
X	X	X				0
	X	X	X	X		0
		X	X	X	X	0
						0

The progeny of *l(2)2132/CyO-GFP; hs-G4* X *l(2)2132/CyO-GFP; UAS-CG3941/TM6B* were heat shocked for 1 hour at 37°C at the times indicated by an "X". At least 100 flies emerged from the populations that were heat shocked once.
l(2)2132; hs-G4/UAS-CG3941 males are fertile, but females are sterile.

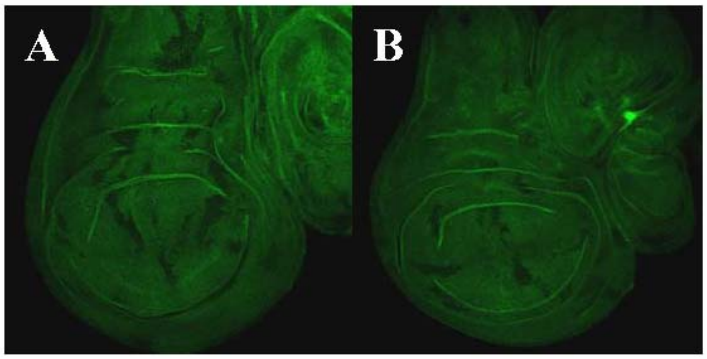

Figure 2.11: Absence of effect of overexpression of *pita* on clonal size
Progeny of *flp122; tub>y+ GFP>Gal 4* virgin females X *yw* **(A)** or *UAS-pita* **(B)** were heat shocked for 1 hour at 37°C at 72 hrs AED, dissected for their wing discs at the wandering 3rd instar stage, and stained for GFP.

RNAi (Figure 2.12C and D). Two copies of *UAS-drice-RNAi* rescues modestly (Figure 2.12E), but one copy each of *UAS-drice-RNAi* and UAS-*dcp-1-RNAi* rescues better (Figure 2.12F); two copies of each restores the eye to nearly wt (Figure 2.12G). Similar observations were obtained with *GMR-hid10* (Figure 2.13) and *GMR-grim* (Figure 2.14). These results show that *dcp-1* and *drice* act synergistically and are epistatic to *rpr*, *hid*, and *grim*.

2.4 Conclusion

When caspases were first identified in *Drosophila*, only *dcp-1* out of a total of seven contained mutations causing loss-of-function. Simultaneous disruption of *pita* at the same locus, however, confounded the phenotypic analysis of the P-alleles. These studies sought to clarify the contribution of the loss of each gene to the phenotypes and demonstrated that all the somatic phenotypes associated with *l(2)2132* and *l(2)1862* are attributed to the loss of *pita* rather than *dcp-1*. One *pita* mutant in a Zn finger domain was isolated from an EMS mutagenesis screen, and *UAS-pita* could rescue mutant larvae to adulthood. All this has been corroborated by Peterson *et al* (2003), who also isolated additional *pita* alleles in other Zn finger domains of the gene in addition to an amber mutation. Furthermore, they generated a *dcp-1* mutant that is homozygous viable with no obvious somatic phenotypes but displays a germline defect in cell death under starvation conditions.

Experiments with *UAS-dcp-1-RNAi* and *UAS-drice-RNAi* demonstrated *in vivo* the epistatic relationship of *dcp-1* and *drice* to *rpr*, *hid*, and *grim* as well as

the possibility of their having distinct functions. Other studies with RNAi and those with mutations generated in *dcp-1* and *drice* have elaborated on these observations (Muro *et al.*, 2006;Xu *et al.*, 2006;Leulier *et al.*, 2006).

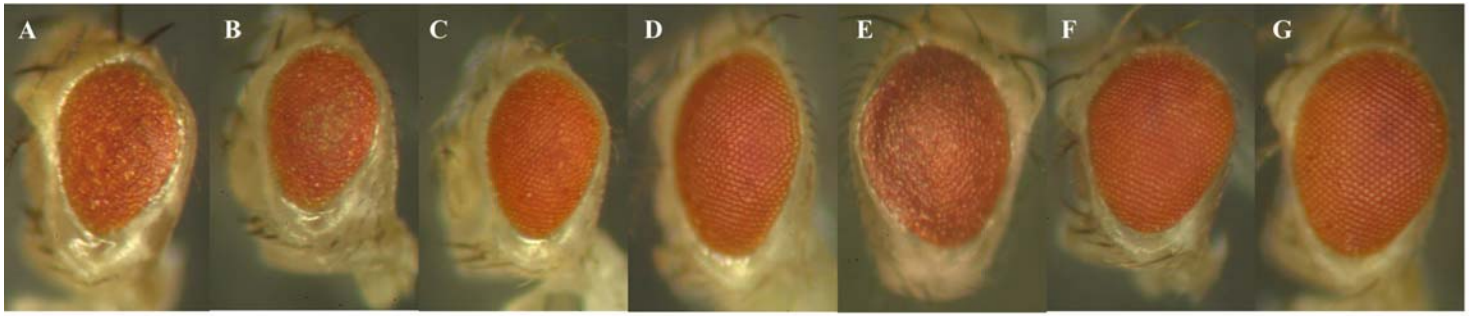

Figure 2.12: Suppression of *GMR-rpr* by reduction of effector caspases

A. *GMR-rpr; Sco/CyO; Sb/TM6B*
B. *GMR-rpr; GMR-G4/CyO; Sb/TM6B*
C. *GMR-rpr; GMR-G4/CyO; UAS-dcp-1-RNAi (2X)/TM6B*
D. *GMR-rpr; GMR-G4/CyO; UAS-dcp-1-RNAi (4X)*
E. *GMR-rpr; GMR-G4/CyO; UAS-drice-RNAi (2X)*
F. *GMR-rpr; GMR-G4/CyO; UAS-dcp-1-RNAi, UAS-drice-RNAi/TM6B*
G. *GMR-rpr; GMR-G4/CyO; UAS-dcp-1-RNAi (2X), UAS-drice-RNAi (2X)*

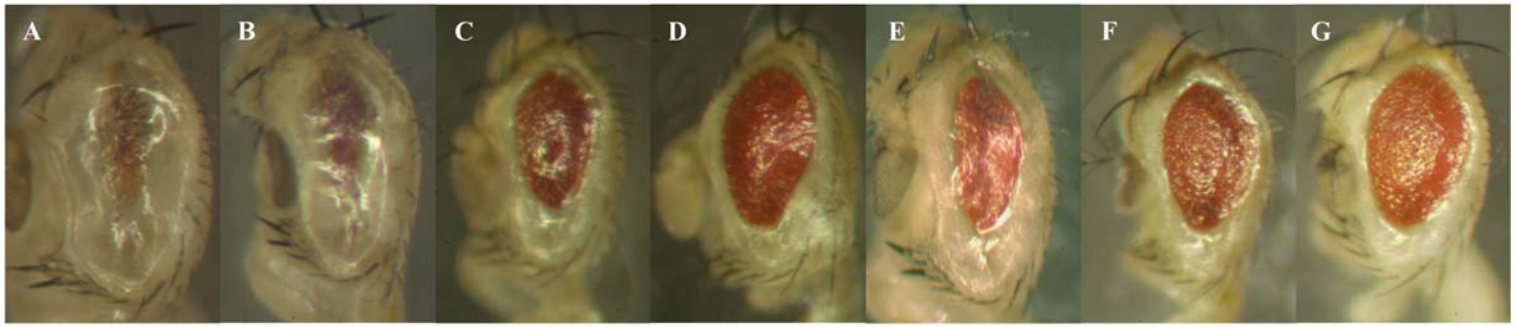

Figure 2.13: Suppression of *GMR-hid* by reduction of effector caspases

A. *GMR-hid10/CyO; Sb/TM6B*
B. *GMR-G4/Y; GMR-hid10/CyO; Sb/TM6B*
C. *GMR-G4/Y; GMR-hid10/CyO; UAS-dcp-1-RNAi (2X)/TM6B*
D. *GMR-G4/Y; GMR-hid10/CyO; UAS-dcp-1-RNAi (4X)*
E. *GMR-G4/Y; GMR-hid10/CyO; UAS-drice-RNAi (2X)*
F. *GMR-G4/Y; GMR-hid10/CyO; UAS-dcp-1-RNAi, UAS-drice-RNAi/TM6B*
G. *GMR-G4/Y; GMR-hid10/CyO; UAS-dcp-1-RNAi(2X), UAS-drice-RNAi (2X)*

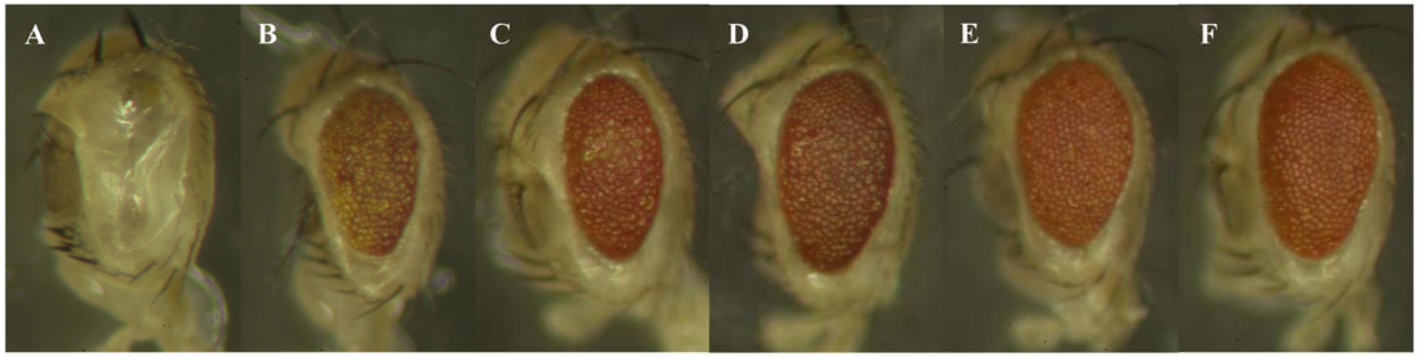

Figure 2.14: Suppression of *GMR-grim* by reduction of effector caspases

A. *GMR-G4/Y; GMR-grim; Sb/TM6B*
B. *GMR-G4/Y; GMR-grim; UAS-dcp-1-RNAi (2X)/TM6B*
C. *GMR-G4/Y; GMR-grim; UAS-dcp-1-RNAi (4x)*
D. *GMR-G4/Y; GMR-grim; UAS-drice-RNAi (2X)*
E. *GMR-G4/Y; GMR-grim; UAS-dcp-1-RNAi, UAS-drice-RNAi/TM6B*
F. *GMR-G4/Y; GMR-grim; UAS-dcp-1-RNAi(2X), UAS-drice-RNAi (2X)*

3 Promoter analysis of *reaper* to identify a factor that mediates death from improper differentiation

3.1 Introduction

Deploying the apoptotic machinery to remove cells during abnormal development plays as important a role in the welfare of an organism as the culling of excess, unnecessary cells produced in normal development. Indeed, well before cell death had become a field of intense investigation, this phenomenon had already been documented in *Drosophila* mutants (Fristrom, 1968;Fristrom, 1969). Since then, many instances of cell death resulting from aberrant development have been reported. Mutations in the maternal gap gene *oskar* (*osk*), for example, result in, among other defects, a failure of the embryonic abdominal region to undergo segmentation and its eventual death (Lehmann and Nusslein-Volhard, 1986). Similar connections have been made between cell death and patterning defects of segment polarity genes (Perrimon and Mahowald, 1987;Magrassi and Lawrence, 1988;Klingensmith *et al.*, 1989). The onset of studying the process of cell death led to the confirmation that these types of developmental mutants as well as others are, indeed, apoptotic in nature (Abrams *et al.*, 1993;White *et al.*, 1994;Nordstrom *et al.*, 1996;Pazdera *et al.*, 1998;Hughes and Krause, 2001). Continued interest has spurred numerous reports of apoptosis resulting from many other mutations. The disruption of *Drosophila hand* leading to the death of cardiac cells (Han *et al.*, 2006) and loss of *polycomb group* genes leading to death of neuroblasts (Bello *et al.*, 2007) are

more recent examples. However, how a developmental mishap engages the cell death machinery has yet to be discovered. A cell that receives insufficient or conflicting signals as to how it should proceed along a developmental path gets confused and frustrated. How this is detected intracellularly or extracellulary and how the detection leads to the elimination of that cell constitute an extremely complicated and intriguing riddle to solve (Figure 3.1). Steller and colleagues have hypothesized that various pro-apoptotic signals may be integrated at the *rpr* promoter (Steller and Grether, 1994;Steller *et al.*, 1994;Steller, 1995;McCall and Steller, 1997). This has been supported by recent studies demonstrating the transcriptional activation of *rpr* during developmental PCD (Robinow *et al.*, 1997;Jiang *et al.*, 2000;Lohmann *et al.*, 2002;Chandrasekaran *et al.*, 2003;Miguel-Aliaga *et al.*, 2004;Manjon *et al.*, 2007) as well as in response to genotoxic stress (Brodsky *et al.*, 2000). More importantly, elements responsible for *rpr* transcriptional upregulation in the developmental mutants *crb*, *srp3*, and *ph* have been mapped to a 4 kb region that does not respond to genotoxic stress (Lamblin and Steller, unpublished.) Further analysis of this region and the identification of factors that bind to it will shed light on the link between developmental frustration and death.

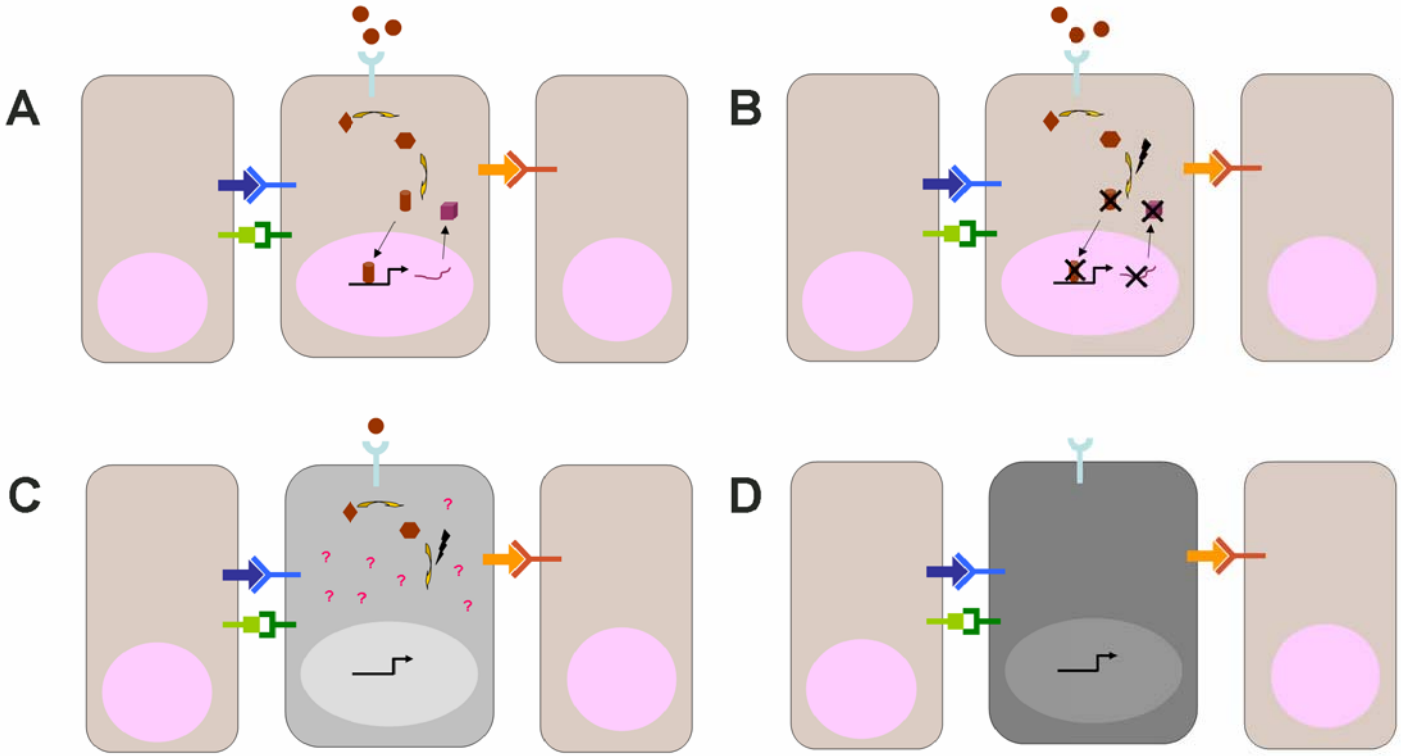

Figure 3.1: A schematic of death by frustration. The proper differentiation of a cell requires input from a combination of many pathways **(A)**. When a mutation causing a lesion in an essential pathway occurs **(B)**, a cell becomes confused and frustrated in its developmental state **(C)** and often undergoes apoptosis as a result **(D)**.

3.2 Materials and Methods

3.2.1 *Drosophila* stocks:

Fly stocks were maintained on conventional cornmeal-agar-molasses medium at 25°C. The following fly lines were used in these studies:

10 kb rpr-LacZ	*crb/TM6B*
4 kb rpr-LacZ	*srp3/TM6B*
4s1-4s7 (Lohmann et al, 2002)	dl^{1}*/CyO* (K. Anderson)
at1-at7 LacZ reporter lines	dl^{5}*/CyO* (K. Anderson)
at5a, at5b, at5c LacZ reporter lines	*bcdE1/TM3* (K. Anderson)
at5i and at5ii LacZ reporter lines	*bcdE3/TM3* (K. Anderson)
UAS-p8	*ph504/FM7c*

3.2.2 Generation of transgenic flies

rpr promoter regions were cloned by PCR from yw genomic DNA with primers designed with 5' SpeI and 3' XhoI overhangs and inserted into a pH-Pelican vector (Barolo et al, 2000). 4s1, 4s3, and 4s7 were recloned according to Lohmann et al (2002) and reinjected to generate additional insertions. The sequences of the other truncated promoter regions are as follows:

at1:

TACTAGTCCGAGCACTACGGATCACTTGGCAATTGTCTTTGTTTCTTTGCCC
CGTCTGGGCTTTCTAAATGGGAAATCAAATAAAACGAAATATACATTTCTGA
CAAGATCGAAAGGGAGACCAGAAACCAGACCACCAGTTGGGATCATAAAAA
ATTAACACAAATTAACGAAACGAAGCCGCAGCCGAAAAAGATACCCAAACAC
CAAAGTGTGAGAAATTGAGAGTTTTCGAGATTGAAAACAGTGCGGGAGCAA

CAAAGAGATGACAATATTCTGTTCGAGAACGTTGCGCAATTCTTGGAATATT

ATTAAGCATTGGCTGGGCTCGAGA

at2

TACTAGTATTATTAAGCATTGGCTGGGGGCGGGGGGGAGCAACCTGACTGAG

AGGAAACTTTAAGAATGAGTGATGATTTCGGCCCAATTATTTTATTACTGCAT

ATAAGGATAGAGGAAGGAGGTTCCAATCCTGCAACTTTACTCCAACGGTTTT

CGTTTAATATTTAAATAATGGGTAATGCAGGGAATATATAGGAAAATTTAAAA

TATAGGTCTAAAATAAATTGTAATGTAAAAGCTATCAATTTATCCACTGAATAT

AACATAAATGATCCAATAGTAGAATTACAAATGAAATGGAACGAGAGAAAGC

TGAAACCTCGAGA

at3

TACTAGTGTAATGCAGGGAATATATAGGAAAATTTAAAATATAGGTCTAAAAT

AAATTGTAATGTAAAAGCTATCAATTTATCCACTGAATATAACATAAATGATC

CAATAGTAGAATTACAAATGAAATGGAACGAGAGAAAGCTGAAACCTCGAGA

at4

TACTAGTCTAGTCCGAGCACTACGGATCACTTGGCAATTGTCTTTGTTTCTTT

GCCCCGTCTGGGCTTTCTAAATGGGAAATCAAATAAAACGAAATATACATTT

CTGACAAGATCGAAAGGGAGACCAGAAACCAGACCACCAGTTGGGATCATA

AAAAATTAACACAAATTAACGAAACGAAGCCGCAGCCGAAAAAGATACCCAA

ACACCAAAGTGTGAGAAATTGAGAGTTTTCGAGATTGAAAACAGTGCGGGA

GCAACAAAGAGATGACAATATTCTGTTCGAGAACGTTGCGCAATTCTTGGAA

TATTATTAAGCATTGGCTGGGGGCGGGGGGGAGCAACCTGACTGAGAGGAA

ACTTTAAGAATGAGTGATGATTTCGGCCCAATTATTTTATTACTGCATATAAG

GATAGAGGAAGGAGGTTCCAATCCTGCAACTTTACTCCAACGGTTTTCGTTT

AATATTTAAATAATGGGTAATGCAGGGAATATATAGGAAAACTCGAGA

at5:

TACTAGTCCGAGCACTACGGATCACTTGGCAATTGTCTTTGTTTCTTTGCCC

CGTCTGGGCTTTCTAAATGGGAAATCAAATAAAACGAAATATACATTTCTGA

CAAGATCGAAAGGGAGACCAGAAACCAGACCACCAGTTGGGATCATAAAAA

ATTAACACAAATTAACGAAACGAAGCCCCTCGAGA

at6

TACTAGTCAAATTAACGAAACGAAGCCGCAGCCGAAAAAGATACCCAAACA

CCAAAGTGTGAGAAATTGAGAGTTTTCGAGATTGAAAACAGTGCGGGAGCA

ACAAAGAGATGACAATATTCTGTTCGAGAACGTTGCGCAATTCTTGGAATAT

TATTAAGCATTGGCTGGGCTCGAGA

at7

TACTAGTATTATTAAGCATTGGCTGGGGGCGGGGGGAGCAACCTGACTGAG

AGGAAACTTTAAGAATGAGTGATGATTTCGGCCCAATTATTTTATTACTGCAT

ATAAGGATAGAGGAAGGAGGTTCCAATCCTGCAACTTTACTCCAACGGTTTT

CGTTTAATATTTAAATAATGGGTAATGCAGGGAATATATCTCGAGA

at5a

CCGAGCACTACGGATCACTTGGCAATTGTCTTTGTTTCTTTGCCCCGTCTGG

GCTTTCTAAATGGGAAATCAAATAAAACGAAATATACATTTCTGACAAGATCG

AAAGGGAG

at5b

TTGCCCCGTCTGGGCTTTCTAAATGGGAAATCAAATAAAACGAAATATACAT

TTCTGACAAGATCGAAAGGGAGACCAGAAACCAGACCACCAGTTGGGATCA

at5c

CGAAATATACATTTCTGACAAGATCGAAAGGGAGACCAGAAACCAGACCAC

CAGTTGGGATCATAAAAAATTAACACAAATTAACGAAACGAAGCC

at5i

CTACGGATCACTTGGCAATTGTCTTTGTTTCTTTGC

at5ii

AAATGGGAAATCAAATAAAACGAAATATACAT

The coding sequence of p8 was obtained by PCR from genomic DNA and cloned into pUAST. All constructs were injected into *yw* embryos following standard protocols.

3.2.3 Antibody staining of embryos

Embryos were dechorionated for 3 minutes in 50% bleach, collected into a cell strainer, and rinsed thoroughly with water. Fixation occurred by a 20-minute continuous agitation in a solution containing a 1:1 ratio of heptane and PBS with 4% paraformaldehyde and 0.1% Triton X-100. Following the removal of the fixative phase and the addition of an equal volume of methanol, the embryos were then vortexed for 30 seconds for devitellinization. Non-devitellinized embryos were removed, and the devitellinized embryos were rinsed 3 times in methanol and 3 times in ethanol and may then be stored at -20°C. Rehydration required a series of 5-minute washes in $PBT_{0.1\%}$ with 75%, 50%, and 25% ethanol. The embryos were then washed 3 X 10 minutes in $PBT_{0.1\%}$ and might

be blocked by rocking for 1 hour at room temperature in $PBT_{0.1\%}$ with 5% normal goat serum and 1 mg/mL BSA (bovine serum albumin). Embryos were rocked in primary antibody diluted in $PBT_{0.1\%}$ at 4°C overnight, and afterwards washed 3 X 10 minutes in $PBT_{0.1\%}$. They were then rocked in secondary antibody for two hours at room temperature and washed again for 3 X 10 minutes in $PBT_{0.1\%}$. The $PBT_{0.1\%}$ was removed and 80% glycerol was added. The embryos were stored at 4°C until they sank and were then mounted onto slides.

3.2.4 Antibody staining of imaginal discs

Done as described in Section 2.2.3.

3.2.5 X-gal staining of embryos

Embryos were dechorionated for 3 minutes in 50% bleach, collected into a cell strainer, and rinsed thoroughly with water. Fixation occurred by a 20-minute continuous agitation in heptane previously saturated with an equal volume of a solution containing 17.8% formaldehyde in PBS. The heptane was removed and the embryos were rinsed twice in fresh heptane. The embryos were devitellinized by vortexing for 30 seconds in a solution containing equal volumes of heptane and methanol. All liquid and non-devitellinized embryos were removed as quickly as possible, and the devitellinized embryos were subjected to two rapid rinses in methanol followed by two rinses in 75% ethanol. The embryos were then rinsed three times in $PBT_{0.5\%}$ and washed 8 X 5 minutes in $PBT_{0.5\%}$ to remove all traces of ethanol. X-gal staining solution containing 10mM phosphate buffer, pH7.4, 150 mM NaCl, 1mM $MgCl_2$, 3mM $K_4FeII(CN)_6 \bullet 3H_2O$, 3mM $K_3FeIII(CN)_6$, and 0.3% Triton X-100 is heated to 65°C, and X-gal was

added at a final concentration of 2mg/mL. The embryos were rocked in this solution at 37°C until a signal was achieved. They were then washed once in $PBT_{0.5\%}$, and 80% glycerol was added. The embryos were stored at 4°C until they sink and were then mounted.

3.2.6 TUNEL staining of embryos

The embryos were dechorionated and devitellinized as for antibody staining. Once they were rehydrated in PBS, they were treated with 10 ug/mL proteinase K in PBS with rocking for 2 minutes, after which they were immediately washed 2 X 5 minutes in $PTW_{0.1\%}$. The embryos were then subjected to a second round of fixation in 4% paraformaldehyde in PBS for 20 minutes at room temperature and were washed afterwards 5 X 5minutes in PBS. A mixture of 50 uL enzyme solution and 450 uL label solution from the In Situ Cell Death Detection Kit, TMR red from Roche (Cat. #12-156-792-910) was incubated with the embryos at 37°C for two hours. The embryos were washed 3 X 10 minutes in PBS. 80% glycerol was added, and the embryos were stored at 4°C until they sank and were then mounted.

3.2.7 RNA *in situ* hybridization of embryos

Embryos were dechorionated for 3 minutes in 50% bleach, collected into a cell strainer, and rinsed thoroughly with water. Fixation occurred by a 20-minute continuous agitation in a solution containing a 1:1 ratio of heptane and PBS with 4% paraformaldehyde and 2mM $MgSO_4$ and 2mM EGTA. Following the removal of the fixative phase and the addition of an equal volume of methanol, the embryos were then vortexed for 30 seconds for devitellinization. The non-

devitellinized embryos were removed with the fixative, and the devitellinized embryos were rinsed twice in methanol and were then rehydrated by washing for 5 minutes in the following ratios of methanol: 4% paraformaldehyde in PBS solutions: 3:1, 1:1, 1:3. The embryos were fixed again by rocking at room temperature in 4% paraformaldehyde in PBS and washed for 2 X 5 minutes in PBS. They were then dehydrated by 5-minute washes in 25%, 50%, and 75% ethanol, and stored at -20°C until use. Rehydration occurred through a reverse series of washes in 75%, 50%, and 25% ethanol. After the embryos are washed 3 X 5 minutes in $PTW_{0.1\%}$ (PBS + 0.1% Tween-20), they were treated with 50 ug/mL proteinase K in $PTW_{0.1\%}$ for 8 minutes with rocking. The proteinase K is removed and the embryos were washed first with 2 mg/mL glycine in $PTW_{0.1\%}$ for 2 minutes and then 2 X 5 minutes in $PTW_{0.1\%}$. The embryos were fixed again in 4% paraformaldehyde in PBS with rocking for 20 minutes and washed 5 X 5 minutes in $PTW_{0.1\%}$. Embryos were then equilibrated in hybridization buffer (50% formamide, 5X SSC, 100 ug/mL yeast tRNA, 50 ug/mL heparin, 100 ug/mL sonicated salmon sperm DNA, and 0.1% Tween 20) by incubating them first in a 1:1 solution of $PTW_{0.1\%}$: hybridization buffer for 10 minutes at room temperature and then in hybridization buffer alone for another 10 minutes. Prehybridization of the embryos occurred in fresh hybridization buffer at 60°C for 1 hour. The probe, made with the Roche DIG RNA Labeling Kit (SP6/T7) (cat# 11 175 025 910) and diluted in hybridization buffer, was denatured at 80°C for 5 minutes, chilled on wet ice, and applied to embryos. Hybridization was allowed to occur overnight at 60°C. 500 uL of prewarmed hybridization buffer was used to rinse the embryos,

followed by a 30-minute wash in fresh buffer. A 1:1 ratio of hybridization buffer : TBST was then used for another 30-minute wash in 60°C. 3 X 5-minute washes in TBST (137 mM NaCl; 2.7 mM KCl; 2.5 mM Tris-HCl, pH 7.4; 1.1% Tween-20) and a single 5-minute wash in TAE took place at room temperature. Probe not hybridized to RNA was electro-eluted from the embryos by placing them into large wells in an agarose gel and electrophoresing for 30 minutes at 100V. The embryos were then washed for 5 minutes in TBST and blocked for 1 hour at room temperature in TBST with 5% HINGS (heat-inactivated normal goat serum) and 1 mg/mL BSA. The embryos were then incubated overnight with anti-DIG-AP antibody diluted to 1:2500 in block solution at 4°C. The embryos were rinsed 3 times and washed 3 X 30 minutes with rocking at room temperature in TBST. Finally, they were washed 2 X 10 minutes in NTMT (100 mM NaCl; 50 mM $MgCl_2$; 100 mM Tris, pH 9.5; 0.1% Tween-20; 1 mM Levamisole). They were incubated with the BCIP (5-Bromo-4-Chloro-3'-Indolyphosphate p-Toluidine Salt) /NBT (Nitro-Blue Tetrazolium Chloride) (Sigma, cat # B-1911) until signal appears, after which point they were rinse twice with TBST. 80% glycerol was added, and the embryos are stored at 4°C until they sank and were then mounted.

3.2.8 Yeast 1-hybrid assay

Yeast one-hybrid was conducted using the BD Clontech One-Hybrid Matchmaker Library Construction & Screening Kit (cat #630304). *rpr* promoter sequences *at5* was cloned into the pHIS2 vector as a single or triple copy. The coding sequence of p8 was cloned into the pGADT7-Rec2 vector. Total RNA was isolated from embryos with Trizol reagent from Invitrogen (cat. #15596-018),

according to the manufacturer's protocol. PolyA+ RNA was isoloated from total RNA using PolyATtract mRNA Isolation System (Promega, Z5300), and 1 ug was used to generate the cDNA library.

3.2.9 Generation of αP8 antibody

The coding sequence of *p8*, omitting its ATG, was obtained by PCR of genomic DNA using 5'AATGGATCCTCCGAGGCCCACTTCGATGA3' and 5'AATGCGGCCGCTCAGTTCTTGCAGGCGGCGG3' with BamHI and NotI overhangs, respectively, and cloned into pET28a(+) using those restriction sites. P8 protein was expressed in BL21 Star (DE3) pLysS competent cells from Invitrogen (cat #C6020-03) by growing the cells to OD_{600} of 0.8 at room temperature and inducing with 1mM IPTG for 18 hours at room temperature. Cells were harvested into a pellet and frozen at -80°C. The pellet was resuspended in 10 volumes of lysis buffer containing 10 mM phosphate buffer, pH 7.4, 0.5 M NaCl, and 20 mM imidazole, and homogenized in a dounce. Benzonase nuclease (Novagen, cat #70664-3) was added at 1 uL/mL lysis buffer and incubated with rocking at room temperature for 15 minutes. The suspension was sonicated for a total of 9 cycles of 10 seconds with 30-second rests in between at 4°C, and then centrifuged at 16000g for 20 minutes at 4°C. The supernatant was filtered with a 0.45 uM filter, and then applied with a syringe through a His Trap FF crude nickel column (GE Healthcare, cat #11-00048-58) by hand. The column was washed sequentially with 10 mM phosphate buffer, pH 7.4 and 0.5 M NaCl with the following concentrations of imidazole: 175 mM, 300 mM, 500 mM. Fractions containing greater than 95% purity of P8 protein were

pooled and electrophoresed through a preparatory gel. The band containing P8 was excised and sent Cocalico for antibody production in 2 guinea pigs.

3.2.10Affinity purification of αP8 antibody

The AminoLink Plus Immobilization Kit (Pierce cat #20394) was used for the column affinity purification of the antisera. P8 was expressed and purified as described in section 3.2.9. His Trap FF crude nickel columns (GE Healthcare, cat #11-00048-58) were used for the purification process. After the supernatant was passed through the column, it was washed in 10 mM phosphate buffer, pH 7.4, 0.5 M NaCl, 100 mM imidazole and eluted in 10 mM phosphate buffer, pH 7.4, 0.5 M NaCl, 0.5 M imidazole. 9 mg of the protein in a total volume of 3 mL was dialyzed first against 10 mM phosphate buffer, pH 7.4; 0.5 M Na Cl, 4 M urea and then against the same buffer but with 2 M urea. After the column was equilibrated with 10 mM phosphate buffer, pH 7.4; 0.5 M Na Cl, 2 M urea, the protein and $NaCNBH_3$ at 50 mM final concentration was added to the column and rocked for 6 hours at room temperature. The column, drained of its contents, was washed first in 10 mM phosphate buffer, pH 7.4 and 0.5 M Na Cl with decreasing amounts of urea: 2 M, 1 M, 0.5 M, 0 M. After passing 4 mL of Quenching Buffer through the column, the column was rocked in 2 mL Quenching Buffer with 40 uL $NaCNBH_3$ for 30 minutes at room temperature. The column was washed with 30 mL 1M NaCl with 0.05% NaN_3, and then with 5 mL of PBS with 0.05% NaN_3, in which the matrix is stored until use. When ready to use, the column was washed in 10 mL PBS. The antiserum was diluted 10-fold into PBS and applied to the column. Every 1.5 mL antisera that enters the gel

bed was allowed to incubate there for 15-30 minutes before it was drained. The column was washed with 12 mL PBS, followed by 12 mL 1 M NaCl, and again with 6 mL PBS. The antibody was eluted with 0.2 M glycine•HCl, pH 2.5 in 1 mL fractions that were neutralized in either 1 M sodium phosphate or 1 M Tris, pH 9.

3.3 Identification of *reaper* cis-regulatory sequences responding to defects in cell differentiation

3.3.1 Background

Previous characterization of *rpr* transcript patterns in the embryo revealed that its expression begins at stage 5, preceding the onset of apoptosis at stage 11 as a normal part of embryonic development, as assayed by acridine orange and TUNEL staining (Abrams *et al.*, 1993;White *et al.*, 1994). Embryos transgenic for a *10kb rpr-LacZ* reporter that contains approximately 10 kb of the *rpr* promoter region exhibit a LacZ expression pattern that comprises a large subset, although not all, of the expression pattern of endogenous *rpr* transcript, and can therefore be used to assess the nature of its transcriptional state (Lamblin and Steller, unpublished). Robust upregulation of *rpr* RNA can be elicited by subjecting embryos to genotoxic stress by exposure to either X or UV irradiation or by crossing the embryos to mutations that cause differentiation and developmental defects (Lamblin and Steller, unpublished). Truncations of the *10 kb rpr-LacZ* reporter into smaller reporter fragments of *4 kb rpr-LacZ* and *1.3 kb rpr-LacZ* revealed that genotoxic and developmental stress transcriptionally activate *rpr* at different cis-regulatory regions. Specifically, whereas the *1.3 kb*

rpr-LacZ reporter showed no upregulation in response to either class of stress induction, the *4 kb rpr-LacZ* reporter did respond in the background of developmental mutants *crb*, *srp*, and *ph*, but not to X or UV irradiation (Lamblin and Steller, unpublished). Hence, signals in response to various stresses are integrated at different regions of the *rpr* promoter.

The identification of promoter sequences responsive to developmental aberrations requires a finer inspection of the 4 kb region and the continued use of *crb* and *srp3* as paradigms. *crb* is necessary to maintain apical-basal polarity and epithelial cell differentiation; in *crb* mutants, epithelial cells undergo apoptosis (Tepass *et al.*, 1990;Abrams *et al.*, 1993;Tepass and Knust, 1993). *srp* is necessary for gut and hematopoietic development, and mutants exhibit upregulated *rpr* RNA in the fore, mid, and hindgut areas (Reuter, 1994;Frank and Rushlow, 1996). First, the *10 kb* and *4 kb rpr-LacZ* lines were shown to be reproducibly activated in *crb* and *srp3* backgrounds both by β-gal antibody staining and by X-gal activity assay (Figure 3.2). The *10 kb rpr-LacZ* alone exhibits a narrow segmental pattern as was previously documented (Figure 3.2A and A'; Lamblin and Steller, unpublished), that is disrupted and becomes grossly elevated in a *crb* background and is additionally upregulated in the gut region in a *srp3* background (Figure 3.2B, B', C, C'; Lamblin and Steller unpublished). Staining of the *4kb rpr-LacZ* transgenic embryos alone show almost no background (Figure 3.2D and D'), and its upregulation in *crb* and *srp3* backgrounds is less intense, though highly reproducible (Figure 3.2E, E', F, F').

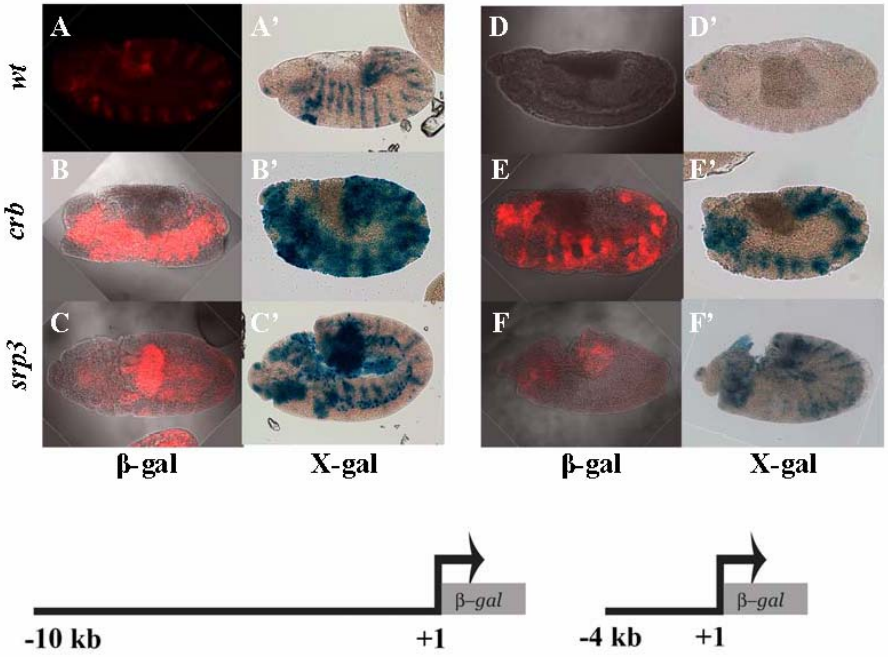

Figure 3.2: Upregulation of *rpr-LacZ* lines in *crb* and *srp3* mutants
(A and A') *10 kb rpr-LacZ/CyO* **(D and D')** *4 kb rpr-LacZ/CyO*
(B and B') *10 kb rpr-LacZ/CyO; crb* **(E and E')** *4 kb rpr-LacZ/CyO; crb*
(C and C') *10 kb rpr-Lac Z/CyO; srp* **(F and F')** *4 kb rpr-LacZ/CyO; srp3*
Embryos were stained either for α β-gal antibody **(A-F)** or with X-gal **(A'-F')**.

3.3.2 Identification of responsive elements in ~600bp region

Shorter *rpr-LacZ* reporter lines, named *4s1* to *4s7*, were derived from the 4 kb region by Lohmann *et al* (2002). Additional transgenic lines were generated for the 4s1, 4s6, and 4s7 constructs, and multiple independent insertions from each 4s construct were used to investigate the transcriptional activation of *rpr* in response to developmental mutations (Table 3.1; Figure 3.3). The *4s7* line exhibits no endogenous staining on its own (Figure 3.3A and A'), and only a low level in *crb* (Figure 3.3B and B') but none in *srp3* embryos (Figure 3.3C and C'). The *4s6* line alone shows staining restricted to the anterior region only in late-stage embryos (Figure 3.3D and D'), and like *4s7*, modest staining in a *crb* background but none in *srp3* (Figure 3.3E, E', F, and F'). Staining of *4s5* reveals an endogenous segmental pattern as well as staining in the head region (Figure 3.3G and G'); the positive staining in *crb* and *srp3* backgrounds, is therefore mostly attributed to its endogenous pattern rather than any upregulation (Figure 3.3H, H', I, and I'). Likewise, *4s4* shows significant endogenous staining in the amnioserosa and head regions (Figure 3.3J and J') that are also present in the *crb* and *srp3* backgrounds; the X-gal activity stain shows a small amount of additional staining in the *crb* background not revealed in the antibody staining (Figure 3.3 K and K'), but no additional staining is seen in the *srp3* background (Figure 3.3L and L'). *4s3* shows neither endogenous staining nor an upregulation in either mutant background (Figure 3.3M-O and M'-O'). *4s2* shows some scattered staining in the head and gut regions (Figure 3.3P and P'), but the antibody staining of embryos in a *crb* background reveals a significant

Table 3.1: Independent transgenic lines from 4s constructs.

Transgene	# Lines Obtained	# Lines Tested	# Lines w/ Consistent Staining
4s1	7	4	3
4s2	1	1	1
4s3	2	2	2
4s4	2	2	2
4s5	2	2	2
4s6	4	3	3
4s7	4	3	3

Fig 3.3: Analysis of ~600 bp promoter segments from a 4 kb region
Overlapping reporter constructs containing truncated segments from a 4 kb promoter region 5' to the *rpr* transcriptional start site are named 4s1-4s7. Embryos were stained with either an α β-gal antibody **(A-U)** or for X-gal activity **(A'-U')**. Staining of embryos with reporter constructs by themselves **(A, A', D, D', G, G', J, J', M, M', P, P', S, S')** show endogenous levels of expression. **(B, B', E, E', H, H', K, K', N, N', Q, Q', T, T')** show embryos transgenic for the reporter constructs in a *crb* background, and **(C, C', F, F', I, I', L, L', O, O',R, R',U, U')** show embryos transgenic for reporter constructs in a *srp3* background.

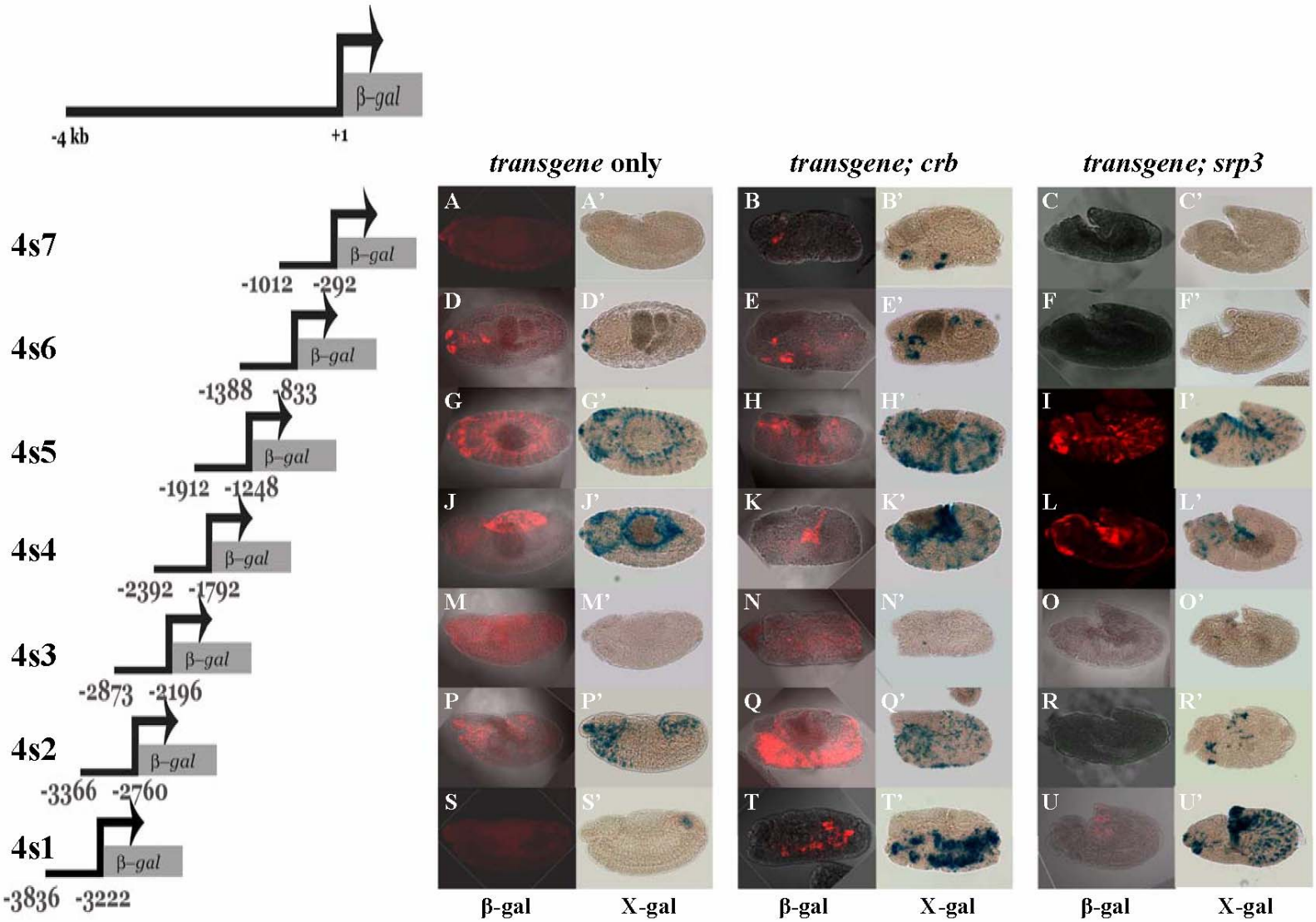
β–gal
-4 kb
+1
4s7
-1012 -292
4s6
-1388 -833
4s5
-1912 -1248
4s4
-2392 -1792
4s3
-2873 -2196
4s2
-3366 -2760
4s1
-3836 -3222
transgene only
transgene; crb
transgene; srp3
β-gal
X-gal

upregulation not reproduced by the X-gal staining (Figure 3.3Q and Q'), whereas none is seen in the *srp3* background (Figure 3.3R and R'). Finally, *4s1*, with a very modest hindgut endogenous staining (Figure 3.3S and S'), shows impressive upregulation in both *crb* and *srp3* backgrounds (Figure 3.3T, T', U, and U'), and hence was chosen for further promoter analysis.

3.3.3 Identification of response elements in *at5*, a 175bp *reaper* promoter fragment

Flies transgenic for reporters constructed with shorter promoter regions derived from *4s1* were made (Table 3.2) and embryos were, as before, evaluated for β-gal expression patterns and X-gal activity in the *crb* and *srp3* backgrounds. *at4*, the fragment containing 75% of the sequences of *4s1* distal to the *rpr* transcription start site, shows a low level of staining in the hindgut (Figure 3.4A and A'), and scored positively in β-gal upregulation in both *crb* and *srp3* backgrounds (Figure 3.4B, B', C, and C'). *at1* and *at2* split the 4s1 fragment in half; the former, with modest endogenous gut staining (Figure 3.4D and D'), exhibited a significant upregulation in *crb* and *srp3* mutant backgrounds (Figure 3.4E, E', F, and F'), while the latter, with endogenous tracheal staining in late embryogenesis (Figure 3.4G and G'), showed upregulation only in *crb* (Figure 3.4H and H') but not in *srp3* (Figure 3.4I and I') background. *4s1* was additionally subdivided into four subfragments. Of those, the two most proximal to the transcription start site, *at7* and *at3*, did not exhibit any upregulation (Figure 3.4P-U, P'-U'). *at6* showed a strong endogenous salivary gland staining (Figure 3.4M and M') but no additional upregulation in *crb* or *srp3* backgrounds that can be

Table 3.2: Independent transgenic lines from at1 to at7 constructs.

Transgene	# Lines Obtained	# Lines Tested	# Lines w/ Consistent Staining
at1	9	5	4
at2	5	4	3
at3	7	3	3
at4	10	4	3
at5	4	3	2
at6	8	3	3
at7	6	3	3

Fig 3.4: Analysis of promoter segments truncated from 4s1 region

Overlapping reporter constructs containing truncated segments from the 4s1 promoter region are named at1-at7. Embryos were stained with either an α β-gal antibody **(A-U)** or for X-gal activity **(A'-U')**. Staining of embryos with reporter constructs by themselves **(A, A', D, D', G, G', J, J', M, M', P, P', S, S')** show endogenous levels of expression. **(B, B', E, E', H, H', K, K', N, N', Q, Q', T, T')** show embryos transgenic for the reporter constructs in a *crb* background, and **(C, C', F, F', I, I', L, L', O, O',R, R',U, U')** show embryos transgenic for reporter constructs in a *srp3* background.

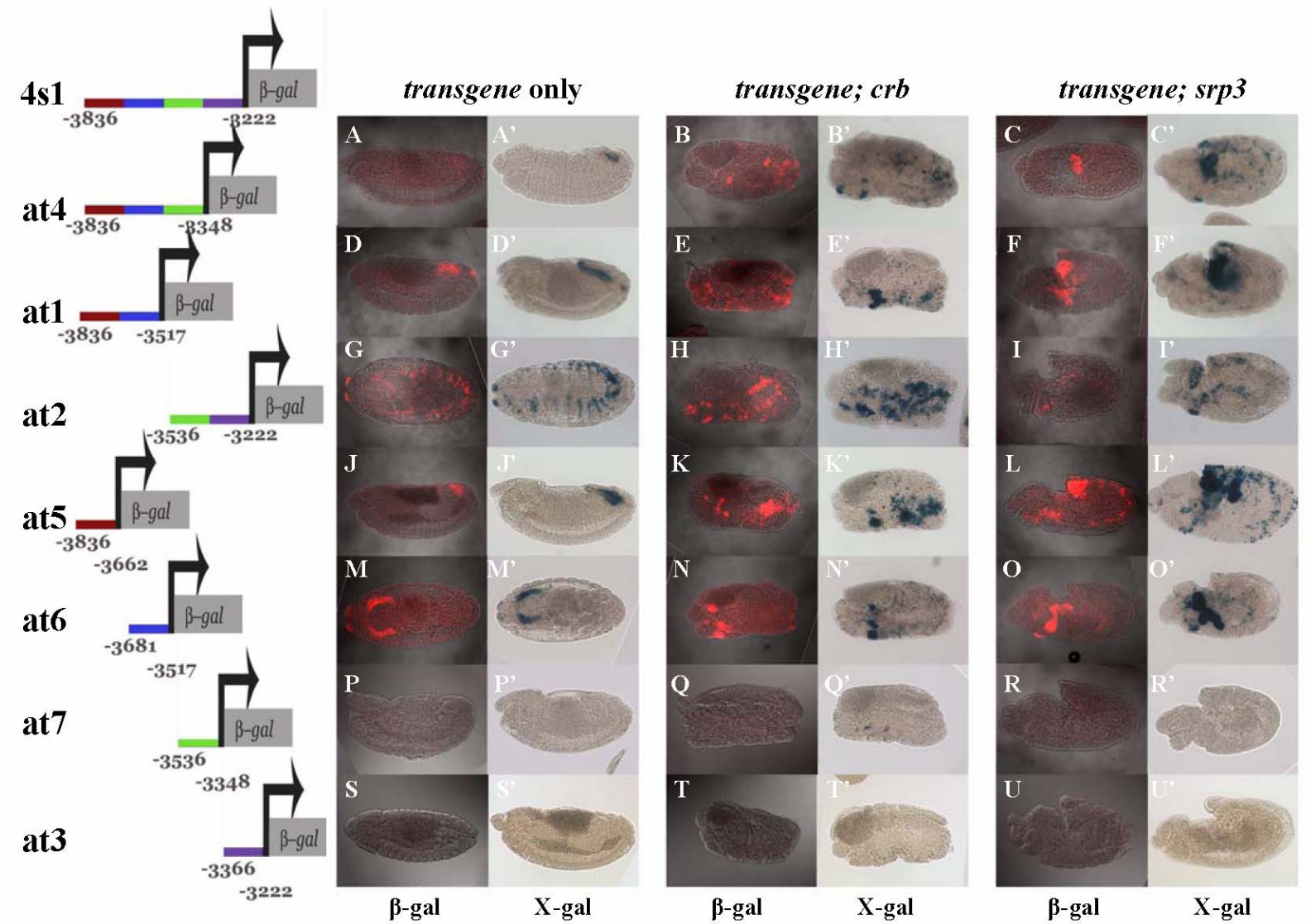
4s1
-3836
-3222
β-gal
at4
-3836
-3348
β-gal
at1
-3836
-3517
β-gal
at2
-3536
-3222
β-gal
at5
-3836
-3662
β-gal
at6
-3681
-3517
β-gal
at7
-3536
-3348
β-gal
at3
-3366
-3222
β-gal
transgene only
transgene; crb
transgene; srp3
A
A'
B
B'
C
C'
D
D'
E
E'
F
F'
G
G'
H
H'
I
I'
J
J'
K
K'
L
L'
M
M'
N
N'
O
O'
P
P'
Q
Q'
R
R'
S
S'
T
T'
U
U'
β-gal
X-gal
β-gal
X-gal
β-gal
X-gal

distinguished from the endogenous pattern (Figure 3.4N, N', O, and O'). *at5*, however, did show robust upregulation in both mutant backgrounds (Figure 3.4K, K', L, L') above the endogenous hindgut signal (Figure 3.4J and J'). Signals resulting from developmental mutants may therefore be integrated upon this 175-bp stretch.

3.3.4 Further truncations of 175bp *at5* region

at5 was further truncated into 3 smaller, overlapping reporter constructs: *at5a*, *at5b*, and *at5c* (Figure 3.5G). Four independent lines from each construct were tested in *crb* and *srp3* mutant backgrounds, and at least three showed similar staining patterns. Only *at5a* showed modest upregulation in both backgrounds of *crb* and *srp3* (Figure 3.5A-C, A'-C'). *at5b* actually showed better upregulation in *crb* background (Figure 3.5E and E') distinguishable from its endogenous salivary gland staining (Figure 3.5D and D'), but the staining seen in the *srp3* background did not localize to the gut region (Figure 3.5F and F'). *at5c*, however, did not show appreciable upregulation at all (Figure 3.5G-I and G'-I').

The sequence of *at5a* was then aligned with those from three other *Drosophila* species: *D. pseudoobscura*, *D. mojavenesis*, and *D. virilis*. Examination of the sequences revealed that significant homology exists in 2 stretches within *at5a* (Figure 3.6A and B). Reporter lines were made with quadruplicate copies of each stretch and were named *at5i* and *at5ii* (highlighted in blue and green, respectively, in Figure 3.6A). Four lines from each were tested. Antibody staining of transgenic embryos showed an upregulation of β-gal

Fig 3.5: Analysis of promoter segments truncated from at5
Overlapping reporter constructs containing truncated segments from the at5 promoter region are named at5a, at5b, and at5c. Embryos were stained with either an α β-gal antibody **(A-I)** or for X-gal activity **(A'-I')**. Staining of embryos with reporter constructs by themselves **(A, A', D, D', G, G')** show endogenous levels of expression. **(B, B', E, E', H, H')** show embryos transgenic for the reporter constructs in a *crb* background, and **(C, C', F, F', I, I')** show embryos transgenic for reporter constructs in a *srp3* background. **(G)** Sequence of each of the at5, at5a, at5b, and at5c regions.

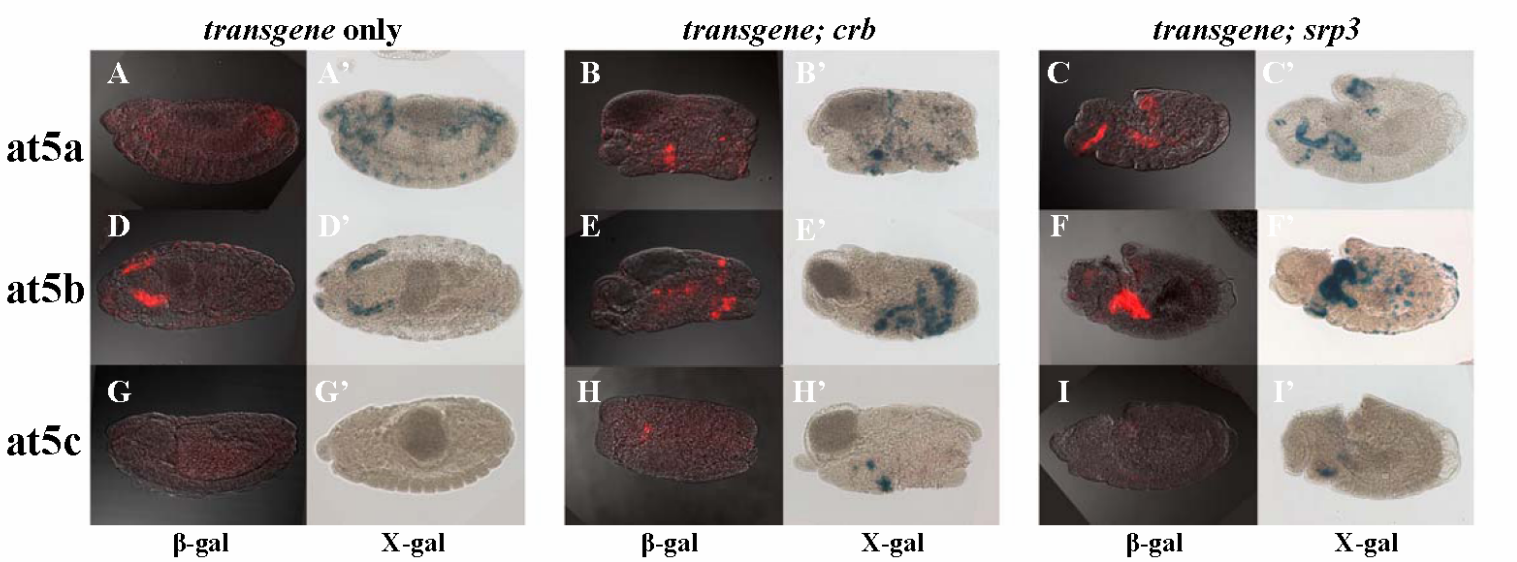
transgene only
transgene; crb
transgene; srp3
at5a
at5b
at5c
A
A'
B
B'
C
C'
D
D'
E
E'
F
F'
G
G'
H
H'
I
I'
β-gal
X-gal
β-gal
X-gal
β-gal
X-gal

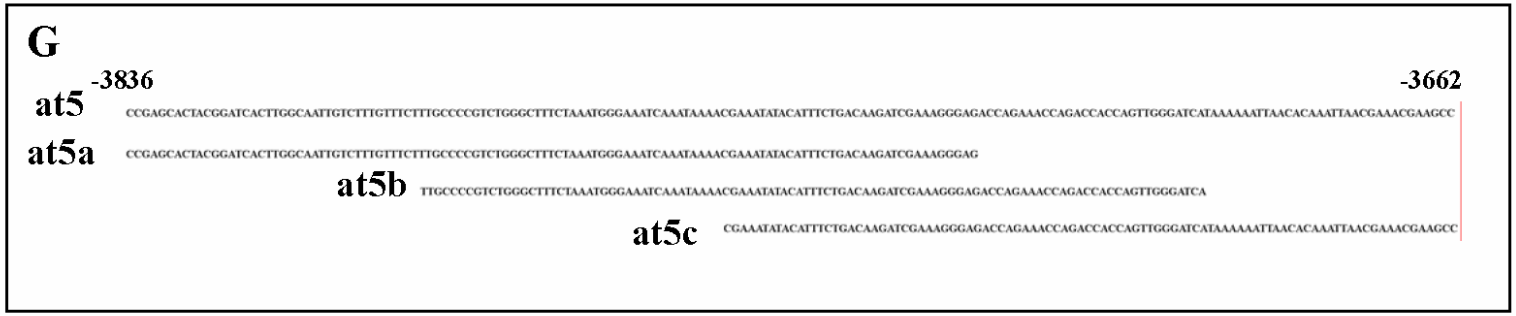
G
-3836
-3662
at5
CCGAGCACTACGGATCACTTGGCAATTGTCTTTGTTTCTTTGCCCCGTCTGGGCTTTCTAAATGGGAAATCAAATAAAACGAAATATACATTTCTGACAAGATCGAAAGGGAGACCAGAAACCAGACCACCAGTTGGGATCATAAAAAATTAACACAAATTAACGAAACGAAGCC
at5a
CCGAGCACTACGGATCACTTGGCAATTGTCTTTGTTTCTTTGCCCCGTCTGGGCTTTCTAAATGGGAAATCAAATAAAACGAAATATACATTTCTGACAAGATCGAAAGGGAG
at5b
TTGCCCCGTCTGGGCTTTCTAAATGGGAAATCAAATAAAACGAAATATACATTTCTGACAAGATCGAAAGGGAGACCAGAAACCAGACCACCAGTTGGGATCA
at5c
CGAAATATACATTTCTGACAAGATCGAAAGGGAGACCAGAAACCAGACCACCAGTTGGGATCATAAAAAATTAACACAAATTAACGAAACGAAGCC

A

CCGAGCACTACGGATCACTTGGCAATTGTCTTTGTTTCTTTGCCCCGTCTGGGCTTTCTAAATGGGAAATCAAATAAAACGAAATATACATTTCTGACAAGATCGAAAGGGAG

at5i at5ii

B

CTACGGATCACTTGGCAATTGTCTTTGTTTCTTTGC	*D. melanogaster*	AAATGGGAAATCAAATAAAACGAAATATACAT
CTACGGATCACTTGGCAATTGTCTTTGTTCCTCTCT	*D. pseudoobscura*	AAATGGGAAATCAAATAATACAAAATATACAT
CAACGGATCACCCAGCAATTGGAATTGTCTTTGTTT	*D. mojavenesis*	AAATGGAAAA-CAAATAAAAGAAAAAATATTT
CAACGGATCACCCAGCAATTGTCTTTGTTTCGGTGC	*D. virilis*	AAATGGAAAA-CAAATAAAAGTATCTGTCGGC

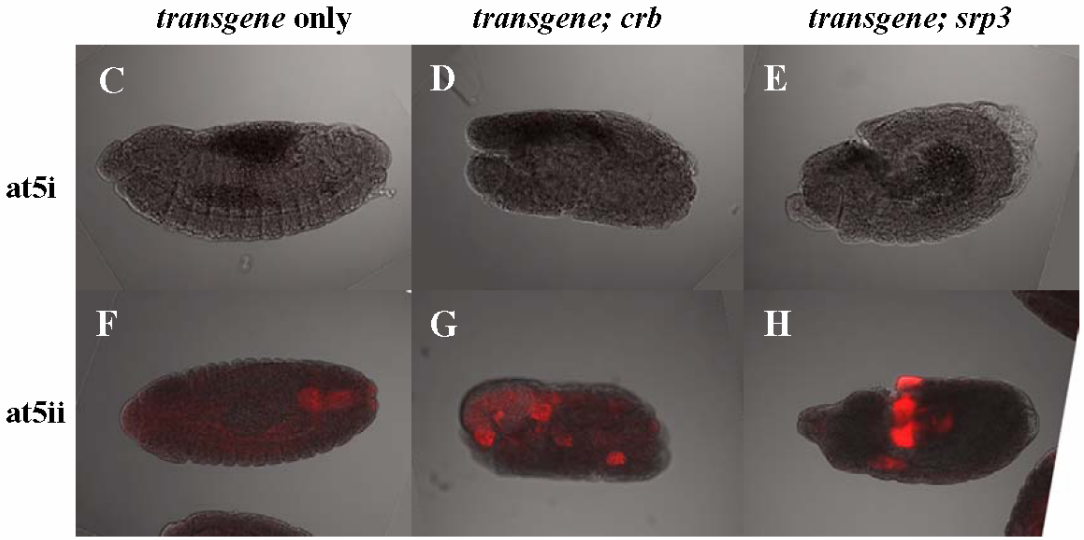

Fig 3.6: Subdivision of fragment at5a

(A) The sequence of at5a is highlighted in two regions of conservation: at5i in blue and at5ii in green. **(B)** The highlighted regions are shown in comparison to the homologous sequences of three other Drosophila species; identical bases are shown in red. Flies transgenic for quadruplicate copies of each of at5i and at5ii cloned in reporter constructs were made. Embryos from at5i-LacZ **(C)** and at5ii-LacZ **(F)** were stained with an α β-gal antibody to show endogenous staining. **(D and G)** show the reporter lines in a *crb* background, and **(E and H)** show them in a *srp3* background.

in two *at5ii* lines in *crb* and *srp3* backgrounds (Figure 3.6F-H) but none in embryos with *at5i* (Figure 3.6C-E). Therefore, the *at5ii* region may contain elements that mediate *rpr* RNA transcriptional activation in response to *crb* and *srp3* mutations.

3.3.5 Role of the *at5 reaper* response elements in other developmental mutants

crb and *srp3* are only two mutants whose developmental misregulation leads to the transcriptional activation at a small stretch of *cis*-regulatory region on the *rpr* promoter. To test whether this is true of other developmental mutants, maternal mutants *dorsal* (*dl*) and *bicoid* (*bcd*) were used. Virgin females transheterozygous for different alleles of both mutants, *bcdE1/bcdE3* and dl^1/dl^5, were crossed to *10 kb rpr-LacZ*, *4 kb rpr-LacZ*, and *4s1* reporter lines, and staining of the embryos revealed that while upregulation was observed in embryos from crosses with the *10* and *4 kb rpr-LacZ* lines (Figure 3.7A, B, D, and E), those from the crosses *4s1* lines showed no staining (Figure 3.7C and F). To test whether *rpr* transcription was activated through the other *4s* lines, dl^1/dl^5 virgin females were crossed to each of the other *4s* lines, and embryos were stained for X-gal activity. Surprisingly, none of those lines exhibited upregulation (Figure 3.7G-M).

Multiple binding sites spanning a distance greater than each of the approximately 600 bp stretch of the *4s* lines may be required to transmit this signal. To test this, the 4 kb region was therefore truncated into two asymmetric and overlapping pieces and cloned into LacZ reporter constructs named *4s1-2*

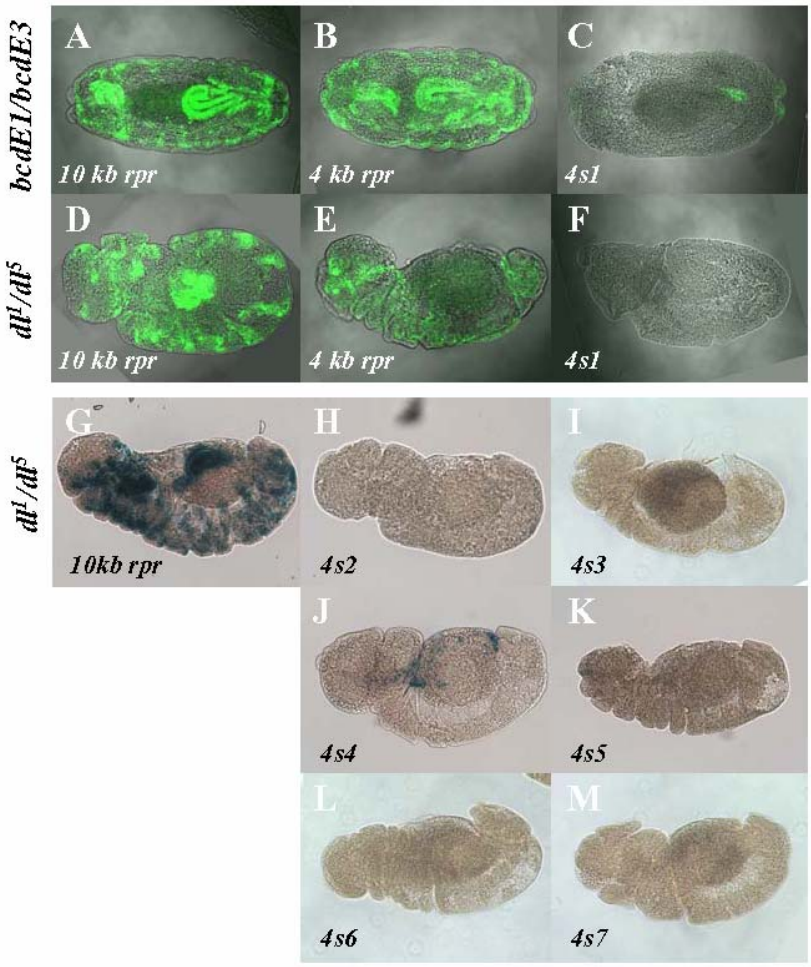

Figure 3.7: Determination of extent of the requirement of *rpr* promoter sequences for a transcriptional response to *bcd* and *dl*

Embryos from *bcdE1/bcdE3* females crossed to *10 kb rpr-LacZ* **(A)**, *4 kb rpr-LacZ* **(B)**, and *4s1* **(C)**, and those from dl^1/dl^5 females crossed to *10 kb rpr-LacZ* **(D)**, *4 kb rpr-LacZ* **(E)**, and *4s1* **(F)** were stained with an α β-gal antibody. Embryos from dl^1/dl^5 females crossed to *10 kb rpr-LacZ* **(G)**, *4s2* **(H)**, *4s3* **(I)**, *4s4* **(J)**, *4s5* **(K)**, *4s6* **(L)**, and *4s7* **(M)** were stained for X-gal activity.

and *4s3-7*, to denote the 4s regions of which each is comprised (Figure 3.8A). These transgenes were first tested in *crb* and *srp3* backgrounds. Modest upregulation was detected for *4s1-2* embryos in those mutants (Figure 3.8B-D and B'-D'). Its lower level of staining compared to *4s1* (Figure 3.3T, T', U, and U') and *at5* (Figure 3.4K, K', L, and L') may indicate the presence of elements bound by inhibitory proteins. No upregulation occurred with *4s3-7* transgenic embryos in those mutant backgrounds (Figure 3.8E-G and E'-G') above the endogenous X-gal filling of the amnioserosa and staining in the head region (Figure 3.8E'-G'), confirming that no convincing upregulation was found in the individual *4s3* to *4s7* transgenes (Figure 3.3A-O and A'-O'). The *4s1-2* and *4s3-7* transgenic animals were then tested in *dl* and and *bcd* backgrounds. Again, surprisingly, upregulation is seen in neither *4s1-2* nor *4s3-7* in embryos from crosses with *bcdE1/bcdE3* (Figure 3.9A, A', B, and B') or (Figure 3.9C, C', D, and D') females, aside from the positive staining in the amnioserosa of *4s3-7* that is seen in embryos harboring only the transgene alone (Figure 3.8E'). Embryos from crosses from *bcdE1/bcdE3* females with *4s3-7* inexplicably do not display the endogenous amnioserosal staining seen in embryos from dl^1/dl^5 females and *4s3-7* males. Transmission of the apoptotic signal, therefore, may require multiple binding sites all along the 4 kb promoter region in response to these two maternal effect mutants.

The mutant *polyhomeotic* (*ph*), that displays cell death in the ventral epidermal region (Dura *et al.*, 1987;Smouse and Perrimon, 1990), was also tested. Hemizygous male embryos obtained from crossing *ph/FM7c* females to

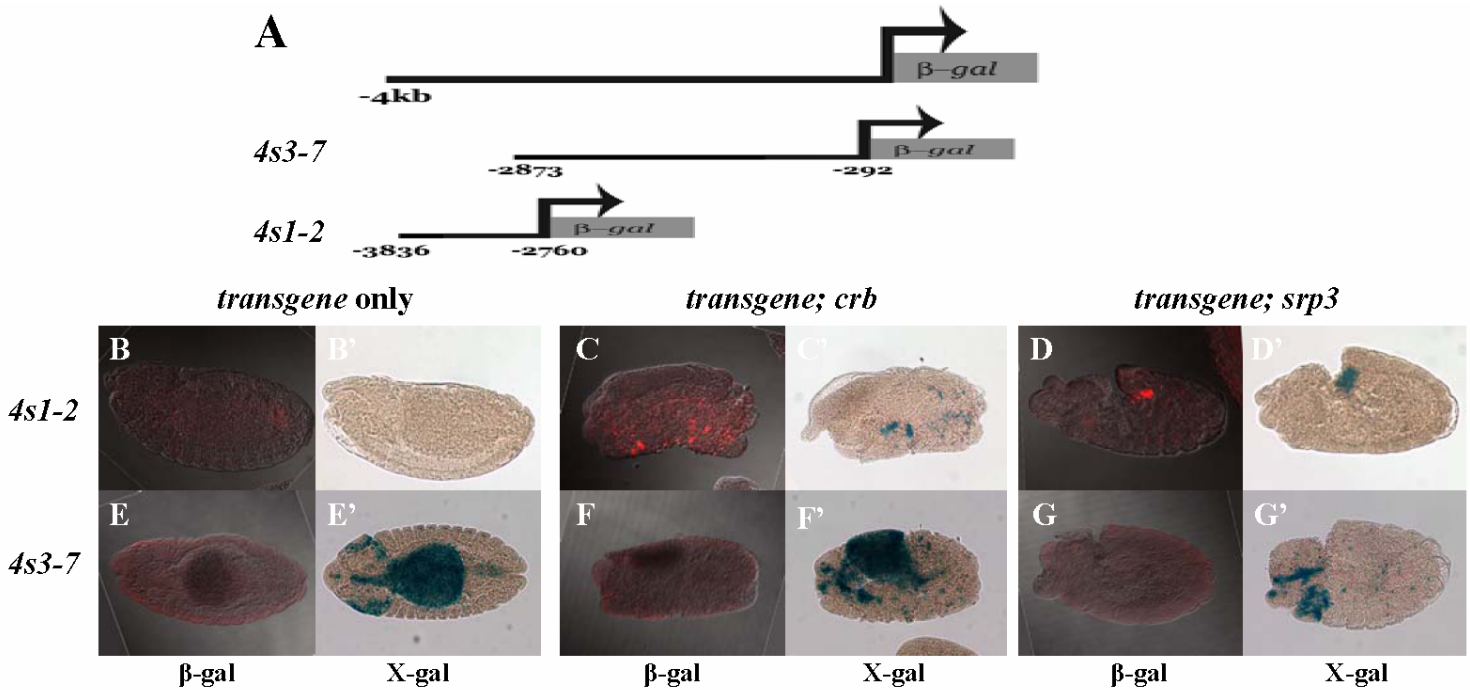

Figure 3.8: Subdivsion of 4 kb promoter region
(A) The 4 kb promoter region is subdivided into two overlapping regions named 4s1-2 and 4s3-7. Embryos were stained with either an α β-gal antibody **(B-G)** or for X-gal activity **(B'-G')**. Staining of embryos with reporter constructs by themselves **(B, B', E, E')** show endogenous levels of expression. **(C, C', F, F')** show embryos transgenic for the reporter constructs in a *crb* background, and **(D, D', G, G')** show embryos transgenic for reporter constructs in a *srp3* background.

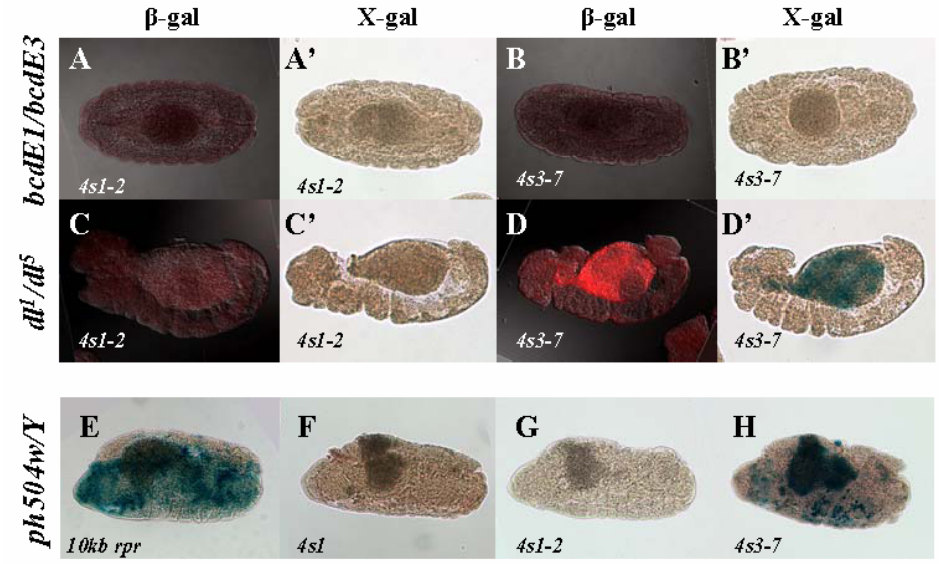

Figure 3.9: Reporter upregulation in *ph* but not *dl* or *bcd*
Embryos from *bcdE1/bcdE3* females crossed to *4s1-2* **(A and A')** and to *4s3-7* **(B and B')** are stained with an α β-gal antibody **(A and B)** or for X-gal activity **(A' and B')**. Likewise, embryos from dl^1/dl^6 females crossed to *4s1-2* **(C and C')** and to *4s3-7* **(D and D')** are stained with an α β-gal antibody **(C and D)** or for X-gal activity **(C' and D').** Embryos from *ph504/FM7c-GFP* females crossed with *10 kb rpr-LacZ* **(E)**, *4s1* **(F)**, *4s1-2* **(G)**, and *4s3-7* **(H)** are stained for X-gal activity.

10 kb rpr-LacZ males show massive upregulation of X-gal activity (Figure 3.9E), but like the maternal effect mutants, no upregulation was seen in embryos from crosses to *4s1* (Figure 3.9F). However, X-gal staining did reveal an upregulation in *ph/Y; 4s3-7/+* embryos (Figure 3.9H), but not in *ph/Y; 4s1-2/+* embryos (Figure 3.9G). Therefore, the apoptotic signals resulting from different developmental aberrations transcriptionally activate *reaper* through distinct elements in its promoter region. This suggests that different pathways, rather than a single master pathway, mediate this response and that the *rpr* promoter is the central integrator of all these signals.

3.4 Identification of *p8* as a putative transcriptional activator of *reaper*

3.4.1 Yeast 1-hybrid assay to screen for putative factors

The 175 bp sequence comprising *at5* was cloned in single and triple copies into the *pHIS2* vector, and two yeast 1-hybrid assays were conducted: one with the triple copy of *at5* as bait and a cDNA library made from *yw* embryos and one with a single copy of *at5* as bait and a cDNA library made from embryos laid by *crb/TM6B* flies. Yeast strain Y187 was first transformed with either *(1x)at5-pHIS2* or *(3x)at5-pHIS2*, and transformation with the libraries followed. Out of approximately one million clones plated for each assay, the clones that grew on SD/-Trp/-Leu/-His media are tabulated in Tables 3.3 and 3.4. Of the known genes, many encode ribosomal binding proteins, some of which were represented in multiple clones. Other known genes as well as some unknown

Table 3.3: Candidates from yeast 1-hybrid screen performed with triplicate *at5* as bait

#Clones	Symbol	Name	Descriptor
5	*Hrb98DE*	*heterogeneous nuclear ribonucleoprotein at 98DE*	mRNA binding, processing, and localization
2	*His3.3A*	*histone 3.3A*	nucleosome assembly
3	*RpL32*	*ribosomal protein L32*	mRNA binding; protein biosynthesis
1	*RpLP0*	*ribosomal protein LP0*	mRNA binding; protein biosynthesis
1	*RpL40*	*ribosomal protein L40*	ribosome biogenesis
1	*RpL17*	*ribosomal protein L17*	protein biosynthesis
1	*RpL18A*	*ribosomal protein L18A*	protein biosynthesis
1	*RpS29*	*ribosomal protein S29*	protein biosynthesis
1	*RpS15*	*ribosomal protein S15*	protein biosynthesis
1	*α-tub84B*	*α-tubulin at 84B*	structural constituent of cytoskeleton
1	*ß-tub56D*	*ß-tubulin st 56D*	structural constituent of cytoskeleton
1	*ent2*	*equilibrative nucleoside transporter 2*	nucleotide and nucleic acid transport
1	*cdc2*		cell cycle regulation
1	*cact*	*cactus*	I-κB/NF-κB cascade
1	*rtnl1*		intracellular protein transport
2	*CG6770*	*p8*	
2	*CG10098*		peptidase family U34
2	*CG1354*		DUF 933 family of several GFP-binding proteins
1	*CG30185*		Glutathione S-transferase homolog
1	*CG6904*		glycogen synthase homolog
1	*CG7852*		Rab6 interacting protein 1 homolog
1	*CG6347*		papain family cysteine peptidase homolog
1	*CG17259*		seryl-tRNA synthetase
1	*CG6995*		unknown; RNA-binding motif
1	*CG15211*		unknown; MARVEL domain often found in lipid-associating proteins
1	*CG7802*		unknown; specific to insects
1	*CG13427*		unknown; specific to *Drosophila*
1	*CG7341*		unknown; specific to *Drosophila*
1	*CG15213*		unknown; specific to *Drosophila*

Table 3.4: Candidates from yeast 1-hybrid screen performed with single *at5* as bait

# Clones	Symbol	Name	Descriptor
3	*RpL32*	*ribosomal protein L32*	mRNA binding; protein biosythesis
1	*RpS16*	*ribosomal protein S16*	protein biosynthesis
1	*RpL17*	*ribosomal protein L17*	protein biosynthesis
2	*RpL27A*	*ribosomal protein L27A*	protein biosynthesis
1	*RpL13*	*ribosomal protein L13*	protein biosynthesis
1	*Lp0*		protein biosynthesis
1	*Hrb98DE*	*heterogeneous nuclear ribonucleoprotein at 98DE*	mRNA binding, processing, and localization
1	*TFIIS*	*RNA polymerase II elongation factor*	regulation of transcription
1	*eIF-5A*		regulation of translation
1	*Ef1a48D*	*Elongation factor 1a at 48D*	regulation of translation
1	*Dmef2*	*Myocyte enhancing factor 2*	transcription factor in muscle differentiation
1	*14-3-3ζ*		protein-binding partner functioning in cell cycle checkpoint, polarity determination, learning
1	*14-3-3ε*		protein-binding partner functioning in cell cycle checkpoint, polarity determination, learning
1	*ent2*	*equilibrative nucleoside transporter 2*	nucleotide and nucleic acid transport
1	*cdc2*		cell cycle regulation
1	*stg*	*string (cdc25)*	cell cycle regulation
2	*cact*	*cactus*	I-κB/NF-κB cascade
1	*fkh*	*forkhead*	transcription factor in gut, Malpighian tubule, and salivary gland development
1	*Bx42*		embryonic development
1	*Afu*	*another transcription unit*	unknown
1	*Cys*	*Cystatin-like*	unknown
1	*Act5c*	*actin 5C*	structural constituent of cytoskeleton
1	*frc*	*fringe connection*	carbohydrate transport; patterning
1	*Cad87A*	*cadherin at 87A*	homophilic cell adhesion
1	*MKK3/kic*	*licorne*	TGFβ pathway
1	*MP20*	*muscle protein 20*	structural constituent of cytoskeleton
1	*GstD1*	*glutathione S transferase D1*	glutathion transferase
1	*ran*		actin filament organization , cell adhesion, cell shape
1	*nuf*	*nuclear fallout*	microtubule binding; actin cytoskeleton reorganization
1	*Mtch*	*mitochondrial carrier homolog 1*	unknown
1	*CG6579*		unknown
1	*CG8580*		unknown
1	*CG6151*		unknown
1	*CG17052*		chitin binding
1	*CG7992*		unknown
1	*CG11985*		pre-mRNA splicing
1	*CG30372*		regulation of GTPase activity
1	*CG15828*		lipid transport
1	*CG9216*		unknown
1	*CG6370*		ribophorin II domain; functions in N-linked glycosylation
1	*CG4330*		unknown
1	*CG9877*		unknown
1	*CG2116*		zinc finger domain

ones encode unlikely candidates as they are known to function as protein binding partners. The most likely candidate is represented by 2 clones and encodes a *Drosophila* gene *CG6770*, a homolog of human *p8*. Initial confirmation of the interaction of the protein with the DNA sequences requires the ability of yeast to grow when transformed with *at5-HIS2* constructs and the original clones and a *Gal4-CG6770*. Transformation of the DNA from the original clone or *Gal4-CG6770* with *(3x)at5-HIS2* resulted in very few colonies, but PCR analysis revealed that the original strain *Y187* transformed with *(3x)at5-HIS2* resulted in a recombination event that eliminated two of the copies of at5. When the possibility that the interaction of *CG6770* occurs only with a single copy of *at5* was tested, the numbers of colonies increased in excess of a log: either clone from the original screen as well as *Gal4-CG6770* transformed into *Y187* with *at5-HIS2* resulted in robust growth in SD/-Trp/-His/-Leu media, confirming that, indeed, *CG6770* is a bona fide candidate.

CG6770 is located in 33B on the left arm of the second chromosome (Figure 3.12A) and encodes a protein homologous to one already identified in mammals, *p8*. Alignment of the primary amino acid sequence shows considerable homology (Figure 3.10). It was independently identified by two groups originally as a transcript that was rapidly induced in experimental pancreatitits (Mallo *et al.*, 1997) and in metastatic tumor cells of rats injected with human carcinoma cells (Ree *et al.*, 1999). Further demonstrations of its upregulation in reponse to serum starvation and treatment with staurosporine, cycloheximide, ceramide, and dexamethasone may indicate a role for p8 in

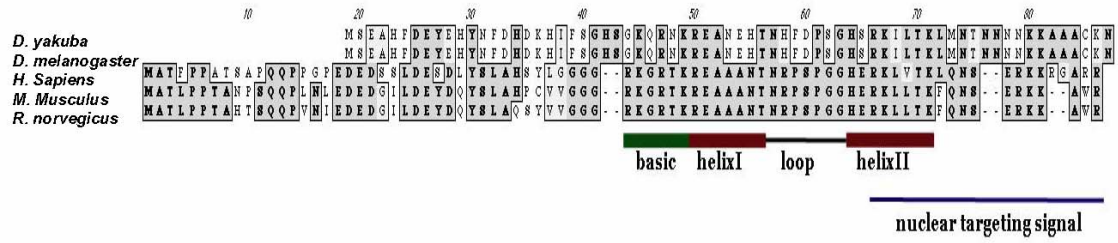

Figure 3.10: Alignment of P8 protein sequence between *Drosophila* and mammalian species

Identical amino acids are highlighted in bold, and similar ones are boxed. Locations of the bHLH motif and nuclear localization signal are indicated as predicted by Mallo et al (1997).

stress response (Mallo *et al.*, 1997;Vasseur *et al.*, 1999). Additionally, that *p8-/-* MEFs showed resistance to adriamycin-induced apoptosis and that it mediates cannabinoid-induced apoptosis of tumor cells suggest a role in cell death (Vasseur *et al.*, 2002b;Carracedo *et al.*, 2006). It may also have an additional role in controlling cell division, but those studies have produced conflicting results. On the one hand, cells transfected with *p8* exhibit higher growth rates (Mallo *et al.*, 1997;Vasseur *et al.*, 1999); but on the other hand, *p8-/-* MEFs and pancreatic cell lines with *p8* silenced by siRNA also show higher growth rates relative to control MEFs (Vasseur *et al.*, 2002b;Malicet *et al.*, 2003). Furthermore, predictions based on primary amino acid sequence, biochemical assessments, and *in vitro* binding assays do support a role for P8 as a transcription factor (Mallo *et al.*, 1997;Encinar *et al.*, 2001;Hoffmeister *et al.*, 2002). *p8*, therefore, appeared to be a legitimate candidate to pursue from the yeast 1-hybrid assay.

3.4.2 Evaluation of *p8*

To test whether *p8* may play a role in the cell death that occurs in *crb* and *srp3* embryos, an RNA *in situ* hybridization was performed. The anti-sense probe detects a wide expression of *p8* in embryos. It is more highly concentrated at the anterior and posterior poles in stage 5 embryos (Figure 3.11C) and in the gut and salivary glands of stage 14 embryos (Figure 3.11D). More importantly, *p8* transcript is impressively upregulated in *crb* embryos (Figure 3.11F and G), and particularly upregulated in the gut and salivary glands in *srp3* embryos (Figure 3.11I and J). This correlating increase supports a possible role for *p8* in the apoptosis of cells in these mutants.

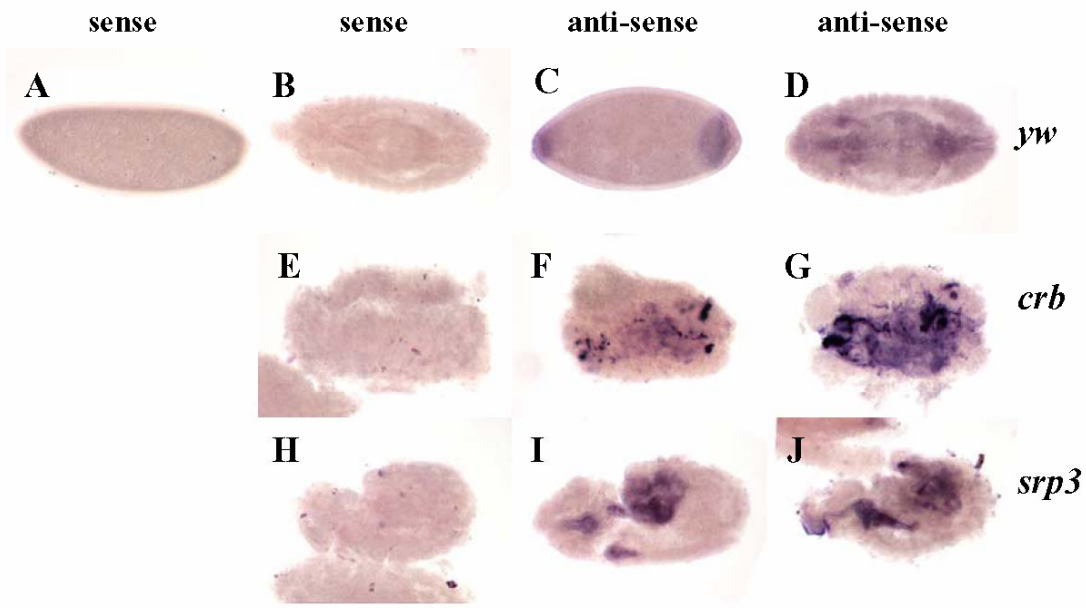

Figure 3.11: RNA *in situ* hybridization of *p8* transcript in embryos
Sense **(A, B, E, H)** and anti-sense **(C, D, F, G, I, J)** *p8* RNA were hybridized to *yw* **(A-D)**, *crb* **(E-F)**, and *srp3* **(H-J)** embryos

There are three *Drosophila* strains P-elements inserted at the locus of *p8*: *EP(2)2459*, *EP(2)EY294*, and *EP(2)2377*; the first two are located in the coding region, while the third is in the 3'UTR (Figure 3.12A). Northern analysis with total RNA isolated from adults reveal that they are loss-of-function alleles (Figure 3.12B). The animals, however, are homozygous viable and fertile and appear grossly normal. To test whether these mutants have an effect on the *rpr* reporter lines, flies harboring an *at5* or *4s1* reporter line, a *p8* P-allele, and *crb* or *srp3* were created, i.e. *at5; EP(2)EY294/CyO, twi-GFP; srp3/TM6B*. Embryos were stained for GFP and β-gal; GFP is used to distinguish between embryos homozygous and heterozygous for the p-allele, and morphology is used to distinguish between *srp3* (or *crb*) homozygotes and heterozygotes. While the antibody staining of *at5; EP(2)EY294/TM3, twi-GFP; srp3/TM6B* embryos did not reveal an all or none immunoreactivity to the α β-gal antibody in *EP(2)EY294* heterozygotes versus the homozygotes, a difference in the range of the levels of staining was noticeable. When a qualitative value is assigned to each embryo from 1 to 5 in order of increasing intensity, embryos homozygous for *EP(2)EY294* showed a lower range in staining intensity than their heterozygous siblings (Table 3.5), and the numbers of embryos scored satisfy the Mann-Whitney test that the distribution of their staining would not occur randomly. Embryos from the 4s1#99; *EP(2)EY294/TM3, twi-GFP; crb/TM6B* line were stained and scored with similar results (Table 3.6). Furthermore, additional lines that were tested, including a different P-allele, *EP(2)2377*, also showed a similar trend (Table 3.7). More importantly, Western analysis of the embryos reveals a quantitative decrease in

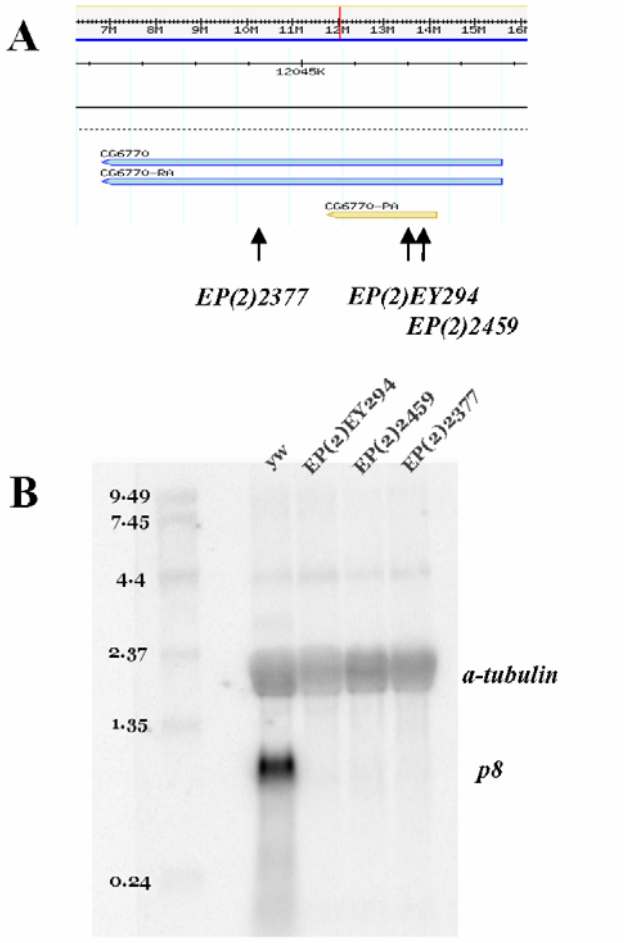

Figure 3.12: Loss-of-function P-alleles of *p8*

(A) Black arrows indicate the locations of 3 EP elements inserted into the *p8* locus.

(B) Northern analysis of total RNA isolated from adult flies shows that the EP insertions cause a loss of function of *p8*.

Table 3.5: Reduction of LacZ expression from *at5* in *p8* mutants

A

at5; EP(2)EY293/+; srp3	Intensity Level	Number of Embryos	% Total
	1	0	0
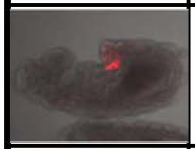	2	7	11
	3	18	29
	4	27	44
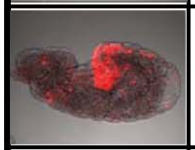	5	10	16
n		*62*	

B

at5; EP(2)EY293; srp3	Intensity Level	Number of Embryos	% Total
	1	5	13
	2	27	71
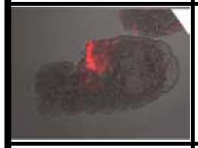	3	6	16
	4	0	0
	5	0	0
n		*38*	

Levels of β-gal immunoreactivity are given estimated intensity levels of 1 to 5, from least intense to most intense. Examples are given for *at5; EP(2)EY294/+; srp3* and *EP(2); EY294; srp3* in **(A)** and **(B)**, respectively. The numbers of embryos for each intensity is counted and a % total is calculated.

Table 3.6: Reduction of LacZ expression from *4s1* in *p8* mutants

A

4s1#99; EP(2)EY294/+; crb	Intensity Level	Number of Embryos	% Total
	1	1	1
	2	10	9
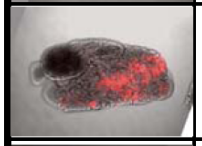	3	65	59
	4	32	29
	5	2	2
n		*110*	

B

4s1#99; EP(2)EY294; crb	Intensity Level	Number of Embryos	% Total
	1	9	15
	2	43	74
	3	5	9
	4	1	2
	5	0	0
n		*58*	

Levels of β-gal immunoreactivity are given estimated intensity levels of 1 to 5, from least intense to most intense. Examples are given for *at5; EP(2)EY294/+; crb* and *EP(2); EY294; crb* in **(A)** and **(B)**, respectively. The numbers of embryos for each intensity is counted and a % total is calculated.

Table 3.7: Tabulation of relative signal intensity in *p8* mutants

	Estimated Intensity					
	1	2	3	4	5	n
at5-4a; EP(2)EY2944; srp3	0 (0%)	7 (11%)	18 (29%)	27 (44%)	10 (16%)	62
at5-4a; EP(2)EY294; srp3	5 (13%)	27 (71%)	6 (16%)	0 (0%)	0 (0%)	38
at5-4a; EP(2)2377/+; srp3	0 (0%)	11 (15%)	55 (74%)	8 (11%)	0 (0%)	74
at5-4a; EP(2)2377; srp3	1 (1.4%)	62 (84.9%)	10 (13.7%)	0 (0%)	0 (0%)	73
4s1#6; EP(2)EY2944; srp3	0 (0%)	15 (18%)	60 (72%)	8 (10%)	0 (0%)	83
4s1#6; EP(2)EY294; srp3	5 (10%)	39 (80%)	5 (10%)	0 (0%)	0 (0%)	49
4s1#99; EP(2)EY2944; srp3	0 (0%)	0 (0%)	18 (69%)	6 (23%)	2 (8%)	26
4s1#99; EP(2)EY294; srp3	0 (0%)	19 (95%)	1 (5%)	0 (0%)	0 (0%)	20
4s1#130; EP(2)EY2944; srp3	0 (0%)	10 (20%)	18 (35%)	21 (41%)	2 (4%)	51
4s1#130; EP(2)EY294; srp3	4 (12%)	23 (66%)	7 (21%)	0 (0%)	0 (0%)	34
	1	2	3	4	5	n
at5-4a; EP(2)EY2944; crb	1 (3%)	31 (97%)	0 (0%)	0 (0%)	0 (0%)	32
at5-4a; EP(2)EY294; crb	1 (7%)	13 (93%)	0 (0%)	0 (0%)	0 (0%)	14
4s1#99; EP(2)EY2944; crb	1 (0.9%)	10 (9.1%)	65 (59.1%)	32 (29.1%)	2 (1.8%)	110
4s1#99; EP(2)EY294; crb	9 (15%)	43 (74%)	5 (9%)	1 (2%)	0 (0%)	58
4s1#130; EP(2)EY2944; crb	3 (14%)	10 (48%)	8 (38%)	0 (0%)	0 (0%)	21
4s1#130; EP(2)EY294; crb	3 (23%)	7 (54%)	3 (23%)	0 (0%)	0 (0%)	13

Signal from immunoreactivity to α β-gal staining is given a range from 1 to 5 in order of progressive intensity, and embryos are counted and a percentage of the total is given in parentheses. The numbers tallied between p8 homozygous and heterozygous genotypes are deemed statistically significant by the Mann-Whitney test.

β-gal levels in *EP(2)EY294* homozygotes in both *crb* and *srp3* backgrounds (Figure 3.13). When total RNA from the embryos were subjected to Northern analysis, however, a decrease in endogenous *rpr* RNA could not be detected (Figure 3.14A, compare "*crb*" and "*EP(2)2377; crb*" lanes). Nor could any decrease in apoptosis be observed when the embryos were stained with TUNEL (Figure3.14B-D). The effect of *p8*, therefore, may only be discernable with more limited regions of the *rpr* promoter comprising the 175 bp of *at5* or the ~600 bp of *4s1*. Additional inputs aside from the contribution of p8 are altogether integrated upon the entire stretch of the *rpr* promoter to determine the fate of the cell.

In order to study the behavior of the P8 protein *in situ*, an antibody was generated in guinea pigs and affinity purified. It readily detects overexpressed P8, as shown by clonal analysis from heat shocking progeny from *flp122; y+GFP; Gal4* X *UAS-p8* and staining their 3rd instar larval imaginal discs (Figure 3.15A-C), but unfortunately does not detect loss of endogenous P8 in loss-of-function clones generated in the progeny of *ey-flp, GMR-Gal4; UAS-GFP, FRT40A* X *FRT40A, EP(2)2377* flies (Figure 3.15D-F). And even though RNA *in situ* hybridization demonstrated an upregulation in *p8* transcripts in *crb* and *srp3* embryos (Figure 3.11), no increase in immunoreactivity to the P8 antibody could be seen (Figure 3.15G-L). This antibody, however, works reliably in Western analyses, and the loss-of-function nature of the three P-alleles of p8 were confirmed for all life stages of the fly (Figure 3.16A-C). And precise and imprecise P-element excision lines created from *EP(2)2459* were confirmed by Western analysis (Figure 3.16D). Western analysis, therefore, was used to

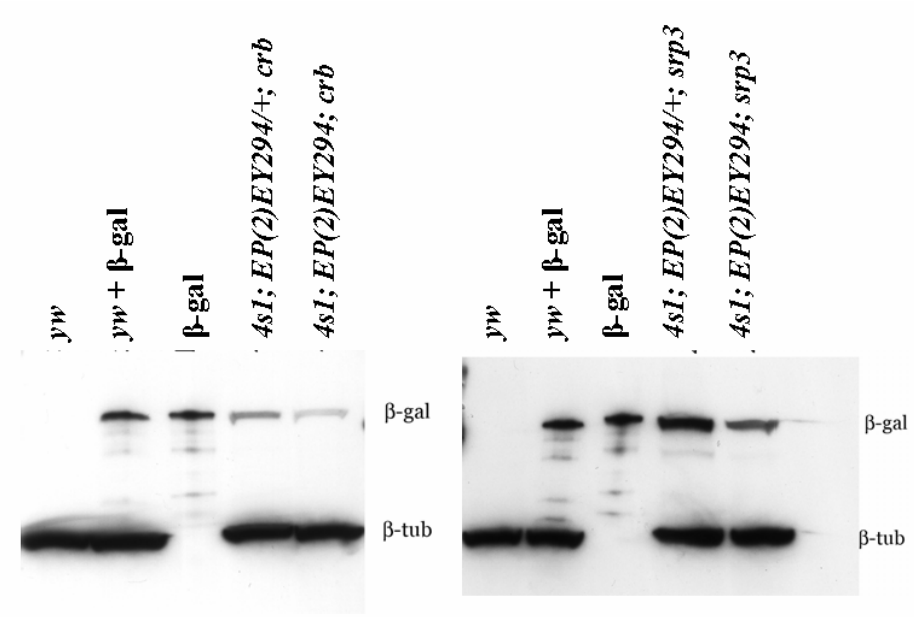

Figure 3.13: Decrease of β-galactosidase in *p8* mutants
4s1; EP(2)EY294/+; crb embryos and their *4s1; EP(2)EY294; crb* siblings (A) or *4s1; EP(2)EY294/+; srp3* and their *4s1; EP(2)EY294/+; srp3* siblings (B) were collected, and their total protein lysates were subjected to Western analysis and probed with α β-gal and α β-tubulin antibodies.

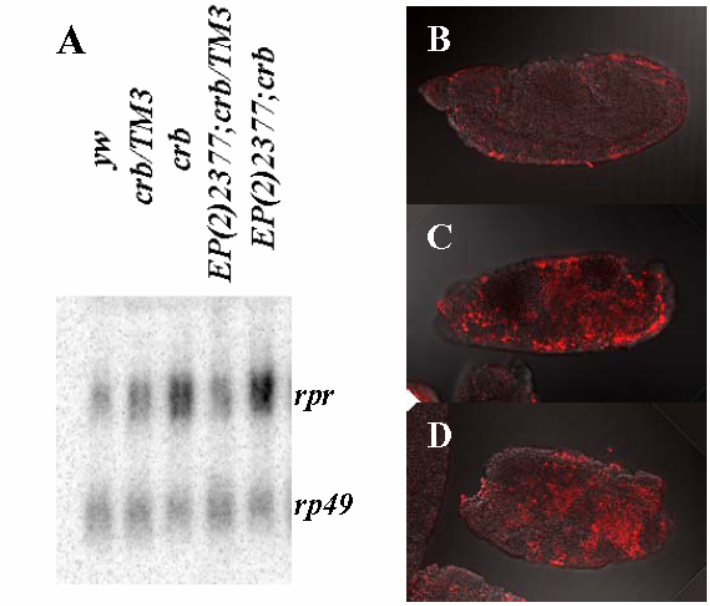

Figure 3.14: Absence of effect on *rpr* endogenous levels and on apoptosis in *p8* mutants
(A) Total RNA was purified from embryos collected from *yw*, *crb/TM3*, *crb*, *EP(2)2377; crb/TM3*, and *EP(2)2377; crb* genotypes and subjected to Northern analysis. The blot was probed for *rpr* and *rp49*. *EP(2)EY294/+; crb* **(C)** and *EP(2)EY294; crb* **(D)** embryos have comparable numbers of Tunel-positive cells that are elevated compared to *EP(2)EY294/+; crb/+* control embryos **(B)**.

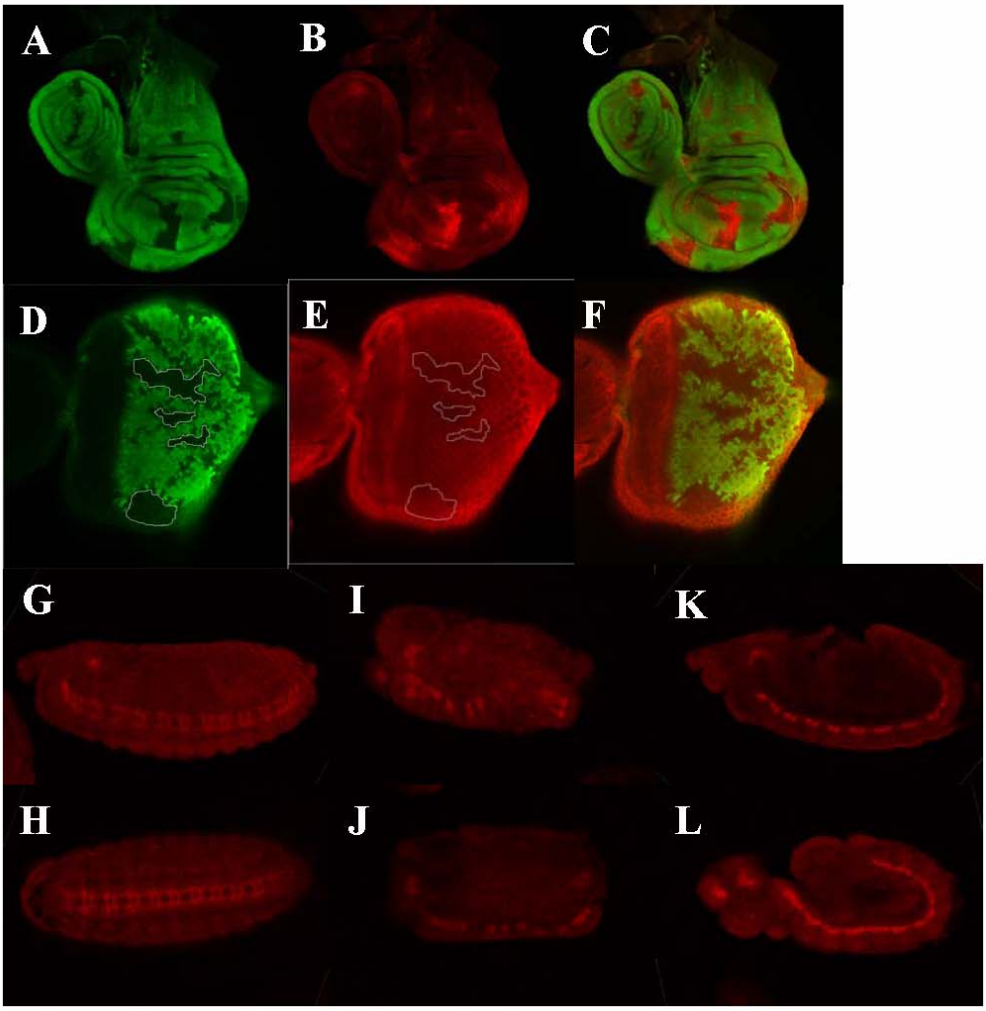

Figure 3.15: α P8 antibody detects overexpressed but not endogenous P8

(A-C) Progeny of *flp122; tub> y+GFP > Gal4 X UAS-p8* are heat shocked and dissected at 3rd instar larval stage for their imaginal discs, which are then stained for GFP **(A)** and P8 **(B)**. **(D-E)** Likewise, eye imaginal discs dissected from 3rd instar larvae of the *ey-flp, GMR-G4; UAS-GFP, FRT40A X FRT40A, EP(2)2377* genotype are stained f or GFP **(D)** and P8 **(E)**. Some of the clones marked by the absence of GFP in **(D)** are delineated and superimposed upon **(E)**. *EP(2)EY294/+* **(G)**, *EP(2)EY294* **(H)**, *EP(2)EY294/+; crb* **(I)**, *EP(2)EY294; crb* **(J)**, *EP(2)EY294/+; srp3* **(K)**, and*EP(2)EY294; srp3* **(L)** embryos were stained with the α P8 antibody.

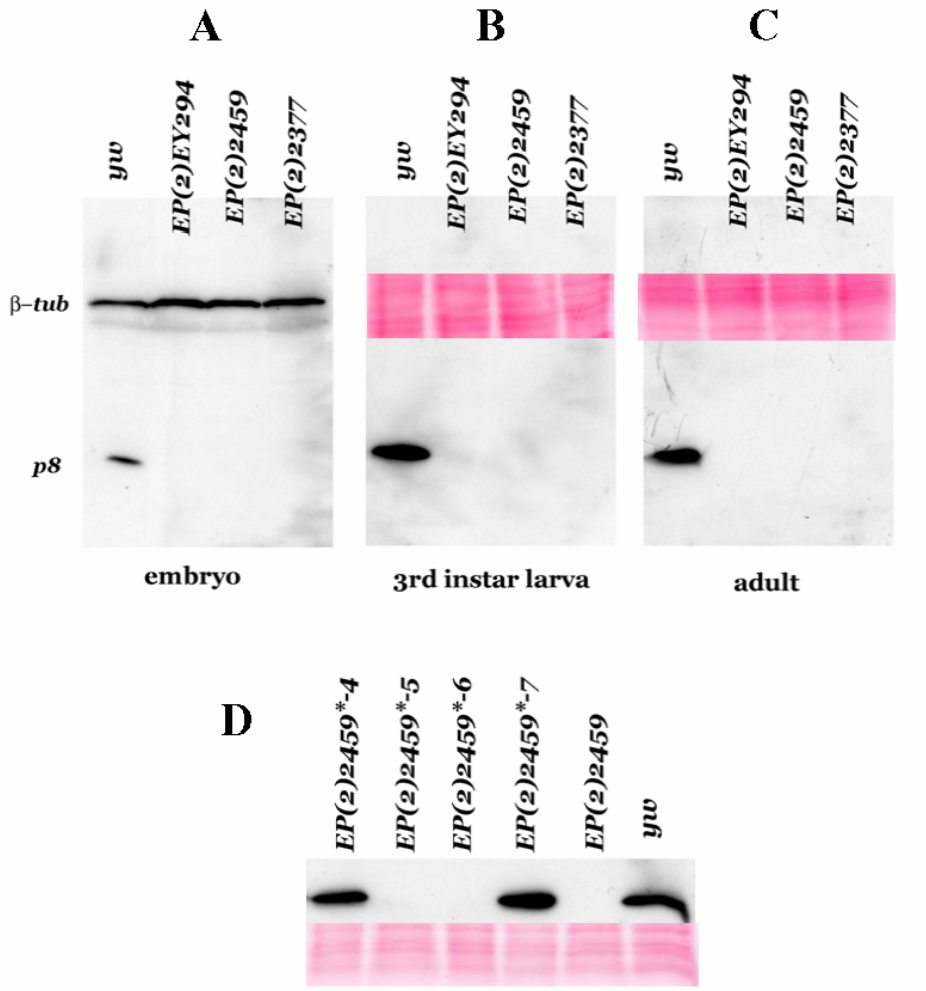

Figure 3.16: Confirmation of *p8* p-alleles as loss-of-function

Lysates were made from embryonic **(A)**, third instar larval **(B)**, and adult **(C)** stages from *yw*, *EP(2)EY294*, *EP(2)2459*, and *EP(2)2377* genotypes and subjected to Western analysis. **(D)** Western analysis was also performed on adult lysates from P-element excision lines that include precise excision lines of *EP(2)2459*-4* and *-7* and imprecise excision lines of *EP(2)2459*-5* and *-6* from which coding sequences were also removed. Either α β-tubulin **(A)** or ponceau **(C-D)** stain was used as loading control.

determine whether P8 levels were increased in *crb* and *srp3* mutants. *crb* and *srp3* embryos were sorted from their *crb/TM3,twi-GFP* and *srp3/TM3, twi-GFP* siblings, and their lysates were subjected to Western analysis, and the blots were probed for P8 and β-tubulin. At 6-8 hours or stages 11-12, the earliest timepoint at which the GFP-marked chromosome could be comfortably used to distinguish between homozygous and heterozygous mutants, P8 levels in both homozygous populations exceeded those in the heterozygous populations, and the most palpable difference between the two populations can be seen at 8-11 hours or stages 12-14 (Figure 3.17). Differences continue to persist up to 11-14 hours or stages 14 to early 16 (Figure 3.17). P8 is therefore upregulated early, suggesting that it is not a consequence of the massive cell death caused by aberrant development in *crb* and *srp3* mutants.

To test whether P8 protein levels become elevated in other contexts, *yw* embryos were collected and irradiated at 4000 rads and allowed to age either 0.5 or 1.5 hours and their lysates were evaluated by Western analysis. At neither time interval of 4.5-7.5 hours or 6.5-12.5 hours did P8 levels in irradiated embryos become greater than in non-irradiated controls, even after those aged for 1.5 hrs after treatment (Figure 3.18A and B).

The two maternal effect mutants *dl* and *bcd* were also assayed for P8 protein levels. Lysates were made from embryos from *yw* males crossed to females of *bcdE1/E3* or their heterozygous sisters (Figure 3.18C) or to dl^1/dl^5 or their heterozygous sisters (Figure 3.18D) and subjected to Western analysis. While progeny from both *bcdE1/E3* and dl^1/dl^5 mothers showed increased levels

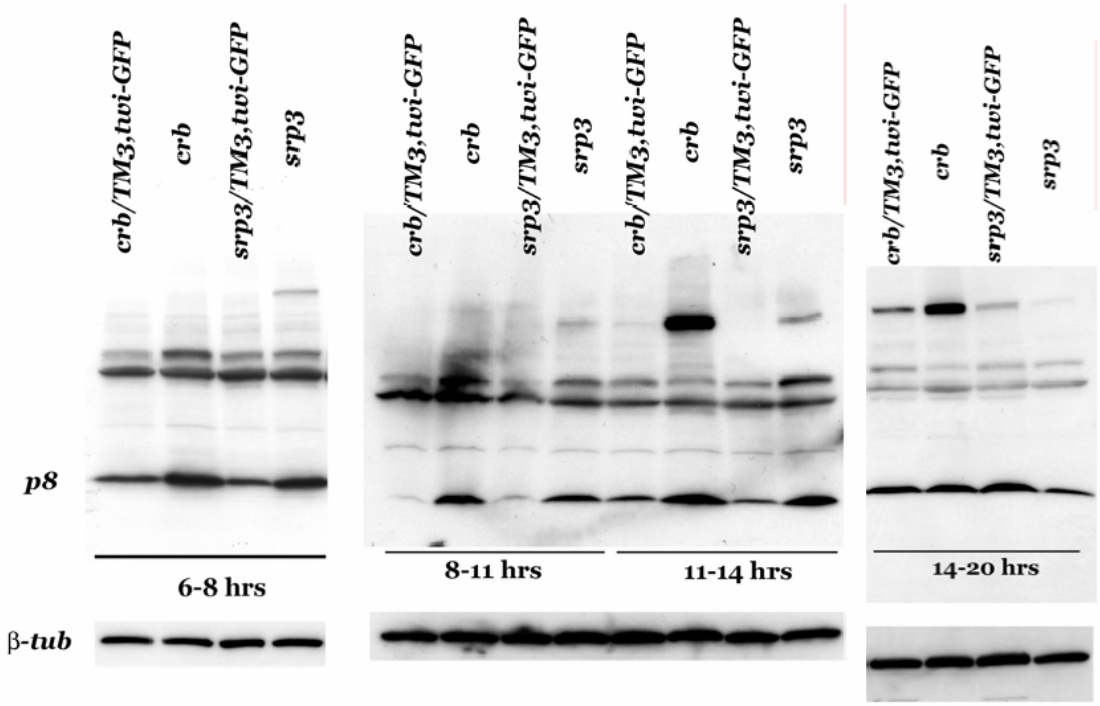

Figure 3.17: Increase of P8 levels in *crb* and *srp3* embryos
Embryos heterozygous and homozygous for *crb* and *srp3* were collected at the indicated time points and lysed for Western analysis. Blots were probed for P8 and β-tubulin.

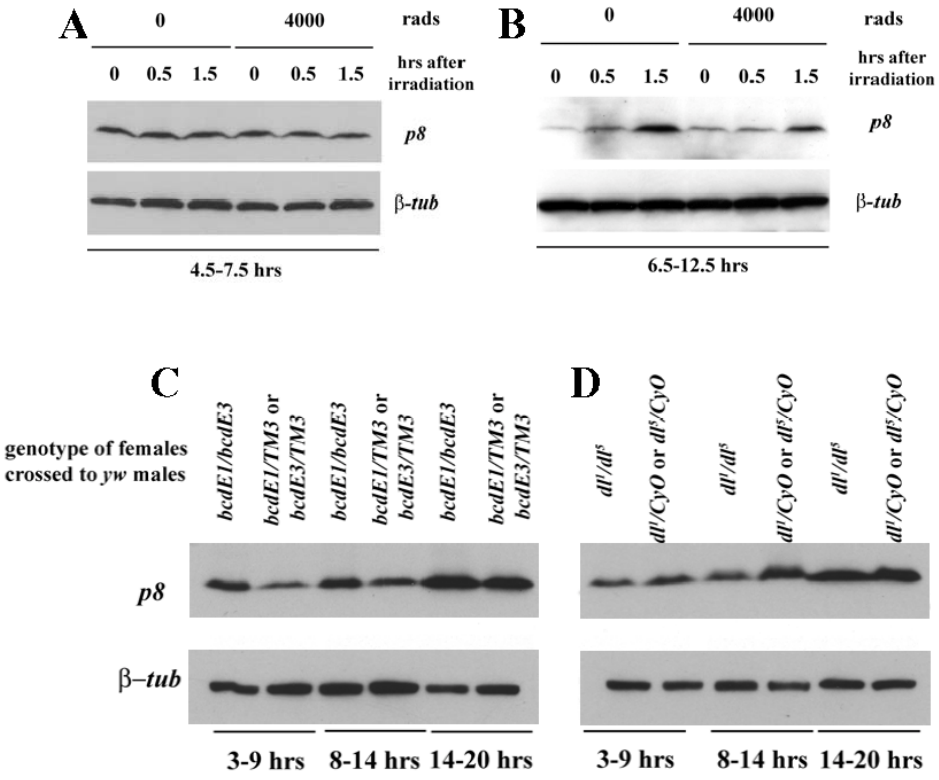

Figure 3.18: P8 is not upregulated in all pro-apoptotic contexts

yw embryos were collected for 3 hrs, aged for 1.5 hrs **(A)** or collected for 6 hrs, aged for 6.5 hrs **(B)**, irradiated and aged for 0.5 or 1.5 hours. *bcdE1/bcdE3* females and their heterozygous female siblings **(C)** or dl^1/dl^5 females and their heterozygous female siblings **(D)** were crossed to *yw* males; embryos were collected over a 6-hour period and aged for either 3, 8, or 14 hours. Lysates were subjected to Western analysis, blots were probed for P8 and β-tubulin.

of P8 in the late timepoint of 14-20 hours, only embryos from the former showed this increase at the earlier timepoint of 3-9 hours. This suggests that not all developmental misregulation events necessarily upregulate P8 protein levels, since the heightened levels at late staged embryos may merely be a consequence of massive death.

Previous studies in mammalian systems have suggested a role for *p8* in both apoptosis and cell division (Mallo *et al.*, 1997;Vasseur *et al.*, 1999;Vasseur *et al.*, 2002a;Vasseur *et al.*, 2002b;Carracedo *et al.*, 2006). To test whether this was true in the case of *Drosophila*, *p8* was overexpressed in flip-out clones from *flp122; tub> y+GFP > Gal4* X *UAS-p8*, and the imaginal discs from the 3rd larval instar progeny were stained for GFP and CM1 (Figure 3.19A-C) or PhosphoH3 (Figure 3.19D-F). In either case, clones did not show an increase in signal as compared to their GFP-expressing siblings, indicating that p8 is not sufficient to cause apoptosis or to drive cell division.

3.5 Conclusion

3.5.1 Integration of different pro-apoptotic signals at the *reaper* promoter in response to developmental frustration

The transcriptional activation of *rpr* occurs in response to many cues, including genotoxic assaults from X- or UV-irradiation as well as normal developmental signaling to sculpt or histolyze tissues. These studies here demonstrate that aberrant development rendering a cell “frustrated” with regards to its differentiation state also leads to the induction of *rpr*. Using *crb* and *srp3*

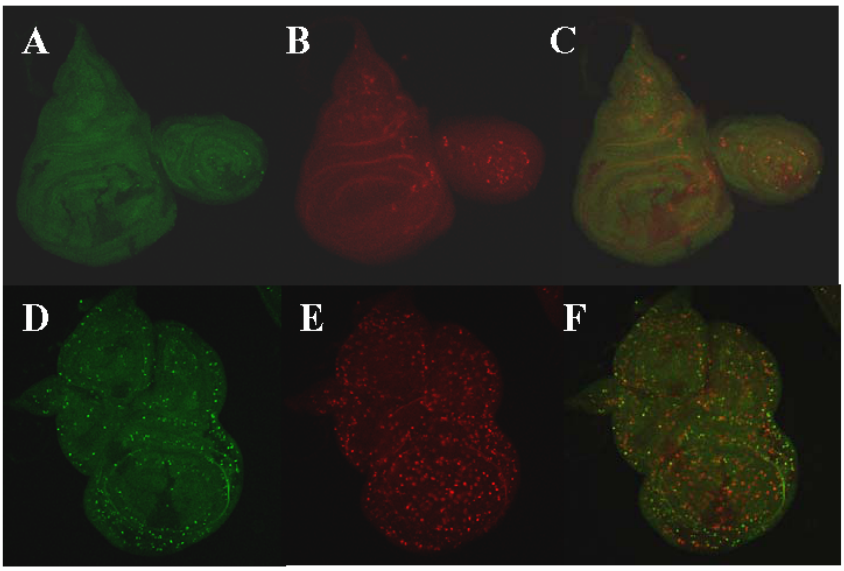

Figure 3.19: P8 is neither sufficient to kill nor to drive cell division

Imaginal discs are dissected from 3rd instar larval progeny of *flp122; y+GFP>Gal 4* X *UAS-p8* that were heat shocked at 37°C for 1 hour at 24 hours AED and stained for GFP **(A and D)** and either CM1 **(B)** or Phospho H3 **(E)**. Merged images are shown in **(C and F)**.

mutants as paradigms for abnormal development, embryos transgenic for reporter contructs with progressively smaller promoter regions were found to have upregulated reporter activity. A 32-bp stretch named *at5ii* was the shortest sequence found to mediate this reponse (Figure 3.6F-H). However, the most robust signal in both mutants was produced by a 175-bp piece, *at5* (Figure 3.4J-L and J'-L'), suggesting the involvement of multiple response elements. Indeed, comparison of *at5* to other larger reporter constructs also containing the *at5* region reveal varying intensities of transcriptional response. *at1* (Figure 3.4E and E') and *at4* (Figure 3.4B and B'), for example, exhibit a relative decrease in response in a *crb* background compared to *at5* (Figure 3.4K and K'). *4s1-2* (Figure3.8B-D and B'-D'), a reporter construct combining elements from *4s1* and *4s2*, also displayed a much more limited signal than *4s1* alone (Figure 3.3S-U and S'-U'). This may be attributed to inhibitory elements present in the additional sequences. *4s1* (Figure 3.3T and T'), on the other, showed a more robust upregulation in β-gal than *at5* (Figure 3.4K and K') in a *crb* background, probably due to the presence of additional elements for transcriptional activators. That multiple response elements participate in *rpr* activation in developmentally abnormal situations is further supported by the observation that a small stretch of response elements that was sufficient to elicit a transcriptional response in *crb* and *srp3* is not engaged in other developmental mutant backgrounds. The maternal effect mutants *dl* and *bcd*, for example, cannot induce *rpr* transcription with any subset of response elements smaller than the 4 kb piece (Figures 3.7 and 3.9A-D and A'-D'). And *ph* requires *4s3-7*, a ~2600 bp stretch that does not

encompass *at5* or *4s1*, to trancriptionally activate *rpr* (Figure 3.9H). Therefore, that developmental frustration leads to a single pathway culminating in the formation of a transcriptional complex that activates *rpr* is an unlikely model. Rather, multiple signals comprising of both pro-apoptotic and anti-apoptotic cues are more probably integrated upon the entire length of the *rpr* promoter and its transcriptional state rests upon their cumulative effect.

3.5.2 *p8* as a modulator of *rpr* transcription

A yeast 1-hybrid screen with the *at5 rpr* promoter region as bait has led to the identification of *p8* as an activator of *rpr* transcription in response to the developmental frustration caused by *crb* and *srp3* mutants. The demonstration that these mutations upregulate the RNA and protein levels of *p8* (Figure 3.11 and 3.17) and that mutations in *p8* lead to a decrease in *at5* and *4s1* reporter signal (Tables 3.3, 3.4, and 3.5; Figure 3.13) support a role for *p8* in activating *rpr* transcription. However, not all developmental aberrations generally induce *p8*, as shown by a similarity in protein levels in the embryonic progeny of *bcdE1/bcdE3* and *bcd/TM3* mothers on the one hand (Figure 3.18C) and by an elevation of P8 protein in the embryonic progeny of dl^1/dl^5 mothers on the other (Figure 3.18D). Furthermore, not all proapoptotic assaults induce *p8*, since X-irradiation does not lead to an increase in protein levels (Figure 3.18D). While *p8* mutants have a transcriptional effect on shorter regions of the *rpr* promoter, endogenous *rpr* RNA transcript levels are not altered in *p8* mutants, and TUNEL staining revealed no change in the degree of apoptosis (Figure 3.14). In addition,

the overexpression of *p8* by itself does not kill (Figure 3.19A-C). Thus, *p8* likely acts in conjunction with other factors, since it is neither necessary nor sufficient. Nonetheless, the identification of *p8* is an important stepping stone to further understanding the upstream signaling that causes *rpr* upregulation resulting from developmental frustration.

4 Implications of the current study and prospects for future research

4.1 Introduction

The current project has greatly expanded on earlier work on the transcriptional regulation of *rpr* in response to defects in development and cellular differentiation. This work was motivated by the hope that studies on the *rpr* promoter will provide insight into the mechanisms by which cells undergo apoptosis in response to aberrant development. The first part entailed the evaluation of reporter constructs made from progressively shorter regions from the *rpr* promoter and has led to the identification of a 32 bp stretch that is sufficient for reporter activation in *crb* and *srp3*. The second part described the identification of *p8* as transcriptional activator of *rpr* from a yeast 1-hybrid screen performed with a 175 bp region. Results from these studies have opened up further questions worth pursuing in the future.

4.2 Further analysis of *reaper* promoter

Promoter analyses performed in these studies have further substantiated the role of the *rpr* promoter region as an integrator of pro-apoptotic signals. Some previous studies have provided evidence that cell death in normal development occurs via the transcriptional regulation of *rpr* at specific elements

(Jiang *et al.*, 2000;Lohmann *et al.*, 2002), while other evidence implicates a role for it without having identified the elements or the factors (Robinow *et al.*, 1997;Chandrasekaran *et al.*, 2003;Miguel-Aliaga *et al.*, 2004;Manjon *et al.*, 2007). The set of fly lines transgenic for relatively short reporter sequence constructs may therefore be used to identify other transcription factors used in normal development. For example, *at1*, *at4*, and *at5* show a staining pattern in the hindgut, *at2* in the trachea, and *at6* in the salivary glands (Figure 3.3). These patterns are not necessarily readily apparent in RNA *in situ* staining (Lohmann, 2003);Lamblin and Steller, unpublished), and possible explanations for the discrepancies may be that *rpr* transcription is normally suppressed in those tissues but activated only because of the absence of inhibitory elements found in longer sequence or that *rpr* is only transiently activated in those tissues. Continued research along this path would further our understanding of how developmental pathways are linked to apoptotic mechanisms.

Moreover, the identification of additional factors would not only be an academic endeavor but would rather contribute to unraveling the complexity involved in how upstream signaling influences *rpr* transcriptional state. The current study, in part, describes the transcriptional activation in response to death from abnormal development and demonstrates that, rather than having the proapoptotic signals integrated upstream of *rpr* and converge upon a single transcription factor that then activates *rpr* transcription, different elements are likely engaged in different mutant contexts. The differential levels of reporter expression also revealed locations of putative inhibitory elements as well, since

reporter constructs with larger pieces of the promoter in some cases exhibited lower levels of upregulation than the shorter pieces in mutant backgrounds. Decoding how the balance of pro and antiapoptotic factors binding to the *rpr* promoter are integrated into a transcriptional activation or repression outcome poses a formidable challenge. As a start, a computational comparison between the *rpr* and *grim* promoters may yield some predictions of other possible binding elements, as these two genes are sometimes found to be co-expressed (Chen *et al.*, 1996;Robinow *et al.*, 1997). And since a transcriptional response has also been found for hid in *bcd* and *oskar* (*osk*) mutants (Werz *et al.*, 2005), a comparison with the *hid* promoter is also warranted. Moreover, as additional genomic sequences from other Drosophila species become annotated, these sequences can be added to the analyses. Furthermore, regions subdivided from *4s1* that may have an inhibitory effect on reporter signal can be used in another yeast 1-hybrid or another kind of screen to identify inhibitory factors. Only when a quorum of players is identified can models be constructed as to how upstream pathways tip the balance between *rpr* activation and repression.

4.3 Further characterization of *p8*

These studies describe the identification of *p8* as a modulator of *rpr* transcription. Its RNA *in situ* pattern, its effect on *rpr* reporter activity, and its own upregulation in developmental mutant backgrounds all indicate a role for *p8* as a mediator of a proapoptotic signal issued in instances of death by confusion. Reports on its mammalian homologue intriguingly suggest roles for p8 in stress

response, apoptosis, and proliferation, although some data appear contradictory at this time. Of particular interest is a recent study demonstrating a role for p8 in mediating cannabinoid-induced apoptosis of tumor cells (Carracedo *et al.*, 2006). Further research in *Drosophila* promises to shed more light upon these issues.

Finding possible binding partners for P8 would be an important undertaking. Because it is neither necessary nor sufficient for the transcriptional activation of *rpr*, it likely acts as a cofactor in a transcriptional complex. Binding partners can be identified by a mass spectroscopy analysis of the products of an immunoprecipitation with the P8 antibody or a yeast 2-hybrid assay using P8 as bait. In fact, prominent higher molecular weight species immunoreactive to the αP8 antibody can be detected in western analysis in a *crb* mutant background (Figure 3.15, 11-14 hrs), and may indicate the presence of a complex. This can be first tested by analyzing samples in a *p8-/-* background to ascertain the relevance of that band. *In vitro* studies with mammalian *p8* have shown that it enhances reporter transactivation activity of the transcription factors Pax2a and Pax2b on the glucagon promoter (Hoffmeister *et al.*, 2002). Identification of the binding partners may therefore provide more revealing hints as to the nature of the upstream signaling that activates *rpr* transcription.

Further analysis of the mutant phenotype of *p8* is also warranted. $p8^{-/-}$ flies are homozygous viable with no ostensible phenotype, but its transcriptional activation in response to developmental aberrations found in *crb* and *srp3* implicates *p8* in stress response. Perhaps only under stress perturbation would the phenotype of *p8* be revealed. Heat shock, hypoxia, and oxidative stress are

examples of stresses that may compromise the viability of *p8*$^{-/-}$ animals. Furthermore, since the JNK pathway is involved in stress response (Kanda and Miura, 2004), testing whether it is affected in a *p8*$^{-/-}$ background would be worthwhile. Apoptosis from ER stress may also be affected since two genes responsive to ER stress are upregulated by *p8* (Carracedo *et al.*, 2006).

p8 may transcriptionally activate the other RHG genes in addition to *rpr*, perhaps doing so with the same or different binding partners. Determining whether the mammalian RHG orthologs are similarly regulated would likewise be interesting.

Since p8 itself is transcriptionally activated in response to stress stimuli, determining the factors that engage its promoter may lead to the identification of further upstream pathways feeding into the activation of the cell death program.

The identification of *p8* therefore represents a starting point from which to study upstream signals that engage the core apoptotic machinery via the transcriptional activation of *rpr* as a response to failure of a cell to differentiate properly. Discovering its binding partners and its own transcriptional regulation may shed light on pathways that activate apoptosis in this context. However, that constitutes only one piece of the puzzle in an extremely complex scenario in which unknown mechanisms evaluate the differentiation state of developing cells and usually, but not always, induce apoptosis in those improperly differentiated ones. This brings up two intriguing questions: (1) How is the differentiation state of a cell monitored; and (2) How does an aberrant cell escape death in cases in which cell fate transformation results from improper differentiation? One study

that addresses the first question suggests a role for the transmembrane proteins, Capricious and Tartan, in providing short-range survival cues in the *Drosophila* wing disc (Milan *et al.*, 2002). And a study that addresses the second question suggests that regions of transformed tissue in *bcd* mutants are kept alive by a survival signal (Werz *et al.*, 2005). Since the analysis of the *rpr* promoter has revealed the presence of both activational and inhibitory elements, that it should integrate some combination of signaling pathways seems likely. The identification of factors that ultimately bind to those elements will not only aid in dissecting out the contributions of pro- and anti-apoptotic signaling that determine the fate of a frustrated cell but will also provide important links to upstream signaling pathways from which one may trace back to the original cue emanating from a frustrated cell.

References

1. Abrams JM, White K, Fessler LI, and Steller H (1993) Programmed cell death during Drosophila embryogenesis. *Development,* **117,** 29-43.

2. Agapite J. Genetic Analysis of Programmed Cell Death in Drosophila melanogaster. 2002. MIT.
   Ref Type: Thesis/Dissertation

3. Alnemri ES, Livingston DJ, Nicholson DW, Salvesen G, Thornberry NA, Wong WW, and Yuan J (1996) Human ICE/CED-3 protease nomenclature. *Cell,* **87,** 171.

4. Arama E, Agapite J, and Steller H (2003) Caspase activity and a specific cytochrome C are required for sperm differentiation in Drosophila. *Dev Cell,* **4,** 687-697.

5. Arama E, Bader M, Srivastava M, Bergmann A, and Steller H (2006) The two Drosophila cytochrome C proteins can function in both respiration and caspase activation. *EMBO J,* **25,** 232-243.

6. Baker NE and Yu SY (2001a) The EGF receptor defines domains of cell cycle progression and survival to regulate cell number in the developing Drosophila eye. *Cell,* **104,** 699-708.

7. Baker NE and Yu SY (2001b) The EGF receptor defines domains of cell cycle progression and survival to regulate cell number in the developing Drosophila eye. *Cell,* **104,** 699-708.

8. Bello B, Holbro N, and Reichert H (2007) Polycomb group genes are required for neural stem cell survival in postembryonic neurogenesis of Drosophila. *Development,* **134,** 1091-1099.

9. Benedict MA, Hu Y, Inohara N, and Nunez G (2000) Expression and functional analysis of Apaf-1 isoforms. Extra Wd-40 repeat is required for cytochrome c binding and regulated activation of procaspase-9. *J Biol Chem,* **275,** 8461-8468.

10. Boyce M, Degterev A, and Yuan J (2004) Caspases: an ancient cellular sword of Damocles. *Cell Death Differ,* **11,** 29-37.

11. Brachmann CB, Jassim OW, Wachsmuth BD, and Cagan RL (2000) The Drosophila bcl-2 family member dBorg-1 functions in the apoptotic response to UV-irradiation. *Curr Biol,* **10,** 547-550.

12. Brodsky MH, Nordstrom W, Tsang G, Kwan E, Rubin GM, and Abrams JM (2000) Drosophila p53 binds a damage response element at the reaper locus. *Cell,* **101,** 103-113.

13. Cakouros D, Daish T, Martin D, Baehrecke EH, and Kumar S (2002) Ecdysone-induced expression of the caspase DRONC during hormone-dependent programmed cell death in Drosophila is regulated by Broad-Complex. *J Cell Biol,* **157,** 985-995.

14. Cakouros D, Daish TJ, and Kumar S (2004) Ecdysone receptor directly binds the promoter of the Drosophila caspase dronc, regulating its expression in specific tissues. *J Cell Biol,* **165,** 631-640.

15. Carracedo A, Lorente M, Egia A, Blazquez C, Garcia S, Giroux V, Malicet C, Villuendas R, Gironella M, Gonzalez-Feria L, Piris MA, Iovanna JL, Guzman M, and Velasco G (2006) The stress-regulated protein p8 mediates cannabinoid-induced apoptosis of tumor cells. *Cancer Cell,* **9,** 301-312.

16. Chai J, Shiozaki E, Srinivasula SM, Wu Q, Datta P, Alnemri ES, and Shi Y (2001) Structural basis of caspase-7 inhibition by XIAP. *Cell,* **104,** 769-780.

17. Chai J, Yan N, Huh JR, Wu JW, Li W, Hay BA, and Shi Y (2003) Molecular mechanism of Reaper-Grim-Hid-mediated suppression of DIAP1-dependent Dronc ubiquitination. *Nat Struct Biol,* **10,** 892-898.

18. Chandrasekaran V and Beckendorf SK (2003) senseless is necessary for the survival of embryonic salivary glands in Drosophila. *Development,* **130,** 4719-4728.

19. Chen F, Hersh BM, Conradt B, Zhou Z, Riemer D, Gruenbaum Y, and Horvitz HR (2000) Translocation of C. elegans CED-4 to nuclear membranes during programmed cell death. *Science,* **287,** 1485-1489.

20. Chen P, Ho SI, Shi Z, and Abrams JM (2004) Bifunctional killing activity encoded by conserved reaper proteins. *Cell Death Differ,* **11,** 704-713.

21. Chen P, Nordstrom W, Gish B, and Abrams JM (1996) grim, a novel cell death gene in Drosophila. *Genes Dev,* **10,** 1773-1782.

22. Chen P, Rodriguez A, Erskine R, Thach T, and Abrams JM (1998) Dredd, a novel effector of the apoptosis activators reaper, grim, and hid in Drosophila. *Dev Biol,* **201,** 202-216.

23. Chew SK, Akdemir F, Chen P, Lu WJ, Mills K, Daish T, Kumar S, Rodriguez A, and Abrams JM (2004) The apical caspase dronc governs programmed and unprogrammed cell death in Drosophila. *Dev Cell,* **7,** 897-907.

24. Choi YJ, Lee G, and Park JH (2006) Programmed cell death mechanisms of identifiable peptidergic neurons in Drosophila melanogaster. *Development,* **133,** 2223-2232.

25. Christich A, Kauppila S, Chen P, Sogame N, Ho SI, and Abrams JM (2002) The damage-responsive Drosophila gene sickle encodes a novel IAP binding protein similar to but distinct from reaper, grim, and hid. *Curr Biol,* **12,** 137-140.

26. Claveria C, Albar JP, Serrano A, Buesa JM, Barbero JL, Martinez A, and Torres M (1998) Drosophila grim induces apoptosis in mammalian cells. *EMBO J,* **17,** 7199-7208.

27. Claveria C, Caminero E, Martinez A, Campuzano S, and Torres M (2002) GH3, a novel proapoptotic domain in Drosophila Grim, promotes a mitochondrial death pathway. *EMBO J,* **21,** 3327-3336.

28. Claveria C, Martinez A, and Torres M (2004a) A Bax/Bak-independent mitochondrial death pathway triggered by Drosophila Grim GH3 domain in mammalian cells. *J Biol Chem,* **279,** 1368-1375.

29. Claveria C, Martinez A, and Torres M (2004b) A Bax/Bak-independent mitochondrial death pathway triggered by Drosophila Grim GH3 domain in mammalian cells. *J Biol Chem,* **279,** 1368-1375.

30. Colussi PA, Quinn LM, Huang DC, Coombe M, Read SH, Richardson H, and Kumar S (2000) Debcl, a proapoptotic Bcl-2 homologue, is a component of the Drosophila melanogaster cell death machinery. *J Cell Biol,* **148,** 703-714.

31. Conradt B and Horvitz HR (1999) The TRA-1A sex determination protein of C. elegans regulates sexually dimorphic cell deaths by repressing the egl-1 cell death activator gene. *Cell,* **98,** 317-327.

32. Conradt B and Horvitz HR (1998) The C. elegans protein EGL-1 is required for programmed cell death and interacts with the Bcl-2-like protein CED-9. *Cell,* **93,** 519-529.

33. Crook NE, Clem RJ, and Miller LK (1993) An apoptosis-inhibiting baculovirus gene with a zinc finger-like motif. *J Virol,* **67,** 2168-2174.

34. Daish TJ, Mills K, and Kumar S (2004) Drosophila caspase DRONC is required for specific developmental cell death pathways and stress-induced apoptosis. *Dev Cell,* **7,** 909-915.

35. Danial NN and Korsmeyer SJ (2004) Cell death: critical control points. *Cell,* **116,** 205-219.

36. Degterev A, Boyce M, and Yuan J (2003b) A decade of caspases. *Oncogene,* **22,** 8543-8567.

37. Degterev A, Boyce M, and Yuan J (2003c) A decade of caspases. *Oncogene,* **22,** 8543-8567.

38. Degterev A, Boyce M, and Yuan J (2003a) A decade of caspases. *Oncogene,* **22,** 8543-8567.

39. Del PL, Gonzalez VM, Inohara N, Ellis RE, and Nunez G (2000) Disruption of the CED-9.CED-4 complex by EGL-1 is a critical step for programmed cell death in Caenorhabditis elegans. *J Biol Chem,* **275,** 27205-27211.

40. Del PL, Gonzalez VM, and Nunez G (1998) Caenorhabditis elegans EGL-1 disrupts the interaction of CED-9 with CED-4 and promotes CED-3 activation. *J Biol Chem,* **273,** 33495-33500.

41. Desai C and Horvitz HR (1989) Caenorhabditis elegans mutants defective in the functioning of the motor neurons responsible for egg laying. *Genetics,* **121,** 703-721.

42. Deveraux QL, Takahashi R, Salvesen GS, and Reed JC (1997) X-linked IAP is a direct inhibitor of cell-death proteases. *Nature,* **388,** 300-304.

43. Dijkers PF, Medema RH, Lammers JW, Koenderman L, and Coffer PJ (2000) Expression of the pro-apoptotic Bcl-2 family member Bim is regulated by the forkhead transcription factor FKHR-L1. *Curr Biol,* **10,** 1201-1204.

44. Dorstyn L, Colussi PA, Quinn LM, Richardson H, and Kumar S (1999a) DRONC, an ecdysone-inducible Drosophila caspase. *Proc Natl Acad Sci U S A,* **96,** 4307-4312.

45. Dorstyn L, Read SH, Quinn LM, Richardson H, and Kumar S (1999b) DECAY, a novel Drosophila caspase related to mammalian caspase-3 and caspase-7. *J Biol Chem,* **274,** 30778-30783.

46. Doumanis J, Quinn L, Richardson H, and Kumar S (2001) STRICA, a novel Drosophila melanogaster caspase with an unusual serine/threonine-rich prodomain, interacts with DIAP1 and DIAP2. *Cell Death Differ,* **8,** 387-394.

47. Du C, Fang M, Li Y, Li L, and Wang X (2000) Smac, a mitochondrial protein that promotes cytochrome c-dependent caspase activation by eliminating IAP inhibition. *Cell,* **102,** 33-42.

48. Duckett CS, Nava VE, Gedrich RW, Clem RJ, Van Dongen JL, Gilfillan MC, Shiels H, Hardwick JM, and Thompson CB (1996) A conserved family

of cellular genes related to the baculovirus iap gene and encoding apoptosis inhibitors. *EMBO J,* **15,** 2685-2694.

49. Dura JM, Randsholt NB, Deatrick J, Erk I, Santamaria P, Freeman JD, Freeman SJ, Weddell D, and Brock HW (1987) A complex genetic locus, polyhomeotic, is required for segmental specification and epidermal development in D. melanogaster. *Cell,* **51,** 829-839.

50. Ellis HM and Horvitz HR (1986) Genetic control of programmed cell death in the nematode C. elegans. *Cell,* **44,** 817-829.

51. Elrod-Erickson M, Mishra S, and Schneider D (2000) Interactions between the cellular and humoral immune responses in Drosophila. *Curr Biol,* **10,** 781-784.

52. Enari M, Sakahira H, Yokoyama H, Okawa K, Iwamatsu A, and Nagata S (1998) A caspase-activated DNase that degrades DNA during apoptosis, and its inhibitor ICAD. *Nature,* **391,** 43-50.

53. Encinar JA, Mallo GV, Mizyrycki C, Giono L, Gonzalez-Ros JM, Rico M, Canepa E, Moreno S, Neira JL, and Iovanna JL (2001) Human p8 is a HMG-I/Y-like protein with DNA binding activity enhanced by phosphorylation. *J Biol Chem,* **276,** 2742-2751.

54. Evans EK, Kuwana T, Strum SL, Smith JJ, Newmeyer DD, and Kornbluth S (1997) Reaper-induced apoptosis in a vertebrate system. *EMBO J,* **16,** 7372-7381.

55. Fernando P, Kelly JF, Balazsi K, Slack RS, and Megeney LA (2002) Caspase 3 activity is required for skeletal muscle differentiation. *Proc Natl Acad Sci U S A,* **99,** 11025-11030.

56. Fischer U, Janicke RU, and Schulze-Osthoff K (2003) Many cuts to ruin: a comprehensive update of caspase substrates. *Cell Death Differ,* **10,** 76-100.

57. Frank LH and Rushlow C (1996) A group of genes required for maintenance of the amnioserosa tissue in Drosophila. *Development,* **122,** 1343-1352.

58. Fraser AG and Evan GI (1997a) Identification of a Drosophila melanogaster ICE/CED-3-related protease, drICE. *EMBO J,* **16,** 2805-2813.

59. Fraser AG, James C, Evan GI, and Hengartner MO (1999) Caenorhabditis elegans inhibitor of apoptosis protein (IAP) homologue BIR-1 plays a conserved role in cytokinesis. *Curr Biol,* **9,** 292-301.

60. Fraser AG, McCarthy NJ, and Evan GI (1997b) drICE is an essential caspase required for apoptotic activity in Drosophila cells. *EMBO J,* **16,** 6192-6199.

61. Fristrom D (1969) Cellular degeneration in the production of some mutant phenotypes in Drosophila melanogaster. *Mol Gen Genet,* **103,** 363-379.

62. Fristrom D (1968) Cellular degeneration in wing development of the mutant vestigial of Drosophila melanogaster. *J Cell Biol,* **39,** 488-491.

63. Furukawa Y, Nishimura N, Furukawa Y, Satoh M, Endo H, Iwase S, Yamada H, Matsuda M, Kano Y, and Nakamura M (2002) Apaf-1 is a mediator of E2F-1-induced apoptosis. *J Biol Chem,* **277,** 39760-39768.

64. Georgel P, Naitza S, Kappler C, Ferrandon D, Zachary D, Swimmer C, Kopczynski C, Duyk G, Reichhart JM, and Hoffmann JA (2001) Drosophila immune deficiency (IMD) is a death domain protein that activates antibacterial defense and can promote apoptosis. *Dev Cell,* **1,** 503-514.

65. Gilley J, Coffer PJ, and Ham J (2003) FOXO transcription factors directly activate bim gene expression and promote apoptosis in sympathetic neurons. *J Cell Biol,* **162,** 613-622.

66. Gottfried Y, Voldavsky E, Yodko L, Sabo E, Ben-Itzhak O, and Larisch S (2004) Expression of the pro-apoptotic protein ARTS in astrocytic tumors: correlation with malignancy grade and survival rate. *Cancer,* **101,** 2614-2621.

67. Goyal L, McCall K, Agapite J, Hartwieg E, and Steller H (2000) Induction of apoptosis by Drosophila reaper, hid and grim through inhibition of IAP function. *EMBO J,* **19,** 589-597.

68. Grether ME, Abrams JM, Agapite J, White K, and Steller H (1995) The head involution defective gene of Drosophila melanogaster functions in programmed cell death. *Genes Dev,* **9,** 1694-1708.

69. Grimes HL, Gilks CB, Chan TO, Porter S, and Tsichlis PN (1996) The Gfi-1 protooncoprotein represses Bax expression and inhibits T-cell death. *Proc Natl Acad Sci U S A,* **93,** 14569-14573.

70. Gupta S, Radha V, Furukawa Y, and Swarup G (2001) Direct transcriptional activation of human caspase-1 by tumor suppressor p53. *J Biol Chem,* **276,** 10585-10588.

71. Haining WN, Carboy-Newcomb C, Wei CL, and Steller H (1999) The proapoptotic function of Drosophila Hid is conserved in mammalian cells. *Proc Natl Acad Sci U S A,* **96,** 4936-4941.

72. Han J, Flemington C, Houghton AB, Gu Z, Zambetti GP, Lutz RJ, Zhu L, and Chittenden T (2001) Expression of bbc3, a pro-apoptotic BH3-only gene, is regulated by diverse cell death and survival signals. *Proc Natl Acad Sci U S A,* **98,** 11318-11323.

73. Han Z, Yi P, Li X, and Olson EN (2006) Hand, an evolutionarily conserved bHLH transcription factor required for Drosophila cardiogenesis and hematopoiesis. *Development,* **133,** 1175-1182.

74. Hanahan D and Weinberg RA (2000) The hallmarks of cancer. *Cell,* **100,** 57-70.

75. Hao H, Dong Y, Bowling MT, Gomez-Gutierrez JG, Zhou HS, and McMasters KM (2007) E2F-1 induces melanoma cell apoptosis via PUMA up-regulation and Bax translocation. *BMC Cancer,* **7,** 24.

76. Harlin H, Reffey SB, Duckett CS, Lindsten T, and Thompson CB (2001) Characterization of XIAP-deficient mice. *Mol Cell Biol,* **21,** 3604-3608.

77. Harvey NL, Daish T, Mills K, Dorstyn L, Quinn LM, Read SH, Richardson H, and Kumar S (2001) Characterization of the Drosophila caspase, DAMM. *J Biol Chem,* **276,** 25342-25350.

78. Hawkins CJ, Wang SL, and Hay BA (1999) A cloning method to identify caspases and their regulators in yeast: identification of Drosophila IAP1 as an inhibitor of the Drosophila caspase DCP-1. *Proc Natl Acad Sci U S A,* **96,** 2885-2890.

79. Hawkins CJ, Yoo SJ, Peterson EP, Wang SL, Vernooy SY, and Hay BA (2000) The Drosophila caspase DRONC cleaves following glutamate or aspartate and is regulated by DIAP1, HID, and GRIM. *J Biol Chem,* **275,** 27084-27093.

80. Hay BA and Guo M (2006) Caspase-dependent cell death in Drosophila. *Annu Rev Cell Dev Biol,* **22,** 623-650.

81. Hay BA, Wassarman DA, and Rubin GM (1995) Drosophila homologs of baculovirus inhibitor of apoptosis proteins function to block cell death. *Cell,* **83,** 1253-1262.

82. Hegde R, Srinivasula SM, Zhang Z, Wassell R, Mukattash R, Cilenti L, DuBois G, Lazebnik Y, Zervos AS, Fernandes-Alnemri T, and Alnemri ES (2002) Identification of Omi/HtrA2 as a mitochondrial apoptotic serine protease that disrupts inhibitor of apoptosis protein-caspase interaction. *J Biol Chem,* **277,** 432-438.

83. Hengartner MO, Ellis RE, and Horvitz HR (1992) Caenorhabditis elegans gene ced-9 protects cells from programmed cell death. *Nature,* **356,** 494-499.

84. Hengartner MO and Horvitz HR (1994a) Programmed cell death in Caenorhabditis elegans. *Curr Opin Genet Dev,* **4,** 581-586.

85. Hengartner MO and Horvitz HR (1994b) The ins and outs of programmed cell death during C. elegans development. *Philos Trans R Soc Lond B Biol Sci,* **345,** 243-246.

86. Hoffmeister A, Ropolo A, Vasseur S, Mallo GV, Bodeker H, Ritz-Laser B, Dressler GR, Vaccaro MI, Dagorn JC, Moreno S, and Iovanna JL (2002) The HMG-I/Y-related protein p8 binds to p300 and Pax2 trans-activation domain-interacting protein to regulate the trans-activation activity of the Pax2A and Pax2B transcription factors on the glucagon gene promoter. *J Biol Chem,* **277,** 22314-22319.

87. Holley CL, Olson MR, Colon-Ramos DA, and Kornbluth S (2002) Reaper eliminates IAP proteins through stimulated IAP degradation and generalized translational inhibition. *Nat Cell Biol,* **4,** 439-444.

88. Hu Y, Ding L, Spencer DM, and Nunez G (1998) WD-40 repeat region regulates Apaf-1 self-association and procaspase-9 activation. *J Biol Chem,* **273,** 33489-33494.

89. Huang DC and Strasser A (2000) BH3-Only proteins-essential initiators of apoptotic cell death. *Cell,* **103,** 839-842.

90. Huang Y, Park YC, Rich RL, Segal D, Myszka DG, and Wu H (2001) Structural basis of caspase inhibition by XIAP: differential roles of the linker versus the BIR domain. *Cell,* **104,** 781-790.

91. Hughes SC and Krause HM (2001) Establishment and maintenance of parasegmental compartments. *Development,* **128,** 1109-1118.

92. Huh JR, Vernooy SY, Yu H, Yan N, Shi Y, Guo M, and Hay BA (2004) Multiple apoptotic caspase cascades are required in nonapoptotic roles for Drosophila spermatid individualization. *PLoS Biol,* **2,** E15.

93. Igaki T, Kanuka H, Inohara N, Sawamoto K, Nunez G, Okano H, and Miura M (2000) Drob-1, a Drosophila member of the Bcl-2/CED-9 family that promotes cell death. *Proc Natl Acad Sci U S A,* **97,** 662-667.

94. Imaizumi K, Tsuda M, Imai Y, Wanaka A, Takagi T, and Tohyama M (1997) Molecular cloning of a novel polypeptide, DP5, induced during programmed neuronal death. *J Biol Chem,* **272,** 18842-18848.

95. Jacobson MD, Burne JF, and Raff MC (1994) Programmed cell death and Bcl-2 protection in the absence of a nucleus. *EMBO J,* **13,** 1899-1910.

96. Jacobson MD, Weil M, and Raff MC (1997) Programmed cell death in animal development. *Cell,* **88,** 347-354.

97. James C, Gschmeissner S, Fraser A, and Evan GI (1997) CED-4 induces chromatin condensation in Schizosaccharomyces pombe and is inhibited by direct physical association with CED-9. *Curr Biol,* **7,** 246-252.

98. Jeffers JR, Parganas E, Lee Y, Yang C, Wang J, Brennan J, MacLean KH, Han J, Chittenden T, Ihle JN, McKinnon PJ, Cleveland JL, and Zambetti GP (2003) Puma is an essential mediator of p53-dependent and -independent apoptotic pathways. *Cancer Cell,* **4,** 321-328.

99. Jiang C, Baehrecke EH, and Thummel CS (1997) Steroid regulated programmed cell death during Drosophila metamorphosis. *Development,* **124,** 4673-4683.

100. Jiang C, Lamblin AF, Steller H, and Thummel CS (2000) A steroid-triggered transcriptional hierarchy controls salivary gland cell death during Drosophila metamorphosis. *Mol Cell,* **5,** 445-455.

101. Jin S, Martinek S, Joo WS, Wortman JR, Mirkovic N, Sali A, Yandell MD, Pavletich NP, Young MW, and Levine AJ (2000) Identification and characterization of a p53 homologue in Drosophila melanogaster. *Proc Natl Acad Sci U S A,* **97,** 7301-7306.

102. Kaiser WJ, Vucic D, and Miller LK (1998) The Drosophila inhibitor of apoptosis D-IAP1 suppresses cell death induced by the caspase drICE. *FEBS Lett,* **440,** 243-248.

103. Kanda H and Miura M (2004) Regulatory roles of JNK in programmed cell death. *J Biochem (Tokyo),* **136,** 1-6.

104. Kannan K, Kaminski N, Rechavi G, Jakob-Hirsch J, Amariglio N, and Givol D (2001) DNA microarray analysis of genes involved in p53 mediated apoptosis: activation of Apaf-1. *Oncogene,* **20,** 3449-3455.

105. Kanuka H, Hisahara S, Sawamoto K, Shoji S, Okano H, and Miura M (1999) Proapoptotic activity of Caenorhabditis elegans CED-4 protein in Drosophila: implicated mechanisms for caspase activation. *Proc Natl Acad Sci U S A,* **96,** 145-150.

106. Kerr JF, Wyllie AH, and Currie AR (1972) Apoptosis: a basic biological phenomenon with wide-ranging implications in tissue kinetics. *Br J Cancer,* **26,** 239-257.

107. Kilpatrick ZE, Cakouros D, and Kumar S (2005) Ecdysone-mediated up-regulation of the effector caspase DRICE is required for hormone-dependent apoptosis in Drosophila cells. *J Biol Chem,* **280,** 11981-11986.

108. Kimble J and Hirsh D (1979) The postembryonic cell lineages of the hermaphrodite and male gonads in Caenorhabditis elegans. *Dev Biol,* **70,** 396-417.

109. Klingensmith J, Noll E, and Perrimon N (1989) The segment polarity phenotype of Drosophila involves differential tendencies toward transformation and cell death. *Dev Biol,* **134,** 130-145.

110. Kluck RM, Bossy-Wetzel E, Green DR, and Newmeyer DD (1997) The release of cytochrome c from mitochondria: a primary site for Bcl-2 regulation of apoptosis. *Science,* **275,** 1132-1136.

111. Kuo CT, Zhu S, Younger S, Jan LY, and Jan YN (2006) Identification of E2/E3 ubiquitinating enzymes and caspase activity regulating Drosophila sensory neuron dendrite pruning. *Neuron,* **51,** 283-290.

112. Lamkanfi M, Declercq W, Kalai M, Saelens X, and Vandenabeele P (2002) Alice in caspase land. A phylogenetic analysis of caspases from worm to man. *Cell Death Differ,* **9,** 358-361.

113. Larisch-Bloch S, Danielpour D, Roche NS, Lotan R, Hsing AY, Kerner H, Hajouj T, Lechleider RJ, and Roberts AB (2000) Selective loss of the transforming growth factor-beta apoptotic signaling pathway in mutant NRP-154 rat prostatic epithelial cells. *Cell Growth Differ,* **11,** 1-10.

114. Laundrie B, Peterson JS, Baum JS, Chang JC, Fileppo D, Thompson SR, and McCall K (2003) Germline cell death is inhibited by P-element insertions disrupting the dcp-1/pita nested gene pair in Drosophila. *Genetics,* **165,** 1881-1888.

115. Lee CY and Baehrecke EH (2000) Genetic regulation of programmed cell death in Drosophila. *Cell Res,* **10,** 193-204.

116. Lee CY, Simon CR, Woodard CT, and Baehrecke EH (2002) Genetic mechanism for the stage- and tissue-specific regulation of steroid triggered programmed cell death in Drosophila. *Dev Biol,* **252,** 138-148.

117. Lee CY, Wendel DP, Reid P, Lam G, Thummel CS, and Baehrecke EH (2000) E93 directs steroid-triggered programmed cell death in Drosophila. *Mol Cell,* **6,** 433-443.

118. Lehmann R and Nusslein-Volhard C (1986) Abdominal segmentation, pole cell formation, and embryonic polarity require the localized activity of oskar, a maternal gene in Drosophila. *Cell,* **47,** 141-152.

119. Leulier F, Ribeiro PS, Palmer E, Tenev T, Takahashi K, Robertson D, Zachariou A, Pichaud F, Ueda R, and Meier P (2006) Systematic in vivo RNAi analysis of putative components of the Drosophila cell death machinery. *Cell Death Differ,* **13,** 1663-1674.

120. Leulier F, Rodriguez A, Khush RS, Abrams JM, and Lemaitre B (2000) The Drosophila caspase Dredd is required to resist gram-negative bacterial infection. *EMBO Rep,* **1,** 353-358.

121. Li P, Nijhawan D, Budihardjo I, Srinivasula SM, Ahmad M, Alnemri ES, and Wang X (1997) Cytochrome c and dATP-dependent formation of Apaf-1/caspase-9 complex initiates an apoptotic protease cascade. *Cell,* **91,** 479-489.

122. Liedtke C, Groger N, Manns MP, and Trautwein C (2003) The human caspase-8 promoter sustains basal activity through SP1 and ETS-like transcription factors and can be up-regulated by a p53-dependent mechanism. *J Biol Chem,* **278,** 27593-27604.

123. Linseman DA, Phelps RA, Bouchard RJ, Le SS, Laessig TA, McClure ML, and Heidenreich KA (2002) Insulin-like growth factor-I blocks Bcl-2 interacting mediator of cell death (Bim) induction and intrinsic death signaling in cerebellar granule neurons. *J Neurosci,* **22,** 9287-9297.

124. Lisi S, Mazzon I, and White K (2000) Diverse domains of THREAD/DIAP1 are required to inhibit apoptosis induced by REAPER and HID in Drosophila. *Genetics,* **154,** 669-678.

125. Liu H, Strauss TJ, Potts MB, and Cameron S (2006) Direct regulation of egl-1 and of programmed cell death by the Hox protein MAB-5 and by CEH-20, a C. elegans homolog of Pbx1. *Development,* **133,** 641-650.

126. Liu X, Zou H, Slaughter C, and Wang X (1997) DFF, a heterodimeric protein that functions downstream of caspase-3 to trigger DNA fragmentation during apoptosis. *Cell,* **89,** 175-184.

127. Liu Z, Sun C, Olejniczak ET, Meadows RP, Betz SF, Oost T, Herrmann J, Wu JC, and Fesik SW (2000) Structural basis for binding of Smac/DIABLO to the XIAP BIR3 domain. *Nature,* **408,** 1004-1008.

128. Lockshin RA and Williams CM (1965) PROGRAMMED CELL DEATH--I. CYTOLOGY OF DEGENERATION IN THE INTERSEGMENTAL MUSCLES OF THE PERNYI SILKMOTH. *J Insect Physiol,* **11,** 123-133.

129. Lohmann I (2003) Dissecting the regulation of the Drosophila cell death activator reaper. *Gene Expr Patterns,* **3,** 159-163.

130. Lohmann I, McGinnis N, Bodmer M, and McGinnis W (2002) The Drosophila Hox gene deformed sculpts head morphology via direct regulation of the apoptosis activator reaper. *Cell,* **110,** 457-466.

131. Los M, Stroh C, Janicke RU, Engels IH, and Schulze-Osthoff K (2001) Caspases: more than just killers? *Trends Immunol,* **22,** 31-34.

132. Lotan R, Rotem A, Gonen H, Finberg JP, Kemeny S, Steller H, Ciechanover A, and Larisch S (2005) Regulation of the proapoptotic ARTS protein by ubiquitin-mediated degradation. *J Biol Chem,* **280,** 25802-25810.

133. Luo X, Puig O, Hyun J, Bohmann D, and Jasper H (2007) Foxo and Fos regulate the decision between cell death and survival in response to UV irradiation. *EMBO J,* **26,** 380-390.

134. Magrassi L and Lawrence PA (1988) The pattern of cell death in fushi tarazu, a segmentation gene of Drosophila. *Development,* **104,** 447-451.

135. Malicet C, Lesavre N, Vasseur S, and Iovanna JL (2003) p8 inhibits the growth of human pancreatic cancer cells and its expression is induced through pathways involved in growth inhibition and repressed by factors promoting cell growth. *Mol Cancer,* **2,** 37.

136. Mallo GV, Fiedler F, Calvo EL, Ortiz EM, Vasseur S, Keim V, Morisset J, and Iovanna JL (1997) Cloning and expression of the rat p8 cDNA, a new gene activated in pancreas during the acute phase of pancreatitis, pancreatic development, and regeneration, and which promotes cellular growth. *J Biol Chem,* **272,** 32360-32369.

137. Manjon C, Sanchez-Herrero E, and Suzanne M (2007) Sharp boundaries of Dpp signalling trigger local cell death required for Drosophila leg morphogenesis. *Nat Cell Biol,* **9,** 57-63.

138. Martinez-Velazquez M, Melendez-Zajgla J, and Maldonado V (2007) Apoptosis induced by cAMP requires Smac/DIABLO transcriptional upregulation. *Cell Signal,* **19,** 1212-1220.

139. Martins LM (2002) The serine protease Omi/HtrA2: a second mammalian protein with a Reaper-like function. *Cell Death Differ,* **9,** 699-701.

140. Maurer CW, Chiorazzi M, and Shaham S (2007) Timing of the onset of a developmental cell death is controlled by transcriptional induction of the C. elegans ced-3 caspase-encoding gene. *Development,* **134,** 1357-1368.

141. McCall K and Steller H (1998) Requirement for DCP-1 caspase during Drosophila oogenesis. *Science,* **279,** 230-234.

142. McCall K and Steller H (1997) Facing death in the fly: genetic analysis of apoptosis in Drosophila. *Trends Genet,* **13,** 222-226.

143. McCarthy JV and Dixit VM (1998) Apoptosis induced by Drosophila reaper and grim in a human system. Attenuation by inhibitor of apoptosis proteins (cIAPs). *J Biol Chem,* **273,** 24009-24015.

144. McDonnell TJ, Deane N, Platt FM, Nunez G, Jaeger U, McKearn JP, and Korsmeyer SJ (1989) bcl-2-immunoglobulin transgenic mice demonstrate extended B cell survival and follicular lymphoproliferation. *Cell,* **57,** 79-88.

145. Meier P, Silke J, Leevers SJ, and Evan GI (2000) The Drosophila caspase DRONC is regulated by DIAP1. *EMBO J,* **19,** 598-611.

146. Mendes CS, Arama E, Brown S, Scherr H, Srivastava M, Bergmann A, Steller H, and Mollereau B (2006) Cytochrome c-d regulates developmental apoptosis in the Drosophila retina. *EMBO Rep,* **7,** 933-939.

147. Miguel-Aliaga I and Thor S (2004) Segment-specific prevention of pioneer neuron apoptosis by cell-autonomous, postmitotic Hox gene activity. *Development,* **131,** 6093-6105.

148. Milan M, Perez L, and Cohen SM (2002) Short-range cell interactions and cell survival in the Drosophila wing. *Dev Cell,* **2,** 797-805.

149. Miller LK (1999) An exegesis of IAPs: salvation and surprises from BIR motifs. *Trends Cell Biol,* **9,** 323-328.

150. Miossec C, Dutilleul V, Fassy F, and Diu-Hercend A (1997) Evidence for CPP32 activation in the absence of apoptosis during T lymphocyte stimulation. *J Biol Chem,* **272,** 13459-13462.

151. Moroni MC, Hickman ES, Lazzerini DE, Caprara G, Colli E, Cecconi F, Muller H, and Helin K (2001) Apaf-1 is a transcriptional target for E2F and p53. *Nat Cell Biol,* **3,** 552-558.

152. Muro I, Berry DL, Huh JR, Chen CH, Huang H, Yoo SJ, Guo M, Baehrecke EH, and Hay BA (2006) The Drosophila caspase Ice is important for many apoptotic cell deaths and for spermatid individualization, a nonapoptotic process. *Development,* **133,** 3305-3315.

153. Muro I, Hay BA, and Clem RJ (2002) The Drosophila DIAP1 protein is required to prevent accumulation of a continuously generated, processed form of the apical caspase DRONC. *J Biol Chem,* **277,** 49644-49650.

154. Nakano K and Vousden KH (2001) PUMA, a novel proapoptotic gene, is induced by p53. *Mol Cell,* **7,** 683-694.

155. Newton K, Harris AW, Bath ML, Smith KG, and Strasser A (1998) A dominant interfering mutant of FADD/MORT1 enhances deletion of autoreactive thymocytes and inhibits proliferation of mature T lymphocytes. *EMBO J,* **17,** 706-718.

156. Nordstrom W, Chen P, Steller H, and Abrams JM (1996) Activation of the reaper gene during ectopic cell killing in Drosophila. *Dev Biol,* **180,** 213-226.

157. Oda E, Ohki R, Murasawa H, Nemoto J, Shibue T, Yamashita T, Tokino T, Taniguchi T, and Tanaka N (2000) Noxa, a BH3-only member of the Bcl-2 family and candidate mediator of p53-induced apoptosis. *Science,* **288,** 1053-1058.

158. Ollmann M, Young LM, Di Como CJ, Karim F, Belvin M, Robertson S, Whittaker K, Demsky M, Fisher WW, Buchman A, Duyk G, Friedman L, Prives C, and Kopczynski C (2000) Drosophila p53 is a structural and functional homolog of the tumor suppressor p53. *Cell,* **101,** 91-101.

159. Orth K, Chinnaiyan AM, Garg M, Froelich CJ, and Dixit VM (1996) The CED-3/ICE-like protease Mch2 is activated during apoptosis and cleaves the death substrate lamin A. *J Biol Chem,* **271,** 16443-16446.

160. Pazdera TM, Janardhan P, and Minden JS (1998) Patterned epidermal cell death in wild-type and segment polarity mutant Drosophila embryos. *Development,* **125,** 3427-3436.

161. Perrimon N and Mahowald AP (1987) Multiple functions of segment polarity genes in Drosophila. *Dev Biol,* **119,** 587-600.

162. Peterson C, Carney GE, Taylor BJ, and White K (2002) reaper is required for neuroblast apoptosis during Drosophila development. *Development,* **129,** 1467-1476.

163. Peterson JS, Barkett M, and McCall K (2003) Stage-specific regulation of caspase activity in drosophila oogenesis. *Dev Biol,* **260,** 113-123.

164. Posmantur R, Wang KK, and Gilbertsen RB (1998) Caspase-3-like activity is necessary for IL-2 release in activated Jurkat T-cells. *Exp Cell Res,* **244,** 302-309.

165. Pronk GJ, Ramer K, Amiri P, and Williams LT (1996) Requirement of an ICE-like protease for induction of apoptosis and ceramide generation by REAPER. *Science,* **271,** 808-810.

166. Putcha GV, Moulder KL, Golden JP, Bouillet P, Adams JA, Strasser A, and Johnson EM (2001) Induction of BIM, a proapoptotic BH3-only BCL-2 family member, is critical for neuronal apoptosis. *Neuron,* **29,** 615-628.

167. Quinn L, Coombe M, Mills K, Daish T, Colussi P, Kumar S, and Richardson H (2003) Buffy, a Drosophila Bcl-2 protein, has anti-apoptotic and cell cycle inhibitory functions. *EMBO J,* **22,** 3568-3579.

168. Quinn LM, Dorstyn L, Mills K, Colussi PA, Chen P, Coombe M, Abrams J, Kumar S, and Richardson H (2000) An essential role for the caspase dronc in developmentally programmed cell death in Drosophila. *J Biol Chem,* **275,** 40416-40424.

169. Ree AH, Tvermyr M, Engebraaten O, Rooman M, Rosok O, Hovig E, Meza-Zepeda LA, Bruland OS, and Fodstad O (1999) Expression of a novel factor in human breast cancer cells with metastatic potential. *Cancer Res,* **59,** 4675-4680.

170. Reuter R (1994) The gene serpent has homeotic properties and specifies endoderm versus ectoderm within the Drosophila gut. *Development,* **120,** 1123-1135.

171. Riedl SJ, Renatus M, Schwarzenbacher R, Zhou Q, Sun C, Fesik SW, Liddington RC, and Salvesen GS (2001) Structural basis for the inhibition of caspase-3 by XIAP. *Cell,* **104,** 791-800.

172. Rikhof B, Corn PG, and El-Deiry WS (2003) Caspase 10 levels are increased following DNA damage in a p53-dependent manner. *Cancer Biol Ther,* **2,** 707-712.

173. Robinow S, Draizen TA, and Truman JW (1997) Genes that induce apoptosis: transcriptional regulation in identified, doomed neurons of the Drosophila CNS. *Dev Biol,* **190,** 206-213.

174. Rodriguez A, Oliver H, Zou H, Chen P, Wang X, and Abrams JM (1999) Dark is a Drosophila homologue of Apaf-1/CED-4 and functions in an evolutionarily conserved death pathway. *Nat Cell Biol,* **1,** 272-279.

175. Rodriguez J and Lazebnik Y (1999) Caspase-9 and APAF-1 form an active holoenzyme. *Genes Dev,* **13,** 3179-3184.

176. Roy N, Deveraux QL, Takahashi R, Salvesen GS, and Reed JC (1997) The c-IAP-1 and c-IAP-2 proteins are direct inhibitors of specific caspases. *EMBO J,* **16,** 6914-6925.

177. Rozenfeld-Granot G, Krishnamurthy J, Kannan K, Toren A, Amariglio N, Givol D, and Rechavi G (2002) A positive feedback mechanism in the transcriptional activation of Apaf-1 by p53 and the coactivator Zac-1. *Oncogene,* **21,** 1469-1476.

178. Ruiz-Ruiz C, Ruiz de AC, Rodriguez A, Ortiz-Ferron G, Redondo JM, and Lopez-Rivas A (2004) The up-regulation of human caspase-8 by

interferon-gamma in breast tumor cells requires the induction and action of the transcription factor interferon regulatory factor-1. *J Biol Chem,* **279,** 19712-19720.

179. Ryoo HD, Bergmann A, Gonen H, Ciechanover A, and Steller H (2002) Regulation of Drosophila IAP1 degradation and apoptosis by reaper and ubcD1. *Nat Cell Biol,* **4,** 432-438.

180. Salvesen GS and Abrams JM (2004) Caspase activation - stepping on the gas or releasing the brakes? Lessons from humans and flies. *Oncogene,* **23,** 2774-2784.

181. Seshagiri S and Miller LK (1997) Caenorhabditis elegans CED-4 stimulates CED-3 processing and CED-3-induced apoptosis. *Curr Biol,* **7,** 455-460.

182. Shaham S and Horvitz HR (1996) An alternatively spliced C. elegans ced-4 RNA encodes a novel cell death inhibitor. *Cell,* **86,** 201-208.

183. Shi Y (2002b) Mechanisms of caspase activation and inhibition during apoptosis. *Mol Cell,* **9,** 459-470.

184. Shi Y (2002a) A conserved tetrapeptide motif: potentiating apoptosis through IAP-binding. *Cell Death Differ,* **9,** 93-95.

185. Shibue T, Takeda K, Oda E, Tanaka H, Murasawa H, Takaoka A, Morishita Y, Akira S, Taniguchi T, and Tanaka N (2003) Integral role of Noxa in p53-mediated apoptotic response. *Genes Dev,* **17,** 2233-2238.

186. Shinjyo T, Kuribara R, Inukai T, Hosoi H, Kinoshita T, Miyajima A, Houghton PJ, Look AT, Ozawa K, and Inaba T (2001) Downregulation of Bim, a proapoptotic relative of Bcl-2, is a pivotal step in cytokine-initiated survival signaling in murine hematopoietic progenitors. *Mol Cell Biol,* **21,** 854-864.

187. Shiozaki EN, Chai J, Rigotti DJ, Riedl SJ, Li P, Srinivasula SM, Alnemri ES, Fairman R, and Shi Y (2003) Mechanism of XIAP-mediated inhibition of caspase-9. *Mol Cell,* **11,** 519-527.

188. Smouse D and Perrimon N (1990) Genetic dissection of a complex neurological mutant, polyhomeotic, in Drosophila. *Dev Biol,* **139,** 169-185.

189. Sogame N, Kim M, and Abrams JM (2003) Drosophila p53 preserves genomic stability by regulating cell death. *Proc Natl Acad Sci U S A,* **100,** 4696-4701.

190. Song Z, Guan B, Bergman A, Nicholson DW, Thornberry NA, Peterson EP, and Steller H (2000) Biochemical and genetic interactions between

Drosophila caspases and the proapoptotic genes rpr, hid, and grim. *Mol Cell Biol,* **20,** 2907-2914.

191. Song Z, McCall K, and Steller H (1997) DCP-1, a Drosophila cell death protease essential for development. *Science,* **275,** 536-540.

192. Song Z and Steller H (1999) Death by design: mechanism and control of apoptosis
2. *Trends Cell Biol,* **9,** M49-M52.

193. Spector MS, Desnoyers S, Hoeppner DJ, and Hengartner MO (1997) Interaction between the C. elegans cell-death regulators CED-9 and CED-4. *Nature,* **385,** 653-656.

194. Srinivasula SM, Datta P, Kobayashi M, Wu JW, Fujioka M, Hegde R, Zhang Z, Mukattash R, Fernandes-Alnemri T, Shi Y, Jaynes JB, and Alnemri ES (2002) sickle, a novel Drosophila death gene in the reaper/hid/grim region, encodes an IAP-inhibitory protein. *Curr Biol,* **12,** 125-130.

195. Stahl M, Dijkers PF, Kops GJ, Lens SM, Coffer PJ, Burgering BM, and Medema RH (2002) The forkhead transcription factor FoxO regulates transcription of p27Kip1 and Bim in response to IL-2. *J Immunol,* **168,** 5024-5031.

196. Steller H (1995) Mechanisms and genes of cellular suicide. *Science,* **267,** 1445-1449.

197. Steller H, Abrams JM, Grether ME, and White K (1994) Programmed cell death in Drosophila. *Philos Trans R Soc Lond B Biol Sci,* **345,** 247-250.

198. Steller H and Grether ME (1994) Programmed cell death in Drosophila. *Neuron,* **13,** 1269-1274.

199. Stoven S, Ando I, Kadalayil L, Engstrom Y, and Hultmark D (2000) Activation of the Drosophila NF-kappaB factor Relish by rapid endoproteolytic cleavage. *EMBO Rep,* **1,** 347-352.

200. Sulston JE and Horvitz HR (1977) Post-embryonic cell lineages of the nematode, Caenorhabditis elegans. *Dev Biol,* **56,** 110-156.

201. Sulston JE, Schierenberg E, White JG, and Thomson JN (1983) The embryonic cell lineage of the nematode Caenorhabditis elegans. *Dev Biol,* **100,** 64-119.

202. Suzuki Y, Imai Y, Nakayama H, Takahashi K, Takio K, and Takahashi R (2001) A serine protease, HtrA2, is released from the mitochondria and interacts with XIAP, inducing cell death. *Mol Cell,* **8,** 613-621.

203. Tait SW, Werner AB, de VE, and Borst J (2004) Mechanism of action of Drosophila Reaper in mammalian cells: Reaper globally inhibits protein synthesis and induces apoptosis independent of mitochondrial permeability. *Cell Death Differ,* **11,** 800-811.

204. Takahashi A, Alnemri ES, Lazebnik YA, Fernandes-Alnemri T, Litwack G, Moir RD, Goldman RD, Poirier GG, Kaufmann SH, and Earnshaw WC (1996) Cleavage of lamin A by Mch2 alpha but not CPP32: multiple interleukin 1 beta-converting enzyme-related proteases with distinct substrate recognition properties are active in apoptosis. *Proc Natl Acad Sci U S A,* **93,** 8395-8400.

205. Tenev T, Zachariou A, Wilson R, Ditzel M, and Meier P (2005) IAPs are functionally non-equivalent and regulate effector caspases through distinct mechanisms. *Nat Cell Biol,* **7,** 70-77.

206. Tenev T, Zachariou A, Wilson R, Paul A, and Meier P (2002) Jafrac2 is an IAP antagonist that promotes cell death by liberating Dronc from DIAP1. *EMBO J,* **21,** 5118-5129.

207. Tepass U and Knust E (1993) Crumbs and stardust act in a genetic pathway that controls the organization of epithelia in Drosophila melanogaster. *Dev Biol,* **159,** 311-326.

208. Tepass U, Theres C, and Knust E (1990) crumbs encodes an EGF-like protein expressed on apical membranes of Drosophila epithelial cells and required for organization of epithelia. *Cell,* **61,** 787-799.

209. Thellmann M, Hatzold J, and Conradt B (2003) The Snail-like CES-1 protein of C. elegans can block the expression of the BH3-only cell-death activator gene egl-1 by antagonizing the function of bHLH proteins. *Development,* **130,** 4057-4071.

210. Thompson CB (1995) Apoptosis in the pathogenesis and treatment of disease. *Science,* **267,** 1456-1462.

211. Thornberry NA, Bull HG, Calaycay JR, Chapman KT, Howard AD, Kostura MJ, Miller DK, Molineaux SM, Weidner JR, Aunins J, and . (1992) A novel heterodimeric cysteine protease is required for interleukin-1 beta processing in monocytes. *Nature,* **356,** 768-774.

212. Thornberry NA and Lazebnik Y (1998) Caspases: enemies within. *Science,* **281,** 1312-1316.

213. Tittel JN and Steller H (2000) A comparison of programmed cell death between species. *Genome Biol,* **1,** REVIEWS0003.

214. Trent C, Tsuing N, and Horvitz HR (1983) Egg-laying defective mutants of the nematode Caenorhabditis elegans. *Genetics,* **104,** 619-647.

215. Uren AG, Pakusch M, Hawkins CJ, Puls KL, and Vaux DL (1996) Cloning and expression of apoptosis inhibitory protein homologs that function to inhibit apoptosis and/or bind tumor necrosis factor receptor-associated factors. *Proc Natl Acad Sci U S A,* **93,** 4974-4978.

216. van LG, van GM, Depuydt B, Srinivasula SM, Rodriguez I, Alnemri ES, Gevaert K, Vandekerckhove J, Declercq W, and Vandenabeele P (2002) The serine protease Omi/HtrA2 is released from mitochondria during apoptosis. Omi interacts with caspase-inhibitor XIAP and induces enhanced caspase activity. *Cell Death Differ,* **9,** 20-26.

217. Varfolomeev EE, Schuchmann M, Luria V, Chiannilkulchai N, Beckmann JS, Mett IL, Rebrikov D, Brodianski VM, Kemper OC, Kollet O, Lapidot T, Soffer D, Sobe T, Avraham KB, Goncharov T, Holtmann H, Lonai P, and Wallach D (1998) Targeted disruption of the mouse Caspase 8 gene ablates cell death induction by the TNF receptors, Fas/Apo1, and DR3 and is lethal prenatally. *Immunity,* **9,** 267-276.

218. Varghese J, Sade H, Vandenabeele P, and Sarin A (2002) Head involution defective (Hid)-triggered apoptosis requires caspase-8 but not FADD (Fas-associated death domain) and is regulated by Erk in mammalian cells. *J Biol Chem,* **277,** 35097-35104.

219. Vasseur S, Hoffmeister A, Garcia S, Bagnis C, Dagorn JC, and Iovanna JL (2002a) p8 is critical for tumour development induced by rasV12 mutated protein and E1A oncogene. *EMBO Rep,* **3,** 165-170.

220. Vasseur S, Hoffmeister A, Garcia-Montero A, Mallo GV, Feil R, Kuhbandner S, Dagorn JC, and Iovanna JL (2002b) p8-deficient fibroblasts grow more rapidly and are more resistant to adriamycin-induced apoptosis. *Oncogene,* **21,** 1685-1694.

221. Vasseur S, Vidal MG, Fiedler F, Bodeker H, Canepa E, Moreno S, and Iovanna JL (1999) Cloning and expression of the human p8, a nuclear protein with mitogenic activity. *Eur J Biochem,* **259,** 670-675.

222. Vaux DL, Aguila HL, and Weissman IL (1992) Bcl-2 prevents death of factor-deprived cells but fails to prevent apoptosis in targets of cell mediated killing. *Int Immunol,* **4,** 821-824.

223. Vaux DL, Cory S, and Adams JM (1988) Bcl-2 gene promotes haemopoietic cell survival and cooperates with c-myc to immortalize pre-B cells. *Nature,* **335,** 440-442.

224. Vaux DL and Silke J (2005) IAPs, RINGs and ubiquitylation. *Nat Rev Mol Cell Biol,* **6,** 287-297.

225. Verhagen AM, Ekert PG, Pakusch M, Silke J, Connolly LM, Reid GE, Moritz RL, Simpson RJ, and Vaux DL (2000) Identification of DIABLO, a mammalian protein that promotes apoptosis by binding to and antagonizing IAP proteins. *Cell,* **102,** 43-53.

226. Verhagen AM, Silke J, Ekert PG, Pakusch M, Kaufmann H, Connolly LM, Day CL, Tikoo A, Burke R, Wrobel C, Moritz RL, Simpson RJ, and Vaux DL (2002) HtrA2 promotes cell death through its serine protease activity and its ability to antagonize inhibitor of apoptosis proteins. *J Biol Chem,* **277,** 445-454.

227. Vernooy SY, Chow V, Su J, Verbrugghe K, Yang J, Cole S, Olson MR, and Hay BA (2002) Drosophila Bruce can potently suppress Rpr- and Grim-dependent but not Hid-dependent cell death. *Curr Biol,* **12,** 1164-1168.

228. Villunger A, Michalak EM, Coultas L, Mullauer F, Bock G, Ausserlechner MJ, Adams JM, and Strasser A (2003) p53- and drug-induced apoptotic responses mediated by BH3-only proteins puma and noxa 38. *Science,* **302,** 1036-1038.

229. Wajapeyee N, Britto R, Ravishankar HM, and Somasundaram K (2006) Apoptosis induction by activator protein 2alpha involves transcriptional repression of Bcl-2. *J Biol Chem,* **281,** 16207-16219.

230. Walsh CM, Wen BG, Chinnaiyan AM, O'Rourke K, Dixit VM, and Hedrick SM (1998) A role for FADD in T cell activation and development. *Immunity,* **8,** 439-449.

231. Wang JM, Chao JR, Chen W, Kuo ML, Yen JJ, and Yang-Yen HF (1999a) The antiapoptotic gene mcl-1 is up-regulated by the phosphatidylinositol 3-kinase/Akt signaling pathway through a transcription factor complex containing CREB. *Mol Cell Biol,* **19,** 6195-6206.

232. Wang SL, Hawkins CJ, Yoo SJ, Muller HA, and Hay BA (1999b) The Drosophila caspase inhibitor DIAP1 is essential for cell survival and is negatively regulated by HID. *Cell,* **98,** 453-463.

233. Wang Z, Malone MH, He H, McColl KS, and Distelhorst CW (2003) Microarray analysis uncovers the induction of the proapoptotic BH3-only protein Bim in multiple models of glucocorticoid-induced apoptosis. *J Biol Chem,* **278,** 23861-23867.

234. Weil M, Jacobson MD, Coles HS, Davies TJ, Gardner RL, Raff KD, and Raff MC (1996) Constitutive expression of the machinery for programmed cell death. *J Cell Biol,* **133,** 1053-1059.

235. Werz C, Lee TV, Lee PL, Lackey M, Bolduc C, Stein DS, and Bergmann A (2005) Mis-specified cells die by an active gene-directed process, and inhibition of this death results in cell fate transformation in Drosophila. *Development,* **132,** 5343-5352.

236. White K, Grether ME, Abrams JM, Young L, Farrell K, and Steller H (1994) Genetic control of programmed cell death in Drosophila. *Science,* **264,** 677-683.

237. White K, Tahaoglu E, and Steller H (1996) Cell killing by the Drosophila gene reaper. *Science,* **271,** 805-807.

238. Whitfield J, Neame SJ, Paquet L, Bernard O, and Ham J (2001) Dominant-negative c-Jun promotes neuronal survival by reducing BIM expression and inhibiting mitochondrial cytochrome c release. *Neuron,* **29,** 629-643.

239. Wilhelm S, Wagner H, and Hacker G (1998) Activation of caspase-3-like enzymes in non-apoptotic T cells. *Eur J Immunol,* **28,** 891-900.

240. Williams DW, Kondo S, Krzyzanowska A, Hiromi Y, and Truman JW (2006) Local caspase activity directs engulfment of dendrites during pruning. *Nat Neurosci,* **9,** 1234-1236.

241. Wilson R, Goyal L, Ditzel M, Zachariou A, Baker DA, Agapite J, Steller H, and Meier P (2002) The DIAP1 RING finger mediates ubiquitination of Dronc and is indispensable for regulating apoptosis. *Nat Cell Biol,* **4,** 445-450.

242. Wing JP, Schreader BA, Yokokura T, Wang Y, Andrews PS, Huseinovic N, Dong CK, Ogdahl JL, Schwartz LM, White K, and Nambu JR (2002) Drosophila Morgue is an F box/ubiquitin conjugase domain protein important for grim-reaper mediated apoptosis. *Nat Cell Biol,* **4,** 451-456.

243. Wing JP, Schwartz LM, and Nambu JR (2001) The RHG motifs of Drosophila Reaper and Grim are important for their distinct cell death-inducing abilities. *Mech Dev,* **102,** 193-203.

244. Wing JP, Zhou L, Schwartz LM, and Nambu JR (1998) Distinct cell killing properties of the Drosophila reaper, head involution defective, and grim genes. *Cell Death Differ,* **5,** 930-939.

245. Wu D, Wallen HD, Inohara N, and Nunez G (1997a) Interaction and regulation of the Caenorhabditis elegans death protease CED-3 by CED-4 and CED-9. *J Biol Chem,* **272,** 21449-21454.

246. Wu D, Wallen HD, and Nunez G (1997b) Interaction and regulation of subcellular localization of CED-4 by CED-9. *Science,* **275,** 1126-1129.

247. Wu G, Chai J, Suber TL, Wu JW, Du C, Wang X, and Shi Y (2000) Structural basis of IAP recognition by Smac/DIABLO. *Nature,* **408,** 1008-1012.

248. Wu JW, Cocina AE, Chai J, Hay BA, and Shi Y (2001) Structural analysis of a functional DIAP1 fragment bound to grim and hid peptides. *Mol Cell,* **8,** 95-104.

249. Xu D, Li Y, Arcaro M, Lackey M, and Bergmann A (2005) The CARD-carrying caspase Dronc is essential for most, but not all, developmental cell death in Drosophila. *Development,* **132,** 2125-2134.

250. Xu D, Wang Y, Willecke R, Chen Z, Ding T, and Bergmann A (2006) The effector caspases drICE and dcp-1 have partially overlapping functions in the apoptotic pathway in Drosophila. *Cell Death Differ,* **13,** 1697-1706.

251. Xue D, Shaham S, and Horvitz HR (1996) The Caenorhabditis elegans cell-death protein CED-3 is a cysteine protease with substrate specificities similar to those of the human CPP32 protease. *Genes Dev,* **10,** 1073-1083.

252. Yan N, Wu JW, Chai J, Li W, and Shi Y (2004) Molecular mechanisms of DrICE inhibition by DIAP1 and removal of inhibition by Reaper, Hid and Grim. *Nat Struct Mol Biol,* **11,** 420-428.

253. Yang J, Liu X, Bhalla K, Kim CN, Ibrado AM, Cai J, Peng TI, Jones DP, and Wang X (1997) Prevention of apoptosis by Bcl-2: release of cytochrome c from mitochondria blocked. *Science,* **275,** 1129-1132.

254. Yang X, Chang HY, and Baltimore D (1998) Essential role of CED-4 oligomerization in CED-3 activation and apoptosis. *Science,* **281,** 1355-1357.

255. Yoo SJ, Huh JR, Muro I, Yu H, Wang L, Wang SL, Feldman RM, Clem RJ, Muller HA, and Hay BA (2002) Hid, Rpr and Grim negatively regulate DIAP1 levels through distinct mechanisms. *Nat Cell Biol,* **4,** 416-424.

256. Yu J, Zhang L, Hwang PM, Kinzler KW, and Vogelstein B (2001) PUMA induces the rapid apoptosis of colorectal cancer cells. *Mol Cell,* **7,** 673-682.

257. Yuan J, Shaham S, Ledoux S, Ellis HM, and Horvitz HR (1993) The C. elegans cell death gene ced-3 encodes a protein similar to mammalian interleukin-1 beta-converting enzyme. *Cell,* **75,** 641-652.

258. Yuan J and Yankner BA (2000) Apoptosis in the nervous system. *Nature,* **407,** 802-809.

259. Yuan JY and Horvitz HR (1990) The Caenorhabditis elegans genes ced-3 and ced-4 act cell autonomously to cause programmed cell death. *Dev Biol,* **138,** 33-41.

260. Zachariou A, Tenev T, Goyal L, Agapite J, Steller H, and Meier P (2003) IAP-antagonists exhibit non-redundant modes of action through differential DIAP1 binding. *EMBO J,* **22,** 6642-6652.

261. Zhang H, Huang Q, Ke N, Matsuyama S, Hammock B, Godzik A, and Reed JC (2000) Drosophila pro-apoptotic Bcl-2/Bax homologue reveals evolutionary conservation of cell death mechanisms. *J Biol Chem,* **275,** 27303-27306.

262. Zhou L, Schnitzler A, Agapite J, Schwartz LM, Steller H, and Nambu JR (1997a) Cooperative functions of the reaper and head involution defective genes in the programmed cell death of Drosophila central nervous system midline cells. *Proc Natl Acad Sci U S A,* **94,** 5131-5136.

263. Zhou L, Song Z, Tittel J, and Steller H (1999) HAC-1, a Drosophila homolog of APAF-1 and CED-4 functions in developmental and radiation-induced apoptosis. *Mol Cell,* **4,** 745-755.

264. Zhou P, Qian L, Kozopas KM, and Craig RW (1997b) Mcl-1, a Bcl-2 family member, delays the death of hematopoietic cells under a variety of apoptosis-inducing conditions. *Blood,* **89,** 630-643.

265. Zou H, Henzel WJ, Liu X, Lutschg A, and Wang X (1997) Apaf-1, a human protein homologous to C. elegans CED-4, participates in cytochrome c-dependent activation of caspase-3. *Cell,* **90,** 405-413.

266. Zou H, Li Y, Liu X, and Wang X (1999) An APAF-1.cytochrome c multimeric complex is a functional apoptosome that activates procaspase-9. *J Biol Chem,* **274,** 11549-11556.